Applied Physics Laboratory
College of Ocean and Fishery Sciences, University of Washington

1943–1993 — 50 Years of Excellence

26 April 1995

To: Defense Technical Information Center
Building 5, Cameron Station
Alexandria, VA 22304-6145

Dear Sir or Madam,

Enclosed please find two copies of a document submitted in compliance with the terms of ONR grant N00014-94-1-0036 for submission of "Final Technical Report, issued at end of grant." The document consists of two preprints, and an extended abstract:

Odom, R.I., M. Park, J.A. Mercer, R.S. Crosson, & P. Paik, "Mode coupling in shallow water with a transversely isotropic bottom", *J. Acoust. Soc. Am.*, submitted, 1994.

Odom, R.I. & J.A. Mercer, "Spectral diffusion of elastic wave energy," *Geophys. J. Int.*, submitted, 1994.

Odom, R.I. & J.A. Mercer, "Modal attenuation and interaction with a transversely isotropic viscoelastic bottom in shallow water acoustic propagation," (extended abstract).

I will forward reprints as the articles are published.

Sincerely,

Robert I. Odom

Cc: Jim Mercer, Monty Bolstad

Encl.

1013 NE 40th Street Seattle, Washington 98105-6698 (206) 543-1300 FAX (206) 543-6785

REPORT DOCUMENTATION PAGE

Form Approved
OPM No. 0704-0188

1. AGENCY USE ONLY *(Leave blank)*	2. REPORT DATE	3. REPORT TYPE AND DATES COVERED
	April 1995	Transmittal document

4. TITLE AND SUBTITLE
Mode Coupling in Shallow Water Acoustic Propagation

5. FUNDING NUMBERS
N00014-94-1-0036

6. AUTHOR(S)
Robert I. Odom and James A. Mercer

7. PERFORMING ORGANIZATION NAME(S) AND ADDRESS(ES)
Applied Physics Laboratory
University of Washington
1013 NE 40th Street
Seattle, WA 98105-6698

8. PERFORMING ORGANIZATION REPORT NUMBER

9. SPONSORING / MONITORING AGENCY NAME(S) AND ADDRESS(ES)
Defense Technical Information Center
Building 5, Cameron Station
Alexandria, VA 22304-6145

10. SPONSORING / MONITORING AGENCY REPORT NUMBER

11. SUPPLEMENTARY NOTES
Preprints of papers submitted to fulfill grant obligation.
Reprints will be furnished upon publication.

12a. DISTRIBUTION / AVAILABILITY STATEMENT
Unlimited

12b. DISTRIBUTION CODE

13. ABSTRACT *(Maximum 200 words)*

Characterization of sound propagation in shallow water requires a detailed understanding of the propagation processes and environmental properties, and how they are linked. This report contains three separate sections that address the effects of range dependence, sediment transverse isotropy, and high attenuation on acoustic propagation in shallow water. The investigations described are theoretical and numerical, and are based on the method of coupled local modes.

14. SUBJECT TERMS
Acoustic propagation, attenuation, coupled modes, shallow water, transverse isotropy

15. NUMBER OF PAGES
105

16. PRICE CODE

17. SECURITY CLASSIFICATION OF REPORT	18. SECURITY CLASSIFICATION OF THIS PAGE	19. SECURITY CLASSIFICATION OF ABSTRACT	20. LIMITATION OF ABSTRACT
Unclassified	Unclassified	Unclassified	SAR

DISCLAIMER NOTICE

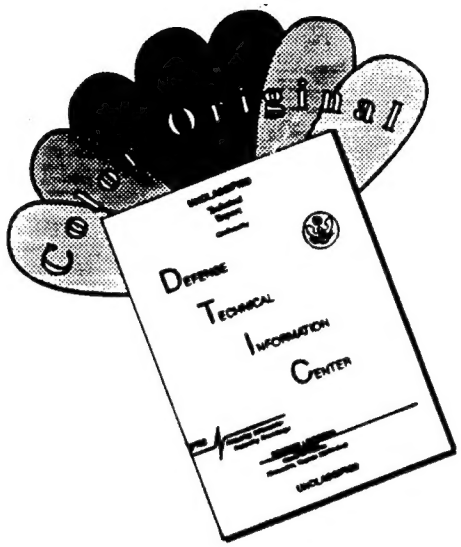

THIS DOCUMENT IS BEST QUALITY AVAILABLE. THE COPY FURNISHED TO DTIC CONTAINED A SIGNIFICANT NUMBER OF COLOR PAGES WHICH DO NOT REPRODUCE LEGIBLY ON BLACK AND WHITE MICROFICHE.

Mode coupling in shallow water with a transversely isotropic bottom

Robert I. Odom[1] Minkyu Park[2] James A. Mercer[1]

Robert S. Crosson[2] Pauline Paik[2]

Received:

PACS 43.30Bp, Ft, Gv, Hw, Ma

[1]Applied Physics Laboratory, 1013 NE 40th Street, and Geophysics Program, AK-50, University of Washington, Seattle, WA 98105 (e-mail: odom@apl.washington.edu)

[2]Geophysics Program, AK-50, University of Washington, Seattle, WA 98195

Abstract

A study of 2-D acoustic mode coupling in range dependent shallow water with a transversely isotropic (TI) bottom is presented. Most marine sediments exhibit a fair degree of transverse isotropy that can have a significant effect on the signal properties of strongly bottom interacting sound. Locally, transverse isotropy has the greatest effect on the fundamental and near fundamental modal overtones. The local shallow water TI modes have reduced amplitude in the sediment relative to the corresponding shallow water modes for an isotropic bottom. Calculations of mode-mode coupling coefficients for a range dependent medium indicate that mode coupling is more strongly confined to modal nearest neighbors for a TI medium characterized predominantly by shear wave anisotropy, when compared to the corresponding isotropic medium. As the frequency increases, the strongest coupling occurs between higher overtones and also becomes more strongly peaked around nearest neighbors. The coupled mode theory of Maupin[Geophys. J. **93**, 173-185 (1988)] is employed to model the coupling. This theory can treat smooth gradients and sloping layer boundaries for all five of the bottom elastic moduli in a TI medium, the densities, and the range dependence of the water column itself. This coupled mode formulation also properly accounts for the continuity of stress and displacement boundary conditions in an exact way at irregular interfaces.

Introduction

Acoustic propagation in shallow water is generally characterized by strong range dependence and interaction with the bottom. The range dependence is both geometric and material in nature. Fluctuations in water depth and layer thicknesses of bottom sediments impose geometric variations of the medium with range. Range dependent gradients in elastic parameters and density of individual layers further complicate the task of characterizing and understanding shallow water acoustic propagation. Adequate modeling and understanding of shallow water signals that interact strongly with the bottom require a proper treatment of the marine sediment and basement properties. Marine sediments typically exhibit finite shear wave speeds that are much less than the sound speed in the water column[1,2]. The vertical gradients of the shear speed can be quite large, and velocity anisotropy is an almost universal feature of marine sediments, with transverse isotropy (TI) being the most common type of anisotropy[3–6].

Strong range dependence causes energy in an initially unidirectional propagating signal to be redistributed among forward and backward discrete and continuum modes. Inclusion of finite shear speed in the sediment is necessary to model the Stoneley wave propagating at the water sediment interface and to properly account for the component of transmission loss due to conversion to shear waves. Acoustic energy can be scattered from the water column into the Stoneley wave by range dependence of the water-sediment interface[7]. Assuming that the bottom properties are isotropic when they are really transversely isotropic can lead to underestimating sediment sound speed gradients, and overestimating sediment thickness and shear velocity[8]. Also, as will be seen below, incorrectly assuming isotropy has a significant effect on the redistribution of acoustic energy through range dependence induced mode coupling.

The original formulation of the coupled mode equations for sound propagation in a range

dependent ocean effected a local separation of the Helmholtz equation for the velocity potential or, equivalently, the pressure (Pierce[9], Milder[10]). The dependent variable is represented as the superposition of a set of range varying basis functions, the "local modes," with range dependent amplitude coefficients. The elements of this local basis are chosen to be the modes of the plane layered structure that corresponds locally in terms of material properties and layer thicknesses to the range dependent structure. This approach leads to another second order differential equation that must be solved to obtain the range dependent modal amplitude coefficients. The right hand side of this equation consists of source terms quantifying the strength of the coupling between different local modes. The formulations presented by Pierce[9] and Milder[10] yield first and second order coupling coefficients that depend on the first and second order derivatives, respectively, with respect to the range coordinate of the local mode functions.

The second order coupling coefficients are cumbersome to deal with analytically. They can be shown to depend on the second derivatives and the squares of the first derivatives with respect to the range coordinate of the boundary slopes and material parameters. Consequently, the second order coupling coefficients have been routinely ignored (Chwieroth et al.[11], Rutherford and Hawker[12], McDaniel[13], Hall[14]).

It is interesting to note, however, that the presence of the second order coupling coefficients is an artifact of the formulation. It is a consequence of working with the Helmholtz equation (a second order differential equation) rather than directly with the coupled first order equations for the pressure and velocity. Odom[15,16] has derived a local coupled mode theory directly from the field quantities pressure and velocity that contains all the modal interaction physics in a single coupling coefficient. This formulation exhibits explicit dependence on geometric and material gradients, and is mathematically and numerically more efficient. Maupin[17] extended the results of Refs.(15,16) to take elastic effects including anisotropy into account. We have applied Maupin's extensions to the case of fluid-elastic

media in order to examine the mode coupling in a realistic shallow water model.

Theory

This section contains a fairly brief, self-contained summary of the coupled mode theory for layered fluid-elastic media as developed by Maupin[17]. We include this because these techniques seem to be generally unfamiliar to the ocean acoustics community. A particularly important point is the treatment of the boundary conditions at the interface between two geometrically irregular layers. Rutherford and Hawker[12] derived corrections to the eigenfunctions for a plane layered medium that satisfy the boundary conditions at irregular layer interfaces to first order in the interface slope. It is, however, possible to satisfy the boundary conditions at the irregular interface exactly by transforming inhomogeneous boundary conditions to homogeneous boundary conditions and adding an additional source term to the governing system of differential equations[17]. This has recently been rediscovered by Fawcett[18] for fluid media. Gillette[19] introduced a local coordinate transformation that leads to a solution that exactly satisfies the boundary conditions for the case of a single perfectly rigid range dependent boundary. Gillette's problem can also be solved with the local mode theory described here without transforming to a special local coordinate system. In fact the following treatment of the coupled mode problem leads to a solution which exactly satisfies the range dependent boundary conditions at all interfaces with no approximations or neglected terms. As will be seen below, it is not necessary to construct depth functions satisfying boundary conditions involving normal derivatives on a range dependent boundary. This exact solution is also numerically tractible, and may be computed using any good normal mode code as the core program. The treatment is valid for solid-solid as well as fluid-solid and fluid-fluid boundaries. It is also valid for general anisotropic media. Our specific examples are carried out for transversely isotropic media with a vertical axis of symmetry. First we treat the mode coupling due to range dependence within the bottom material. In

the second sub-section we review the additional terms in the mode coupling matrix due to the range dependence of the water column itself and the range dependence of the fluid-solid boundary at the water-bottom interface.

A. Mode Coupling in Solid Elastic Media

We use a Cartesian coordinate system in which the x axis (or x_1 axis) is the direction of the range dependence, y-axis (or x_2 axis) is the axis along which there is no variation in medium properties, and z-axis (or x_3 axis) is the depth axis and taken to be positive downward. The particle displacement vector is $\mathbf{w} = (w_x,\ w_y,\ w_z)$.

For the elastic moduli, the matrix notation of Woodhouse[20] is employed such that

$$(C_{ij})_{kl} = c_{kilj}. \tag{1}$$

Note that this is *not* the same as the widely used abbreviated subscript notation for the elasticity tensor as described by Auld[21] for example. The individual C_{ij}'s in Woodhouse's notation are matrices, not individual matrix elements as in the abbreviated subscript notation.

The equations of motion for an elastic medium are

$$\rho \frac{\partial^2 \mathbf{w}}{\partial t^2} = \nabla_i \mathbf{t}_i + \mathbf{f}, \tag{2}$$

where ρ is the density, $\mathbf{f}$ is an external force and the traction vector $\mathbf{t}$ is defined by

$$\mathbf{t}_i = C_{ij} \left(\frac{\partial \mathbf{w}}{\partial x_j} \right), \tag{3}$$

where $\mathbf{w} = (w_x, w_y, w_z)$ and $\mathbf{t}_i = (\tau_{ix},\ \tau_{iy},\ \tau_{iz})$.

The displacement, Fourier transformed with respect to y and t, is represented as

$$\mathbf{w}(x, z, p, \omega) = \int_{-\infty}^{+\infty} \int_{-\infty}^{+\infty} \mathbf{w}(x, y, z, t) \exp(i(py - \omega t)) dy dt \tag{4}$$

where p is the spatial wave number in the y-direction. The equations of motion can then be written as

$$-\rho\omega^2\mathbf{w} = \frac{\partial \mathbf{t}_1}{\partial x} - ip\mathbf{t}_2 + \frac{\partial \mathbf{t}_3}{\partial z} + \mathbf{f} \tag{5}$$

where

$$\mathbf{t}_i = C_{i1}\frac{\partial \mathbf{w}}{\partial x} - ipC_{i2}\mathbf{w} + C_{i3}\frac{\partial \mathbf{w}}{\partial z}. \tag{6}$$

The same symbol $\mathbf{w}$ is used for both the transformed and untransformed displacement. The subsequent development is carried out completely in the (x, z, p, ω) domain, and there should be no confusion. The use of i as both an index and as $\sqrt{-1}$ should also be clear from context.

Introducing the 6-component displacement-stress vector $\mathbf{u} = (\mathbf{w}, \mathbf{t})^{\mathbf{T}}$ where $\mathbf{w}$ is as defined above and $\mathbf{t} = \mathbf{t}_1 = (\tau_{xx},\ \tau_{xy},\ \tau_{xz})$, the equations of motion can be written as the first order system where the derivatives with respect to the propagation direction, that is, the direction of the range dependence of the structure, appear only on the left hand side of equation

$$\frac{\partial \mathbf{u}}{\partial x} = A\mathbf{u} - \begin{Bmatrix} 0 \\ \mathbf{f} \end{Bmatrix}. \tag{7}$$

The differential operator

$$A = \begin{pmatrix} -C_{11}^{-1}C_{13}\frac{\partial}{\partial z} + C_{11}^{-1}C_{12}ip & C_{11}^{-1} \\ -\rho\omega^2 - \frac{\partial}{\partial z}\left(Q_{33}\frac{\partial}{\partial z}\right) + ipQ_{23}\frac{\partial}{\partial z} + \frac{\partial}{\partial z}(Q_{32}ip) + p^2Q_{22} & -\frac{\partial}{\partial z}C_{31}C_{11}^{-1} + ipC_{21}C_{11}^{-1} \end{pmatrix} \tag{8}$$

does not depend on the horizontal derivatives. The matrices Q_{ij} are defined as

$$Q_{ij} = C_{ij} - C_{i1}C_{11}^{-1}C_{1j}. \tag{9}$$

The boundary conditions require the continuity of traction and displacement across interfaces. The free surface condition for an elastic (fluid) medium is that the traction (pressure) vanishes and a radiation condition is assumed as $z \to \infty$. The interfaces of the range dependent medium are taken to be of the form $z = h(x)$ with normal $\mathbf{n}$. Thus the slope of m-th interface can be written as

$$\frac{dz_m}{dx} = \frac{\partial h_m}{\partial x} = \dot{h}_m. \tag{10}$$

By introducing the inclination angle $\theta_m = \tan^{-1}(\dot{h}_m)$, the normal vector can be expressed as

$$\mathbf{n} = \sin\theta\hat{\mathbf{i}} - \cos\theta\hat{\mathbf{k}}. \tag{11}$$

The continuity of traction $\mathbf{T} = \mathbf{t}_j n_j$ across m-th interface can be written as

$$\begin{aligned} [\mathbf{T}] &= [\mathbf{t}_1 \sin\theta_m - \mathbf{t}_3 \cos\theta_m]_m \\ &= \frac{1}{\sqrt{1+\dot{h}_m^2}}[\mathbf{t}_3 - \dot{h}_m \mathbf{t}]_m = 0. \end{aligned} \tag{12}$$

The square brackets $[\cdot]_m$ indicate the jump of the enclosed quantity across the m^{th} interface, taken from bottom to top. Consequently, we have

$$[\mathbf{t}_3]_m = \dot{h}_m [\mathbf{t}]_m. \tag{13}$$

The continuity of traction *normal* to a sloping interface is then equivalent to a *jump* in the traction along the vertical axis. The equations of motion (7) along with the interface boundary conditions (13) and the free surface and radiation conditions are an exact formal representation of the equations for the displacement-stress field in a range dependent layered elastic medium. What makes a solution of the problem difficult is the inhomogeneous form of the interface boundary condition Eq.(13). Historically this inhomogeneous boundary condition has been dealt with by ignoring the inhomogeneity[13,15,16,22], and replacing it with the approximate homogeneous condition. That is, the condition that the normal component of the traction be continuous across interfaces was replaced by the condition that only the

vertical component of the traction be continuous. It was pointed out by Maupin[17] that the traction discontinuity in the interface boundary conditions can be converted to a localized volume force located along the interface. This follows from a representation theorem for elastic media investigated by Burridge and Knopoff[23]. The resulting equivalent volume force becomes a source term on the right hand side of Eq.(7), and the interface boundary conditions become homogeneous. Equations (7) and (13) can now be written in the absence of body forces as

$$\frac{\partial \mathbf{u}}{\partial x} = A\mathbf{u} + \sum_m \dot{h}_m \left\{ \begin{array}{c} 0 \\ [\mathbf{t}]_m \delta(z - h_m(x)) \end{array} \right\} \tag{14}$$

with the interface conditions

$$[\mathbf{t}_3]_m = [\mathbf{w}]_m = 0. \tag{15}$$

Equations (14) and (15) are a very important result. This first order system of inhomogeneous equations with homogeneous boundary conditions formally describes the evolution of the displacement-stress fields along the range direction. The solution to this system will now be expressed in terms of coupled local modes. These local modes, defined below, are the eigenfunctions of the *range independent* medium that locally share the same depth dependence as the *range dependent* medium. This means that locally at some point x_0 in range, the density $\rho(x_0, z)$ and the elastic moduli $C_{ij}(x_0, z)$ are taken to be functions of depth only so that

$$\rho(x_0, z) = \rho(z) \quad \text{and} \quad C_{ij}(x_0, z) = C_{ij}(z). \tag{16}$$

The wave propagation problem for a 2-dimensional range dependent medium can be solved exactly in terms of the eigenfunctions of the range independent medium. These eigenfunctions are the homogeneous solutions to Eq.(14) with homogeneous boundary con-

ditions Eq.(15). The boundary conditions at the irregular interfaces are satisfied exactly by including the effective source term in Eq.(14). No approximations have been made.

Local homogeneous solutions of the equations of motion (Eq.(14)) which depend parametrically on x are represented as

$$\mathbf{u}(x_0, z)\exp\{-ik^r(x_0)x\} \tag{17}$$

with $\mathbf{u}$ satisfying

$$-ik^r(x_0)\mathbf{u}^r(x_0, z) = A\mathbf{u}^r(x_0, z) \tag{18}$$

and the homogeneous boundary conditions $[\mathbf{w}^r]_m = 0$ and $[\mathbf{t}_3^r]_m = 0$ across interfaces. The horizontal wave number in the x-direction is $k^r(x_0)$, and taken to be real.

The final definition required is the following scalar product between two local eigenfunctions of index r and q.

$$\langle \mathbf{u}^q, \mathbf{u}^r \rangle = i\int_0^\infty (\mathbf{w}^{q*}\mathbf{t}^r - \mathbf{t}^{q*}\mathbf{w}^r)dz \tag{19}$$

where $*$ indicates complex conjugation. The scalar product (19) is Hermitian, i.e.

$$\langle f, g \rangle = \langle g, f \rangle^*. \tag{20}$$

The local modes at fixed values of frequency and p are orthogonal with respect to this scalar product. The local modes are normalized such that

$$\langle \mathbf{u}^q, \mathbf{u}^r \rangle = \delta_{rq}. \tag{21}$$

Thus, they all carry the same energy flux across planes $x =$ constant.

The basic idea of the coupled local mode technique is to seek a solution for the equations of motion as a coupled set of local modes whose amplitudes and phases vary with laterally

varying structure. The evolution of the range dependent amplitude determines how energy is exchanged between modes as a signal propagates through the medium. The solution of the equations of motion for the displacement-stress field in the range dependent medium is represented as the sum over local modes

$$\mathbf{u} = \left\{ \begin{array}{c} \mathbf{w} \\ \mathbf{t} \end{array} \right\} = \sum_r c_r(x) \exp\left(-i \int_0^x k^r(\zeta) d\zeta\right) \left\{ \begin{array}{c} \mathbf{w}^r(x,z) \\ \mathbf{t}^r(x,z) \end{array} \right\}, \tag{22}$$

where $k(\zeta)$ is the local horizontal wavenumber. The local modes satisfy the homogeneous boundary conditions, Eq.(15), of a plane layered medium, and can therefore be computed with any appropriate normal mode code.

The derivation of the evolution equation for the range dependent amplitude coefficients $c_r(x)$ proceeds in the same fashion as previous coupled mode developments. The representation Eq.(22) is substituted into the equations of motion Eq.(14). The scalar product of the resulting expression is formed with the displacement-stress vector of the qth mode $\mathbf{u}^q$, yielding:

$$\frac{\partial c_q}{\partial x} = B_{qr} c_r \tag{23}$$

with the coupling matrix

$$B_{qr} = \{-\langle \mathbf{u}^q, \frac{\partial \mathbf{u}^r}{\partial x} \rangle + i \sum_m \dot{h}_m \mathbf{w}^{q*} [\mathbf{t}^r]_m\} \exp\left(i \int_0^x (k^q - k^r) d\zeta\right) \tag{24}$$

In the case of very weak range dependence, we can set

$$B_{qr} = 0, \tag{25}$$

indicating that individual modes propagate independently without interacting. This is the

adiabatic approximation[9,10,20,24]. The validity of the adiabatic approximation requires that the medium properties change very slowly with range. The total change can actually be quite large, but the rate of change with range must be small enough so that modes do not exchange energy among each other and are able to adjust their shapes to the local environment. Backscattering is automatically excluded by the adiabatic approximation, as is radiation to the continuum. A medium characterized by layer thicknesses or material properties that change significantly over a mode equivalent ray cycle distance will not be well modeled by the adiabatic approximation.

The form of the coupling matrix in Eq.(24) is not well suited to numerical computation because of the presence of the range derivatives of the local mode functions. The coupling matrix B_{qr} can be transformed so that the only range derivatives appearing in the expression are of the density and elastic moduli within layers and of the interface functions $h_m(x)$ at layer boundaries. We omit the lengthy derivation and refer the interested reader to Reference (17). The final form for the coupling matrix in the solid medium comprising the bottom is then:

$$
\begin{aligned}
B_{qr} \;=\; & \frac{1}{k^q - k^r}\left(\int_0^\infty (\mathbf{w}^{q*}\dot{\rho}\omega^2\mathbf{w}^r - \frac{\partial \mathbf{w}^{q*}}{\partial z}\dot{Q}_{33}\frac{\partial \mathbf{w}^r}{\partial z} - \mathbf{w}^{q*}ip\dot{Q}_{23}\frac{\partial \mathbf{w}^r}{\partial z}\right. \\
& + \frac{\partial \mathbf{w}^{q*}}{\partial z}\dot{Q}_{32}ip\mathbf{w}^r - \mathbf{w}^{q*}\dot{Q}_{22}p^2\mathbf{w}^r - \frac{\partial \mathbf{w}^{q*}}{\partial z}(C_{31}\dot{C}_{11}^{-1})\mathbf{t}^r - \mathbf{w}^{q*}ip(C_{21}\dot{C}_{11}^{-1})\mathbf{t}^r \\
& - \mathbf{t}^{q*}(C_{11}^{-1}\dot{C}_{13})\frac{\partial \mathbf{w}^r}{\partial z} + \mathbf{t}^{q*}(C_{11}^{-1}\dot{C}_{12})ip\mathbf{w}^r + \mathbf{t}^{q*}\dot{C}_{11}^{-1}\mathbf{t}^r)dz \\
& + \sum_m \dot{h}_m\left[-\mathbf{w}^{q*}\rho\omega^2\mathbf{w}^r - \frac{\partial \mathbf{w}^{q*}}{\partial z}Q_{33}\frac{\partial \mathbf{w}^r}{\partial z} + \mathbf{w}^{q*}Q_{22}\mathbf{w}^r p^2 + \frac{\partial \mathbf{w}^{q*}}{\partial z}(C_{31}C_{11}^{-1})\mathbf{t}^r\right. \\
& \left.\left. - \mathbf{t}^{q*}(C_{11}^{-1}C_{13})\frac{\partial \mathbf{w}^r}{\partial z} + \mathbf{t}^q C_{11}^{-1}\mathbf{t}^r\right]_n\right)\exp\left(i\int_0^x (k^q - k^r)d\zeta\right) \qquad (26)
\end{aligned}
$$

The coupling matrix Eq.(26) involves an integral term related to the lateral derivative of the elastic moduli and density inside the layers. The interface term is a combination of an expression derived from the continuity conditions and another arising from jumps in the

lateral derivatives of the elastic coefficients. It is the former of the these two interface terms that appears as the effective volume source term on Eq.(14). There are no range derivatives of the local eigenfunctions, and there is no need to introduce a special coordinate system. The expression(26) describes the coupling in a fully anisotropic 2-dimensional medium. We have derived the form of the matrices C_{ij} and Q_{ij} for a transversely isotropic medium, and listed the result in the Appendix. These have also been given by Maupin[25]. We use the notation of Love[26] for the five elastic moduli required to characterize a transversely isotropic medium. The relationship between Love's[26] notation and the abbreviated subscript notation for the elastic moduli of a TI medium is also given in the Appendix.

B. Coupling Terms for Fluid Layer and Fluid-Elastic Interface

In this subsection we very briefly review the the additional terms required to treat the mode coupling due to the range dependence of the water column and the fluid-solid interface at the water-bottom boundary[17]. We make the two assumptions that: 1. The water column surface is flat; and 2. The water density ρ and incompressibility λ may vary with depth and range but not with time. We assume an ocean of depth $h = h(x)$.

In a fluid medium, the displacement-stress vector $\mathbf{u}$ is

$$\mathbf{u} = \begin{Bmatrix} w_x \\ t \end{Bmatrix} \tag{27}$$

The x component of the particle displacement is w_x, and the scalar t is the pressure. The equations of motion written in first order matrix form are

$$\frac{\partial \mathbf{u}}{\partial x} = A\mathbf{u} + \mathbf{f} \tag{28}$$

where the operator A in the fluid is

$$A = \begin{pmatrix} 0 & \frac{1}{\lambda} - \frac{p^2}{\rho\omega^2} + \frac{\partial}{\partial z}\left(\frac{1}{\rho\omega^2}\frac{\partial}{\partial z}\right) \\ -\rho\omega^2 & 0 \end{pmatrix}, \tag{29}$$

and $\mathbf{f}$ is the source vector. As before p is the spatial wavenumber in the y (cross-range) direction.

An ideal inviscid fluid does not support shear, so the boundary condition at the fluid-solid bottom boundary requiring continuity of the tangential component of displacement is relaxed and replaced with a free slip boundary condition. This free slip boundary condition results in a physically unrealistic discontinuity in the tangential component of displacement w_x, which can be remedied by including a small nonzero viscosity in the equations of motion for the fluid.

The continuity conditions across a fluid-solid interface of the form $z = h(x)$ are

$$[\mathbf{t}_3 - \dot{h}\mathbf{t}_1] = 0, \quad [w_z - \dot{h}w_x] = 0. \tag{30}$$

Again, these continuity conditions can be transformed into continuity conditions across a flat interface plus a volume force located along the fluid-solid interface. A first part of this force applies in the solid part only:

$$\mathbf{f} = \dot{h}[-\mathbf{t}_1]\delta(z - h(x)). \tag{31}$$

A second one can be taken as applying on either side of the interface:

$$f_i = \dot{h}\left([w_x]C_{33ij}\frac{\partial}{\partial x_j}\right)\delta(z - h(x)) \tag{32}$$

where C_{33ij} has to be taken in the layer where we actually choose to apply the force.

The scalar product (19) now becomes:

$$\langle \mathbf{u}^q, \mathbf{u}^r \rangle = i\int_0^h (w_x^{q*}t^r - t^{q*}w_x^r)dz + i\int_h^\infty (\mathbf{w}^{q*}\mathbf{t}_1^r - \mathbf{t}_1^{q*}\mathbf{w}^r)dz \tag{33}$$

To obtain an evolution equation for the amplitude coefficients, one uses the properties of the scalar product (33) and proceeds exactly as in the solid-solid case. The transformation of the coupling matrix B_{qr} also proceeds in an identical manner. The final result requires that several terms be added to the right hand side of Eq.(26). On the solid side of interface it is necessary to add

$$-i\dot{h}(k^q - k^r)(w_x^{q*}\tau_{zz}^r + \tau_{zz}^{q*}w_x^r) \tag{34}$$

to the terms which already hold for a purely solid medium. On the fluid side of the interface it is necessary to add the term

$$-\dot{h}\left(-\frac{\partial t^{q*}}{\partial z}\frac{1}{\rho\omega^2}\frac{\partial t^r}{\partial z} - t^{q*}\left(\frac{1}{\lambda} - \frac{p^2}{\rho\omega^2}\right)t^r + w_x^{q*}\rho\omega^2 w_x^r\right). \tag{35}$$

Finally, inside the fluid layer are the integral terms describing the coupling resulting from the continuous range dependent variations of the water column

$$\int_0^h w_x^{q*}\dot{\rho}\omega^2 w_x^r + t^{q*}\left(\frac{1}{\lambda} - \frac{p^2}{\rho\omega^2}\right)t^r + \frac{\partial t^{q*}}{\partial z}\frac{\dot{1}}{\rho\omega^2}\frac{\partial t^r}{\partial z}dz. \tag{36}$$

These additional terms are multiplied by the global term:

$$\frac{1}{(k^q - k^r)}exp\left(i\int_0^x (k^q - k^r)d\zeta\right) \tag{37}$$

A final note is that the integral in Eq.(26), describing coupling due to continuous range dependence of the density and elastic moduli in the bottom, now extends from the ocean bottom $h(x)$ to infinity. It would also be a simple matter to incorporate an additional solid layer at the surface to model the mode coupling in an ice covered sea.

C. Energy Conservation

As indicated by Eq.(21), the local modes are normalized to carry the same energy flux across planes $x =$ constant. We can obtain a statement of energy conservation for a lossless range dependent medium by substituting the local mode representation of the displacement-stress field Eq.(22) into the scalar product Eq.(19) and setting the derivative with respect to x equal to 0, yielding

$$\begin{aligned}
\frac{\partial}{\partial x}\langle \mathbf{u}^q, \mathbf{u}^r \rangle &= \frac{\partial}{\partial x} \sum_q |c_q(x)|^2 \\
&= \sum_q \left(\frac{\partial}{\partial x} c_q(x) c_q^*(x) + c_q(x) \frac{\partial}{\partial x} c_q^*(x) \right) \\
&= \sum_{q,r} \left(B_{qr} + B_{rq}^* \right) c_r(x) c_q^*(x) \\
&= 0. \qquad (38)
\end{aligned}$$

We have used the fact that

$$\sum_q c_q(x) \left(\sum_r B_{qr}^* c_r^*(x) \right) = \sum_r c_r(x) \left(\sum_q B_{rq}^* c_q^*(x) \right), \qquad (39)$$

since the mode indices $\{q, r\}$ are summed over the same set.

The only way for Eq.(38) to be satisfied generally is for the coupling matrix to be anti-Hermitian, i.e.

$$B_{qr} = -B_{rq}^*. \qquad (40)$$

This anti-Hermiticity is a necessary consequence of energy conservation in a lossless medium. It can be seen by inspection that the coupling matrix B_{qr} given by Eq.(26) is anti-Hermitian. The additional coupling terms for the fluid layer and interface, equations (34), (35) and (36) are also anti-Hermitian.

An obvious consequence of Eq.(40) is that

$$Re(B_{rr}) = 0. \tag{41}$$

If we insist that the phase of the local modes be continuous from point to point in the medium then we should also choose

$$Im(B_{rr}) = 0. \tag{42}$$

D. Evolution of Range Dependent Mode Amplitudes

The theory we have summarized up to this point only describes the local mode-mode interactions caused by the range dependence of the medium. In order to synthesize a complete signal propagating in a strongly range dependent medium for which the adiabatic approximation is not valid, we must solve the evolution equation Eq.(23) for the mode amplitudes. A complete solution for a strongly range dependent medium must account for the interaction of both forward(+) and backward(−) propagating modes. The evolution of both the forward and backward propagating components of a signal is described by

$$\frac{\partial}{\partial x}\begin{pmatrix}\mathbf{c}^{+}(x)\\ \mathbf{c}^{-}(x)\end{pmatrix} = \begin{pmatrix}\mathbf{B}^{++}(x) & \mathbf{B}^{+-}(x)\\ \mathbf{B}^{-+}(x) & \mathbf{B}^{--}(x)\end{pmatrix}\begin{pmatrix}\mathbf{c}^{+}(x)\\ \mathbf{c}^{-}(x)\end{pmatrix} \tag{43}$$

where $\mathbf{c}^{+}$ and $\mathbf{c}^{-}$ are n-dimensional vectors whose elements are the amplitude coefficients of n forward and backward propagating modes. The $n \times n$ matrices $\mathbf{B}^{++}$, $\mathbf{B}^{+-}$, $\mathbf{B}^{-+}$ and $\mathbf{B}^{--}$ describe forward-to-forward, forward-to-backward, backward-to-forward and backward-to-backward coupling, respectively.

If we specify a geometry defined by a heterogeneous region sandwiched between two homogeneous (plane layered) regions, and assume a signal incident from the left onto the heterogeneous region, Eq.(43) defines a $2n \times 2n$ boundary value problem for the amplitudes of

the forward and backward propagating modes. A schematic of a range dependent medium is shown in Figure 1. The boundary values are $\mathbf{c}^+(x_L)$, known at $x = x_L$ on the left side of the heterogeneous region, and $\mathbf{c}^-(x_R) = 0$ on the right side of the heterogeneous region at $x = x_R$. Stable numerical solution of the two point boundary value problem defined by Eq.(43) and the two boundary values is problematic due to presence of growing and decaying mode amplitudes within the heterogeneous region. This situation is exacerbated if the heterogeneous region is extended in range. Kennett[27] reformulated the two point boundary value problem as an initial value problem for the reflection and transmission properties of the heterogeneous region using invariant imbedding techniques.

The procedure is to define a transmission matrix $\mathbf{T}(x_R, x_L)$ that connects the $\mathbf{c}^+(x_L)$ on the left side of the heterogeneous region with the $\mathbf{c}^+(x_R)$ on the right side of the heterogeneous region

$$\mathbf{c}^+(x_R) = \mathbf{T}(x_R, x_L)\mathbf{c}^+(x_L). \tag{44}$$

In addition a reflection matrix $\mathbf{R}(x_R, x_L)$ is defined that relates the backscattered component $\mathbf{c}^-(x_L)$ from the heterogeneous region to the forward propagating component $\mathbf{c}^+(x_L)$ at the left side of the heterogeneous region

$$\mathbf{c}^-(x_L) = \mathbf{R}(x_R, x_L)\mathbf{c}^+(x_L). \tag{45}$$

We differentiate Eqs.(44) and (45) with respect to x_L

$$\frac{\partial}{\partial x_L}\mathbf{c}^+(x_R) = \frac{\partial}{\partial x_L}\mathbf{T}\mathbf{c}^+(x_L) + \mathbf{T}\frac{\partial}{\partial x_L}\mathbf{c}^+(x_L) = 0 \tag{46}$$

$$\frac{\partial}{\partial x_L}\mathbf{c}^-(x_L) = \frac{\partial}{\partial x_L}\mathbf{R}\mathbf{c}^+(x_L) + \mathbf{R}\frac{\partial}{\partial x_L}\mathbf{c}^+(x_L) \tag{47}$$

The derivatives of the amplitude vectors are replaced with their expressions from Eq.(43), and $\mathbf{c}^-(x_L)$ can be removed from the equation using Eq.(45). After removing a common factor of $\mathbf{c}^+(x_R)$, we arrive at coupled matrix Ricatti equations for the reflection and transmission matrices for the heterogeneous region

$$\frac{\partial}{\partial x_L}\mathbf{R} = \mathbf{B}^{-+} + \mathbf{B}^{--}\mathbf{R} - \mathbf{R}\mathbf{B}^{++} - \mathbf{R}\mathbf{B}^{+-}\mathbf{R} \tag{48}$$

and

$$\frac{\partial}{\partial x_L}\mathbf{T} = -\mathbf{T}\mathbf{B}^{++} - \mathbf{T}\mathbf{B}^{+-}\mathbf{T}. \tag{49}$$

The integration begins to the right of the heterogeneous region at x_R and proceeds to the left with the initial conditions

$$\mathbf{T}(x_R, x_R) = \mathbf{I} \quad \text{and} \quad \mathbf{R}(x_R, x_R) = \mathbf{0}. \tag{50}$$

$\mathbf{I}$ is the $n \times n$ identity matrix.

The stability of the coupled set of first order equations (48) and (49) is significantly improved over that of the original two point boundary value problem. If backscattering from the heterogeneous region can be neglected, then we are left with only the equation

$$\frac{\partial}{\partial x_L}\mathbf{T} = -\mathbf{T}\mathbf{B}^{++}. \tag{51}$$

Eq.(51) describes a level of approximation between that implied by the adiabatic approximation Eq.(25) and the complete solution described by Eq.(48) and Eq.(49) with the initial conditions Eq.(50).

This concludes our summary of the complete 2-D coupled mode theory. This theory incorporates an exact treatment of the boundary conditions at sloping interfaces as well as being able to handle smooth gradients in density and all elastic moduli. We have applied

the theory to a transversely isotropic medium with a vertical symmetry axis. The theory is, however, valid for general anisotropic media at the expense of additional algebraic and numerical complexity. In a general anisotropic medium the horizontally polarized shear waves do not decouple from the compressional waves and vertically polarized shear waves. Consequently, the motion is represented by a single 6×6 system of equations rather than the separate 4×4(P-SV) and 2×2(SH) systems required for isotropic and transversely isotropic media.

Numerical Results

In this section we numerically investigate the effects of transverse isotropy on the modal dispersion, eigenfunctions and the coupling matrix B_{qr} for a realistic shallow water model. We are in the process of coding the matrix Ricatti equations (48) and (49), and will present results from the integration of those equations in a future paper.

Elastic anisotropy is a well established geoacoustic property of marine sediments[3–6]. The most common form of anisotropy observed in marine sediments is transverse isotropy(TI) with a vertical axis of symmetry. In a TI medium propagation in all azimuthal directions lying in planes including the symmetry axis is equivalent. In TI marine sediments with vertical symmetry axes, horizontally polarized and horizontally propagating waves travel faster than vertically propagating and vertically polarized waves. The primary mechanisms for transverse isotropy in marine sediments are: 1. aligned cracks and pores; 2. recrystallization of anisotropic minerals; and 3. compositional layering on a very fine scale. If isotropy is erroneously assumed sound speed gradients are underestimated, sediment layer thicknesses can be overestimated and shear velocity can be overestimated[8]. The most likely mechanism for the observed transverse isotropy of sediments at the water-bottom interface is compositional layering. Recrystallization of anisotropic minerals may be important for deeper lying sediments, but to depths of at least $1km$ beneath the ocean bottom, compositional layering

is believed to be the dominant mechanism[6].

We have examined the effect of transverse isotropy on the mode structure and mode coupling of a bottom interacting signal propagating in shallow water. The code used to generate the eigenvalues, eigenfunctions and kinetic energy integrals for a plane layered fluid-elastic TI medium was DISPER80[28]. The computations were carried out on a Sun SPARCstation LX, mostly in double precision. At the highest frequencies it was necessary to employ quadruple precision for the first few eigenvalues and eigenfunctions. Our shallow water model was taken from Berge et al.[29] who analyzed multi-component seismic data from an experiment conducted in $21m$ of water about $10km$ east of New Jersey.

The data analyzed by Berge et al.[29] were collected in 1986 by Roundout Associates Inc. and Woods Hole Oceanographic Institution. Initial attempts at modeling the data assuming isotropy of the bottom material were not considered adequate[29], and led to further modeling efforts employing an anisotropic reflectivity program. The resulting TI models estimated by Berge et al.[29] provided a good fit to their data and constrained four of the five elastic parameters necessary to describe a TI medium. They did not have enough resolution to determine the compressional wave anisotropy and assumed $c_{11} = c_{33}$ ($A = C$ in Love's[26] notation).

In order to specify the anisotropy, we introduce the dimensionless parameters

$$\eta' \quad = \quad 1 - \eta \quad = \quad 1 - \frac{F}{A - 2L}, \tag{52}$$

and

$$\phi' \quad = \quad 1 - \phi \quad = \quad 1 - \frac{C}{A}, \tag{53}$$

Values of

$$\eta' = 0 \quad \text{and} \quad \phi' = 0 \tag{54}$$

indicate isotropy. The departure from isotropy increases as η' and/or ϕ' change from 0.

The dynamic stability of a transversely isotropic medium requires that certain conditions be imposed on the elastic moduli (Auld[21], Postma[30], Backus[31]):

$$\begin{aligned} A \geq N \geq 0, \\ C \geq 0, \\ L \geq 0, \\ F^2 \leq C(A-N). \end{aligned} \tag{55}$$

The most plausible physical mechanism for TI with a vertical symmetry axis within the interfacial sediments is fine compostional layering. This mechanism imposes the additional constraints

$$\begin{aligned} C \geq F, \\ C \geq \frac{4}{3}L, \\ N \geq L \end{aligned} \tag{56}$$

(Backus[31]). A final independent inequality constraint for compositionally layered TI media is

$$(A-L)(C-L) \geq (F+L)^2 \tag{57}$$

(Postma[30], Berryman[32]).

The model, shown in Figure 2, consists of a $21m$ thick isovelocity water layer over $12.5m$ of TI sediments, followed by $12.5m$ of isotropic sediments with a steep gradient in both

compressional and shear speeds. The density of the sediments is taken to be constant at $2100kg/m^3$. The TI layer is characterized by $\eta' = 0.012$ and $\phi' = 0$. The base of the model is an isotropic elastic half-space with a shear speed of $1450m/s$, a compressional speed of $3000m/s$, and a density of $2400kg/m^3$.

We have explicitly focused on the qP-qSV component of propagation in the sediments. The excitation of horizontally polarized shear waves(SH) in the sediments by a propagating acoustic signal in the water requires 3-D heterogeneity or anisotropy of a more general nature than we treat.

Figure 3 illustrates the phase velocity dispersion for the model of Figure 2. The modal phase velocities for the TI model are generally higher than for the corresponding isotropic medium. This was apparently first noted by Stoneley[33], and is a consequence of greater material stiffness sampled by components of wave particle motion parallel to the bedding plane. The difference between the modal phase velocities for the TI and isotropic media increases with increasing frequency. As the frequency increases, the phase velocity of the TI mode can approach the phase velocity of the next higher isotropic mode. This is also evident in the group velocity curves shown in Figure 4.

Despite a relatively small difference in the fundamental mode phase velocity between the TI and isotropic models, the eigenfunctions are substantially different. Because the eigenfunction calculation depends on the inverse of the eigen-phase velocity, small changes in the smallest eigen-phase velocity can have significant effects on the computation of the corresponding eigenfunction. This is also the reason for using quadruple precision at the higher frequencies for the first few modes. DISPER80 directly integrates the equations of motion which become quite stiff at high frequencies. Efficient methods of generating the fluid-elastic modes are important for high frequency applications.

The eigenfunctions for the vertical component of displacement at $10Hz$ and $20Hz$ are shown in Figures 5 and 6, respectively. Although it is not visible on the scale at which the

modes are plotted, all eigenfunctions have been normalized such that the vertical component of displacement is unity at the sea surface. The scale of the other three components of the eigenfunctions is derived from this normalization. This choice of normalization is somewhat arbitrary and merits discussion since the energy integrals and their partial derivatives (Figures 7(a-c), 8 and 9) are computed using this normalization. The purpose of Figures 5 and 6 is to illustrate the effect of the transverse isotropy on the eigenfunctions. The eigenfunctions could have been normalized so the isotropic and corresponding TI eigenfunctions had equal energy, or so that they had equal peak amplitudes or equal amplitudes at the water sediment interface. Although we have not computed the Green's function for the medium, which forces the selection of an explicit source location, we are assuming that the source and receiver are located within the water column or at, or slightly beneath, the water-sediment interface. Our chosen normalization emphasizes differences near the water-sediment interface. Modes with a given surface amplitude will have very different amplitudes at the water-sediment interface depending on whether the bottom is isotropic or anisotropic. Had we chosen a normalization such that the peak vertical displacement was unity, corresponding amplitudes in the water column would be quite different. Our normalization yields eigenfunctions with different energies in isotropic and corresponding TI media, but because they have the same vertical displacement at the surface, the differences in energy reflect the different amount of energy input into the medium required to produce the same surface displacement. The contribution of an individual mode to the Green's function for the medium is directly proportional to the mode amplitude at the chosen source depth. Therefore our choice of normalization will emphasize differences resulting from shallow sources.

Comparison of eigenfunctions between isotropic and anisotropic media is somewhat problematic in any case, since there is no simple method of establishing correspondence between the two. Because of the constraint relations among the elastic parameters listed earlier, it is not possible to arbitrarily perturb one elastic modulus without corresponding perturbations

to other moduli. Arbitrary perturbations to elastic moduli can destroy the symmetry of the elastic stiffness tensor and produce unphysical results in calculations.

In the 10-20Hz frequency range the water depth is approximately $\lambda/4$, which means that the bottom is near an acoustic radiation maximum. A propagating acoustic signal in this band will thus be dominated by the fundamental mode guided along the water sediment interface. For frequencies greater than approximately $7Hz$ for the isotropic medium and $11Hz$ for the TI medium, the phase velocity of the fundamental mode is less than the sediment shear speed at the water sediment interface. The fundamental mode above the threshhold frequency is therefore a Stoneley wave. At frequencies lower than the threshhold, the mode is more properly termed a pseudo-Rayleigh wave.

It can be clearly seen from Figures 5 and 6 that the fundamental carries the most energy in this frequency band. The generally smaller peak amplitude of the low order TI modes relative to the isotropic modes is a consequence of the greater material stiffness for horizontally propagating waves in the TI medium. As the mode number increases for a given frequency, the eigenfunctions persist to greater depths in the structure. The fractional amount of modal energy within the $10m$ thick TI layer decreases, so the influence of the anisotropy on the eigenfunctions also decreases. Also, as the frequency of a given mode increases the component of the mode in the bottom becomes more and more like pure SV. It can be seen from Figure 3 that as the frequency of a mode increases, its phase velocity approaches the shear speed at the sediment interface. The compressional speed is much higher than the sediment shear speed, and so the compressional component of the mode is evanescent, leading to the almost pure SV behavior of the modes at high frequency.

Figures 7(a-c) shows the relative mode kinetic energy as a function of frequency for the first three modes. The kinetic energy E_m of the m^{th} mode is

$$E_m = \omega^2 \int_0^\infty \rho \left(w_x^m w_x^{m*} + w_z^m w_z^{m*} \right) dz. \tag{58}$$

The energy in the Stoneley wave peaks at around $11Hz$. Berge et al.[29] have plotted amplitude vs. frequency for the unfiltered vertical component of the data from one of their profiles. (Their Figure 7, and here reproduced as our Figure 7d.) The main features of the lower frequency part of their spectrum are well represented by our kinetic energy plots. The Stoneley wave peak at about $11Hz$ in Berge et al.'s[29] data appears to be particularly well modeled by our mode calculations. The low amplitude maxima appearing at $1.8Hz$ and $5Hz$ in Figures 7a and 7b, respectively, and the kink at approximately $8Hz$ in Figure 7c occur at the knees of the modal dispersion curves(Figure 3). These knees occur at the frequency at which a mode becomes trapped in the sediment layer. The mode dies out very rapidly in the underlying halfspace, and the phase velocity drops abruptly towards the sediment shear wave speed. The peak at $4.5Hz$ in Figure 7c corresponds to the very sharp minimum in the group velocity curve for $m = 2$(Figure 4). At this point the group velocity rises to meet the phase velocity at the cutoff value. The comparisons between our model calculations and Berge et al.'s[29] data is not direct as we have not attempted to correct our modeling results in such a way that would permit absolute amplitude comparisons with their experimental data.

Berge et al.[29] reported that their synthetic seismograms were quite sensitive to small perturbations in the elastic modulus F (c_{13} in the abbreviated subscript notation). The modulus F affects the the propagation of qP and qSV at angles intermediate between the horizontal and vertical in a TI medium with a vertical symmetry axis. In an attempt to illuminate the sensitivity of a bottom interacting acoustic signal to sediment anisotropy, we computed partial derivatives of mode energy with respect to a parameter η'.

The dimensionless partial derivative of the mode energy is defined by

$$\frac{1}{E_m}\frac{\partial E_m}{\partial \eta'} = \frac{1}{E_m}\frac{\partial F}{\partial \eta'}\frac{\partial E_m}{\partial F} = -\frac{A-2L}{E_m}\frac{\partial E_m}{\partial F}. \quad (59)$$

In Figure 8 the partial derivative Eq(59) is plotted versus $\eta' \times 100$ for the first three modes at $10Hz$. Since a value of $\eta' = 0$ indicates isotropy, the anisotropy increases with increasing values of the abcissa. The magnitudes of the derivatives for the first three modes are relatively large and negative. The negativity of the derivatives indicates that the energy of the modes will decrease with increasing anisotropy as measured by increasing η'. Again, we mention that the vertical component of the eigenfunctions are all normalized to have unit displacement at the surface.

Physically Figure 8 illustrates that, as the elastic modulus F departs from its isotropic value, less energy is required to produce the same vertical surface displacement. (In an isotropic medium, F corresponds to the Lamé parameter λ.) Our perturbation reduces F from its isotropic value, thereby reducing the stiffness of the medium somewhat at angles intermediate between the horizontal and vertical. The effect is the same as reducing the spring constant of a mass-spring system. Less energy is required to produce a given displacement of the mass suspended from a weaker spring. The relatively large dimensionless magnitudes of the derivatives are a measure of the sensitivity of the eigenfunction, and hence the acoustic signal, to anisotropic medium perturbations. Since the fundamental has the largest derivative, it will also be most sensitive to changes in F. Although not shown in Figure 8, at $10Hz$ for the mode $m = 3$, $\partial E_m/\partial \eta'$ is a very weak function of η' and nearly zero. The mode $m = 3$ persists to greater depth into the bottom, and has relatively more energy both in the water column and the underlying halfspace.

We also found for this model that a 2.4% change in η' could produce a 15% change in the phase velocity of the Stoneley wave mode. Over the range of η' from 0 to 0.024, the phase velocity of the fundamental increases from $145.57m/s$ to $169.67m/s$.

The frequency sensitivity of the mode energy for a single value of the anisotropy parameter $\eta' = 0.012$ is illustrated in Figure 9 by a plot of $\partial E_m/\partial \eta'$ versus frequency. The main thing to notice is, that over the $4Hz$ to $20Hz$ frequency range depicted, the magnitude of the derivative is increasing. A shallow water signal with a strongly excited Stoneley wave will become more sensitive to the anisotropy with increasing frequency. Of course as the frequency increases still further, the excitation of the Stoneley wave will drop off, and the influence of the anisotropy on that part of the signal will also decrease.

We have not computed the corresponding partial derivatives with respect to ϕ', which controls the P wave anisotropy, while holding $\eta' = 0$. This combination of anisotropy parameters violates the condition expressed by Eq.(57), while the converse, i.e. $\phi' = 0$ and $\eta' > 0$ does not. We have, however, computed an example that shows the effect of both $\eta' > 0$ and $\phi' > 0$. As previously mentioned, Berge et al.[29] did not investigate the effects of P-wave anisotropy because their profiles were not long enough to resolve it. The length of their long profile was about $200m$. The P-wave anisotropy could be important for longer propagation paths, since values as high as 40% have been reported in shale[34], although 8% to 14% is probably more typical of marine sediments[3].

Figure 10 is a plot of the vertical displacement component of the fundamental eigenfunction for the isotropic case $\eta' = 0$ and $\phi' = 0$ (solid line), and for the two transversely isotropic cases corresponding to $\eta' = 0.012$ and $\phi' = 0$ (dashed line), and $\eta' = 0.012$ and $\phi' = 0.012$ (dotted line). A value of $\eta' = 0.012$ corresponds to Berge et al.'s[29] long profile model (their Table 1). The vertical components of the eigenfunctions are all normalized to have unit displacement at the surface. The amplitude of the fundamental for the case $\eta' = 0.012$ and $\phi' = 0.012$ lies between the the amplitude for the isotropic case and for the case $\eta' = 0.012$ and $\phi' = 0$. The inclusion of this very modest amount of P-wave anisotropy draws the appearance of the fundamental back towards isotropy. It may be possible to increase the P-wave anisotropy enough so that there is essentially no detectable difference between the

shapes of the isotropic and anisotropic eigenfunctions, but, in reality the P-wave anisotropy near the water-sediment interface is likely to be even smaller than the value used for our calculations[8]. The phase velocity of the fundamental for the case $\eta' = 0.012$ and $\phi' = 0$ is $159.83 m/s$, which is actually slightly higher than the horizontally propagating qSV speed $(158.26 m/s)$.

Our ultimate goal is to improve our ability to model and predict shallow water acoustic signal propagation in a range dependent medium. We have computed the coupling matrix B_{qr} (Eq. 26) including the fluid-solid boundary interaction terms described in Eq.(34) and Eq.(35) for the isotropic model ($\eta' = 0$ and $\phi' = 0$) equivalent to Berge et al.'s model (Fig. 11a,b); for the TI model of Berge et al.[29] ($\eta' = 0.012$ and $\phi' = 0$) (Fig. 11c,d); and for a model ($\eta' = 0.012$ and $\phi' = 0.012$) incorporating the weak P-wave anisotropy (Fig. 11e,f). The calculations were done at two frequencies $10 Hz$ and $20 Hz$.

Berge et al.'s[29] TI model is a range independent model. What we have computed is the coupling matrix for a model with the same local vertical structure as Berge et al.[29] The absolute values of the coupling matrix $|B_{qr}|$ in Figure 11 represent the effects of the geometric medium properties only. The layer boundary slopes, $\dot{h}_n = dh_n/dx$, have been set equal to 1. All material parameter horizontal gradients such as $\dot{\rho}$ have been set equal to 0. The absolute values of the elements of all six coupling matrices depicted in Figure 11 have been normalized by dividing all elements by the largest matrix element of the entire set so comparisons can be made between frequencies and between the isotropic and both TI media.

As the frequency increases, the shallow water structure can support a greater number of modes, so there are more modes to participate in the coupling. There is a preferred mode pair for which the strongest coupling occurs in Berge et al.'s[29] model. At 10 Hz this is mode pair $\{1, 2\}$ (Fig. 11c), and at 20 Hz the strongest interaction occurs for pair $\{4, 5\}$ (Fig. 11d). Coupling strength decreases away from the diagonal and also away from the preferred mode pair. The coupling of the preferred pair is stronger in the TI medium than in the equivalent

isotropic medium. This latter effect illustrates the most striking difference between the TI and isotropic media, and is a qualitative indicator of the difficulties that may be encountered by ignoring sediment anisotropy when attempting to model range dependent shallow water acoustic propagation. Away from the diagonal, other mode pairs participate nearly equally in the coupling process. This indicates that a careful examination of the coupling matrix is necessary before deciding on a truncated mode set to employ when synthesizing complete propagating signals in a range dependent medium. Use of too small a mode set will alias the coupling, and affect the amplitude and phase of a synthesized signal, but also, it may occur that coupling is confined to a small number of model configurations leading to more efficiency in calculations.

We have also computed the coupling matrix for a TI medium containing weak P-wave anisotropy in addition to the S-wave anisotropy of Berge et al.'s[29] model (Fig. 11e,f). The addition of weak P-wave anisotropy to the model actually makes the medium appear more isotropic for the case shown. It is, however, important to remember that Figure 11 represents just a local snapshot of coupling interactions. To get a complete picture, the actual range dependent structure of the medium must be imposed and Eqs.(48) and (49) for the reflection from and transmission through the heterogeneous region must be solved. Because of the almost order of magnitude difference between the shear and compressional wavelengths at the water-sediment interface, the effects of the shear wave anisotropy will accumulate much faster for a strongly bottom interacting shallow water acoustic signal.

E.Summary and Conclusions

We have summarized a coupled mode theory for fluid-elastic media that is formulated as a coupled set of first order equations, and accounts exactly for the inhomogeneous boundary condition due to range dependent interface irregularities[17]. We have applied this theory to

a realistic shallow water model derived from experimental data. A particular feature of this work is the inclusion of transversely isotropic bottom sediments.

Our modeling results show that there can be significant qualitative and quantitative differences between the eigenvalues and modes in shallow water models with an isotropic and a tranversely isotropic bottom. These differences are also reflected in the mode coupling induced by range dependence. The Stoneley wave at the water sediment interface is particularly sensitive to the transverse isotropy of the sediments. Conversion to Stoneley waves has been shown to be an important loss mechanism by Hawker[35]. In light of the sensitivity of the Stoneley waves to the transverse isotropy of the bottom, and the apparent ease with which they can be excited by bottom roughness[7], some care should be taken regarding interpretations of strongly bottom interacting acoustic signals derived from models that assume isotropic sediment properties.

Acknowledgements

This research was supported by the Office of Naval Research Contracts N00014-90-J-1369, N00014-94-1-0036 and the Space and Naval Warfare Office PMW-183. We thank Blackwell Scientific Publications Ltd., the publisher of Geophysical Journal International, for permission to use Figure 7d.

References

[1]E.L. Hamilton,"Geoacoustic modeling of the sea floor," J. Acoust. Soc. Am. **68**, 1313-1340 (1980).

[2]J.Ewing, J.A. Carter, G.H. Sutton, and N. Barstow, "Shallow water sediment properties derived from high-frequency shear and interface waves," J. Geophys. Res. **97**, 4739-4762 (1992).

[3]R.T. Bachman, "Acoustic anisotropy in marine sediments and sedimentary rocks," J. Geophys. Res. **84**, 7661-7663 (1979).

[4]R.T. Bachman, "Elastic anisotropy in marine sedimentary rocks," J. Geophys. Res. **88**, 539-545 (1983).

[5]D.W. Oakley and P.J. Vidmar, "Acoustic reflection from transversely isotropic consolidated sediments," J. Acoust. Soc. Am. **73**, 513-519 (1983).

[6]R.L. Carlson, C.H. Schaftenaar, and R.P. Moore, "Causes of compressional wave anisotropy in carbonate-bearing deep sea sediments," Geophysics **49**, 525-532 (1984).

[7]W.A. Kuperman and H. Schmidt, "Self-consistent perturbation approach to rough surface scattering in stratified elastic media," J. Acoust. Soc. Am. **86**, 1511-1522 (1989).

[8]Fryer, G.J. and D.J. Miller, "Effects and consequences of transverse isotropy in the seafloor," in *Ocean Seismo-Acoustics; Low frequency Underwater Acoustics*, edited by T. Akal and J.M. Berkson (Plenum, New York, 1986), pp. 589-597.

[9]A.D. Pierce, "Extension of the method of normal modes to sound propagation in an almost-stratified medium," J. Acoust. Soc. Am. **37**, 19-27 (1965).

[10]D.M. Milder, "Ray and wave invariants for SOFAR channel propagation," J. Acoust. Soc. Am. **46**, 1259-1263 (1969).

[11]F.S. Chwieroth, A. Nagl, H. Überall, and G.L. Zarur, "Mode coupling in a sound channel with range-dependent parabolic velocity profile," J. Acoust. Soc. Am. **64**, 1105-

1112 (1978).

[12]S.R. Rutherford and K.E. Hawker, "Consistent coupled mode theory of sound propagation for a class of non-separable problems," J. Acoust. Soc. Am. **70**, 554-564 (1981).

[13]S.T. McDaniel, "Mode coupling due to interaction with the seabed," J. Acoust. Soc. Am. **72**, 916-923 (1982).

[14]M. Hall, "The effects of variations in sound speed on coupling coefficients between acoustic normal modes in shallow water over a sloping bottom," J. Acoust. Soc. Am. **79**, 332-337 (1986).

[15]R.I. Odom, "Experimental and Theoretical Investigations of Ocean-Earth Acoustic Coupling," Ph.D. Dissertation, Geophysics, University of Washington, Seattle, 1980.

[16]R.I. Odom, "A coupled mode examination of irregular waveguides including the continuum spectrum," Geophys. J.R. Astr. Soc. **86**, 425-453 (1986).

[17]V. Maupin, "Surface waves across 2-D structures: a method based on coupled local modes," Geophys. J. **93**, 173-185 (1988).

[18]J.A. Fawcett, "A derivation of the differential equations of coupled-mode propagation," J. Acoust. Soc. Am. **92**, 290-295 (1993).

[19]G. Gillette, "Coupled modes in a waveguide with a range-dependent rigid basement," J. Acoust. Soc. Am. **95**, 187-200 (1994).

[20]J.H. Woodhouse, " Surface waves in laterally varying structure," Geophys J. R. Astr. Soc. **37**, 461-490 (1974).

[21]B.A. Auld, *Acoustic Fields and Waves in Solids, 2 Volumes* (Krieger, Malabar, FL, 1990), 2nd ed., Vol. I, pp. 64-86.

[22]R.B. Evans, "A coupled mode solution for acoustic propagation in a waveguide with stepwise depth variations of a penetrable bottom," J. Acoust. Soc. Am. **74**, 188-195 (1983).

[23]R. Burridge and L. Knopoff, "Body-force equivalents for seismic dislocations, " Bull. Seism. Soc. Am. **54**, 1875-1888 (1964).

[24]A. Nagl, H. Überall, A.J. Haug and G.L. Zarur, "Adiabatic mode theory of underwater sound propagation in a range dependent environment," J. Acoust. Soc. Am. **63**, 739-749 (1978).

[25]V. Maupin, "Modelling of laterally trapped surface waves with application to Rayleigh waves in the Hawaiian swell," Geophys. J. Int. **110**, 553-570 (1992).

[26]A.E.H. Love, *A Treatise on the Mathematical Theory of Elasticity* (Dover, New York, NY, 1944), p. 160.

[27]B.L.N. Kennett, " Guided-wave propagation in laterally varying media. I. Theoretical development," Geophys. J. R. Astr. Soc. **79**, 235-255 (1984).

[28]M. Saito, "DISPER80: A Subroutine Package for the Calculation of Seismic Normal Mode Solutions," in *SEISMOLOGICAL ALGORITHMS: Computational Methods and Computer Programs*, edited by D. Doornbos (Academic Press, San Diego, 1988), Chap. IV.1, pp. 293-319.

[29]P.A. Berge, S. Mallick, G.J. Fryer, N. Barstow, J.A. Carter, G.H. Sutton and J.I. Ewing, "*In situ* measurement of transverse isotropy in shallow-water marine sediments," Geophys. J. Int. **104**, 241-254 (1991).

[30]G.W. Postma, "Wave propagation in a stratified medium," Geophysics **20**, 780-806 (1955).

[31]G.E. Backus, "Long-wave anisotropy produced by horizontal layering," J. Geophys. Res. **67**, 4427-4440 (1962).

[32]J.G. Berryman, "Long-wave anisotropy in transversely isotropic media," Geophysics **44**, 896-917 (1979).

[33]R. Stoneley, "The seismological implications of aeolotropy in continental structure," Monthly Notices Roy. Astron. Soc., Geophys. Suppl. **5**, 222-232 (1949).

[34]L.F. Urhig and F.A. Van Melle, "Velocity anisotropy in stratified media," Geophysics **20**, 774-779 (1955).

[35]K.E. Hawker, "Influence of Stoneley waves on plane-wave reflection coefficients: Characteristics of bottom reflection loss," J. Acoust. Soc. Am. **64**, 548-555 (1978).

Appendix: Elastic Moduli Matrices for a Transversely Isotropic Medium

We list the elastic moduli matrices C_{ij} and Q_{ij} used in the calculation of the coupling matrix B_{qr}, Eq.(26).

$$C_{11}^{-1} = \begin{pmatrix} 1/A & 0 & 0 \\ 0 & 1/N & 0 \\ 0 & 0 & 1/L \end{pmatrix}$$

$$C_{11}^{-1}C_{12} = \begin{pmatrix} 0 & (A-2N)/A & 0 \\ 1 & 0 & 0 \\ 0 & 0 & 0 \end{pmatrix}$$

$$C_{11}^{-1}C_{13} = \begin{pmatrix} 0 & 0 & F/A \\ 0 & 0 & 0 \\ 1 & 0 & 0 \end{pmatrix}.$$

The Q_{ij}, defined as

$$Q_{ij} = C_{ij} - C_{i1}C_{11}^{-1}C_{1j},$$

are:

$$Q_{22} = \begin{pmatrix} 0 & 0 & 0 \\ 0 & 4N(A-N)/A & 0 \\ 0 & 0 & L \end{pmatrix}$$

$$Q_{23} = \begin{pmatrix} 0 & 0 & 0 \\ 0 & 0 & 2NF/A \\ 0 & L & 0 \end{pmatrix}$$

$$Q_{33} = \begin{pmatrix} 0 & 0 & 0 \\ 0 & L & 0 \\ 0 & 0 & (AC-F^2)/A \end{pmatrix}$$

When $A = C = \lambda + 2\mu$, $L = N = \mu$, and $F = \lambda$ the medium is isotropic.

The relationship between the notation of Love[26] and the abbreviated subscript notation for the elastic moduli of a TI medium is

$$A = c_{11}, \quad F = c_{13}, \quad C = c_{33}, \quad L = c_{44}, \quad N = c_{66}.$$

Figure Captions

Figure 1. The figure illustrates the geometry of the range dependent medium modeled by the coupled Ricatti equations Eq.(48) and Eq.(49). The range dependent region (II) is sandwiched between two plane layered (range independent) regions (I) and (III) that need not be the same. The integration of Eq.(48) and Eq.(49) proceeds backwards from the point x_R to the point x_L.

Figure 2. The transversely isotropic shallow water model of Berge et al.[29] (Their **Table1.**). The 12.5m thick sediment layer immediately below the water sediment interface is transversely isotropic. We have terminated their model with an isotropic half-space with a shear speed of $1450m/s$, a compressional wave speed of $3000m/s$ and a density of $2400kg/m^3$.

Figure 3. Phase velocity dispersion curves for the shallow water model of Fig. 2. Note that the phase velocities in the TI medium are generally higher than in the equivalent isotropic medium. As the frequency increases, the phase velocity of a TI mode can approach the phase velocity of the next higher isotropic mode. This is also true of the group velocities plotted in Fig. 4.

Figure 4. Group velocities of the first three modes for the model shown in Figure 2.

Figure 5. The vertical displacement eigenfunctions for the first four modes at 10Hz. Notice that for mode 3, the isotropic and TI vertical displacements are virtually identical, but that the amplitude of the TI displacement in the halfspace is slightly greater than the isotropic displacement. Modes are normalized to have unit vertical displacement at the water surface. At 10Hz, the signal is dominated by the fundamental (Stoneley) mode.

Figure 6. The vertical displacement eigenfunctions for the first four modes at 20Hz. The isotropic and TI modes are distinct. In fact, although not shown here, there are significant differences between the isotropic and TI modes for the first five modes.

Figure 7. Kinetic energy as a function of frequency for the first three modes (a-c). These match quite well the lower frequency part of the spectrum of some shallow water data (d) shown by Berge et al.[29] (Their Figure 7, used by permission of Blackwell Scientific Publications Ltd.) The Stoneley wave peak at about 11 Hz in Berge et al.[29] appears to particularly well modeled by our mode calculations. Note that the frequency ranges of (a-c) and (d) are not the same.

Figure 8. Nondimensional partial derivatives of mode energy with respect to the parameter η'. The negativity of the derivatives indicates that the mode energy for the first three modes decreases upon departure from isotropy.

Figure 9. The partial derivative of the fundamental mode energy with respect to η' evaluated at $\eta' = 0.012$ as a function of frequency. Note that the absolute value of the magnitude of the derivative generally increases over the plotted frequency range. Indicating an increasing sensitivity with frequency of the fundamental mode to the anisotropy. A value of $\eta' = 0.012$ corresponds to the best fitting TI model for the long profile data of Berge et al.'s[29] (their Table 1).

Figure 10. Vertical displacement component of the fundamental eigenfunction for the isotropic medium(solid line, phase velocity= $145.57m/s$), and for TI media characterized by $\eta' = 0.012$(dashed line, phase velocity= $159.83m/s$) and $\eta' = \phi' = 0.012$(dotted line, phase velocity = $153.73m/s$). They have all been normalized to unit displacement at $z = 0$. The frequency is $10Hz$. The speed of horizontally propagating qSV waves ($\sqrt{L/\rho}$) at the water sediment interface is $158.26m/s$.

Figure 11. The absolute value of the elements of the coupling matrix B_{qr} Eq.(26) for the model in Fig. 2. Layer boundary slopes $\dot{h}$ have been set equal to 1, and all horizontal material parameter gradients such as $\dot{\rho}$ have been set to 0. This emphasizes the effects of geometric (boundary) heterogeneities. The absolute values of the elements of the six coupling matrices have been normalized by the largest matrix element of the entire set so comparisons

can be made between frequencies and between isotropic and TI media. The array elements have been normalized so that dark red is unit coupling and dark blue is zero coupling. The diagonals have been purposely left blank to reflect our choice of phase for the local modes (Eq.(42).

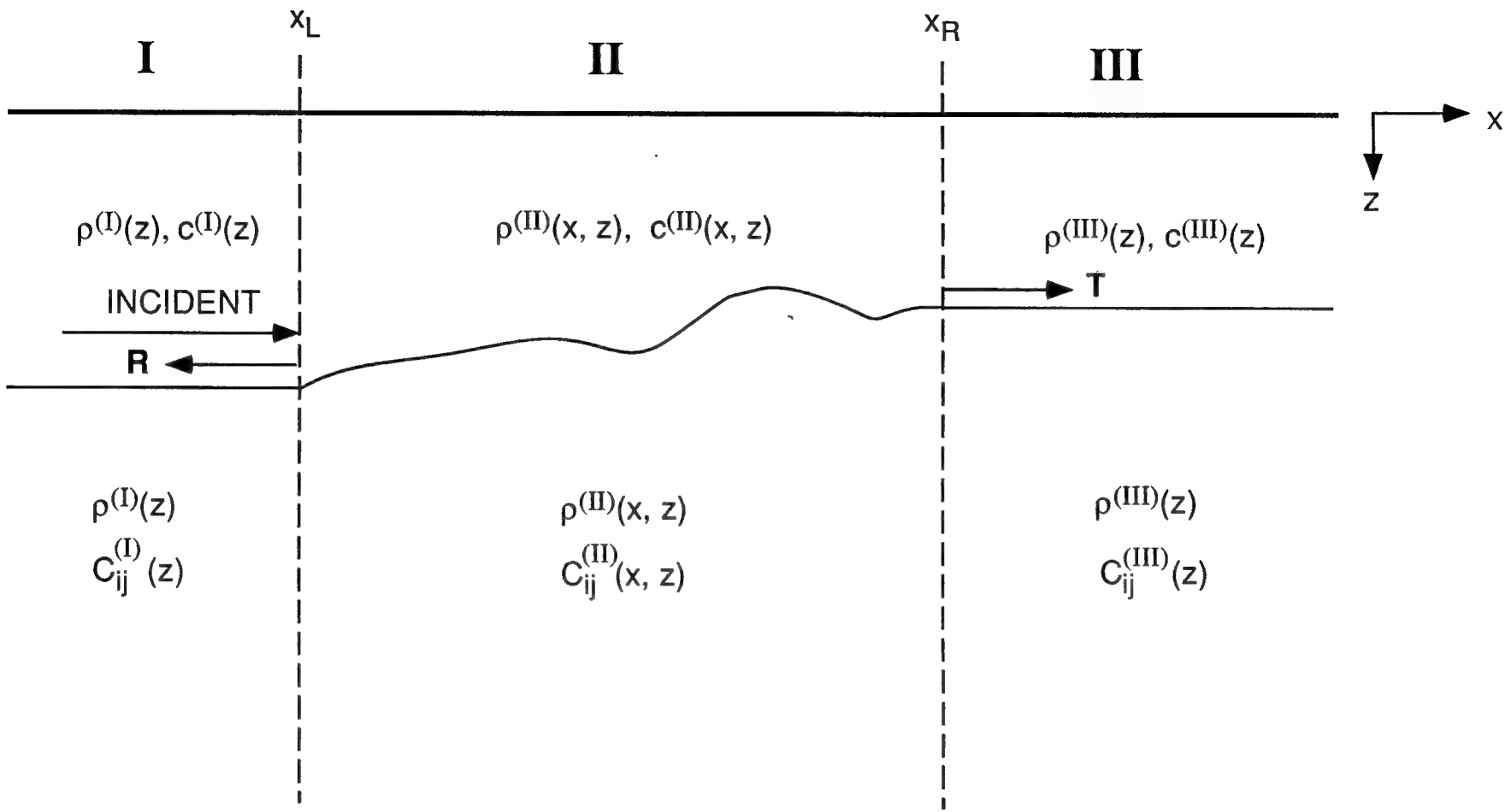
I
II
III
x_L
x_R
x
z
$\rho^{(I)}(z), c^{(I)}(z)$
$\rho^{(II)}(x, z), c^{(II)}(x, z)$
$\rho^{(III)}(z), c^{(III)}(z)$
INCIDENT
R
T
$\rho^{(I)}(z)$
$C_{ij}^{(I)}(z)$
$\rho^{(II)}(x, z)$
$C_{ij}^{(II)}(x, z)$
$\rho^{(III)}(z)$
$C_{ij}^{(III)}(z)$

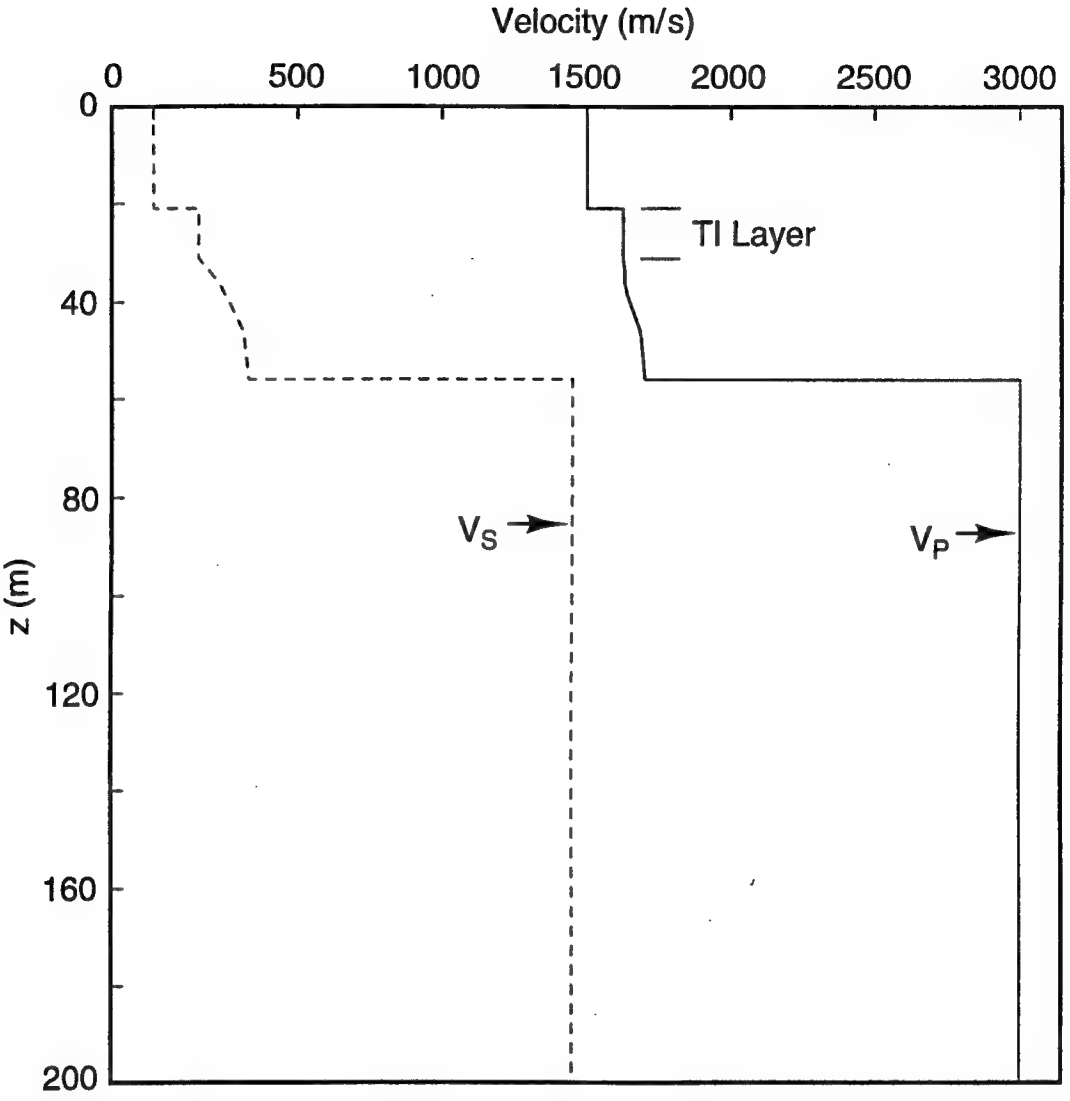
Velocity (m/s)
0
500
1000
1500
2000
2500
3000
0
40
80
120
160
200
z (m)
TI Layer
V_S
V_P

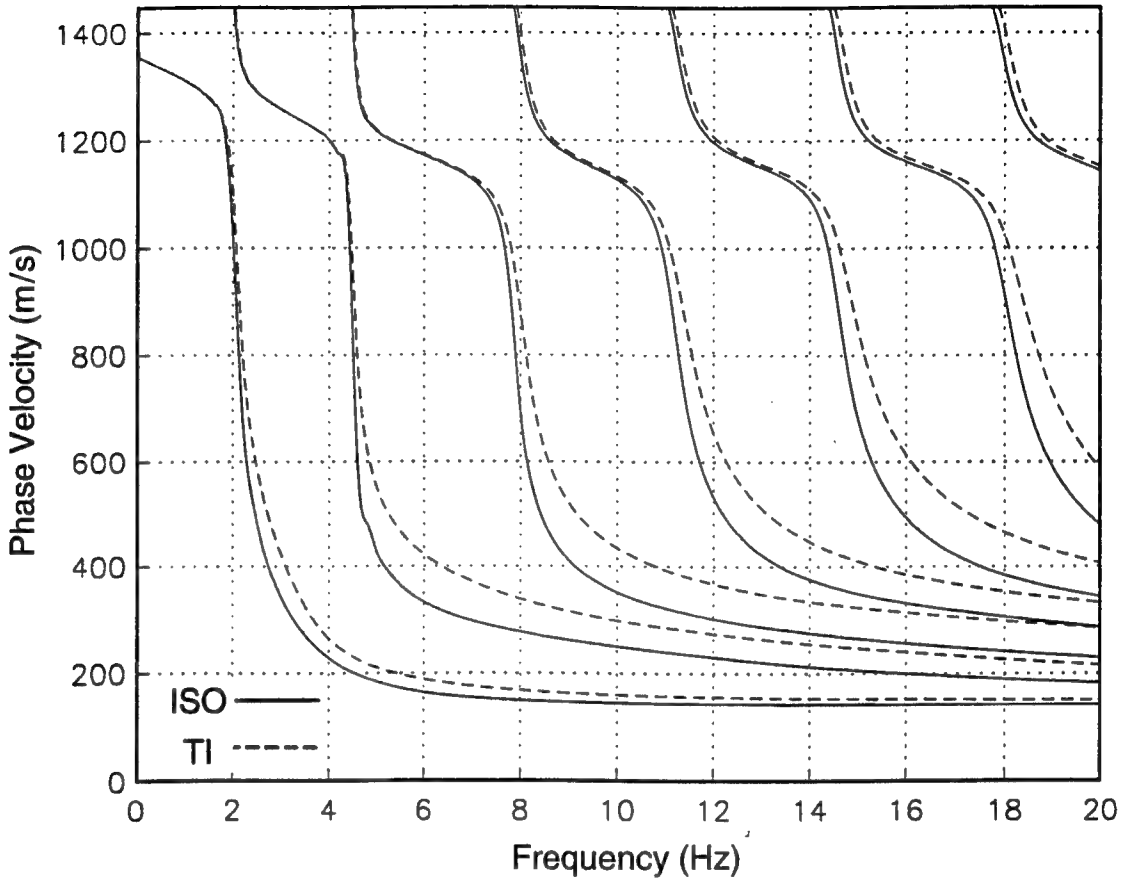
Phase Velocity (m/s)
1400
1200
1000
800
600
400
200
0
0
2
4
6
8
10
12
14
16
18
20
Frequency (Hz)
ISO
TI

Fig 3

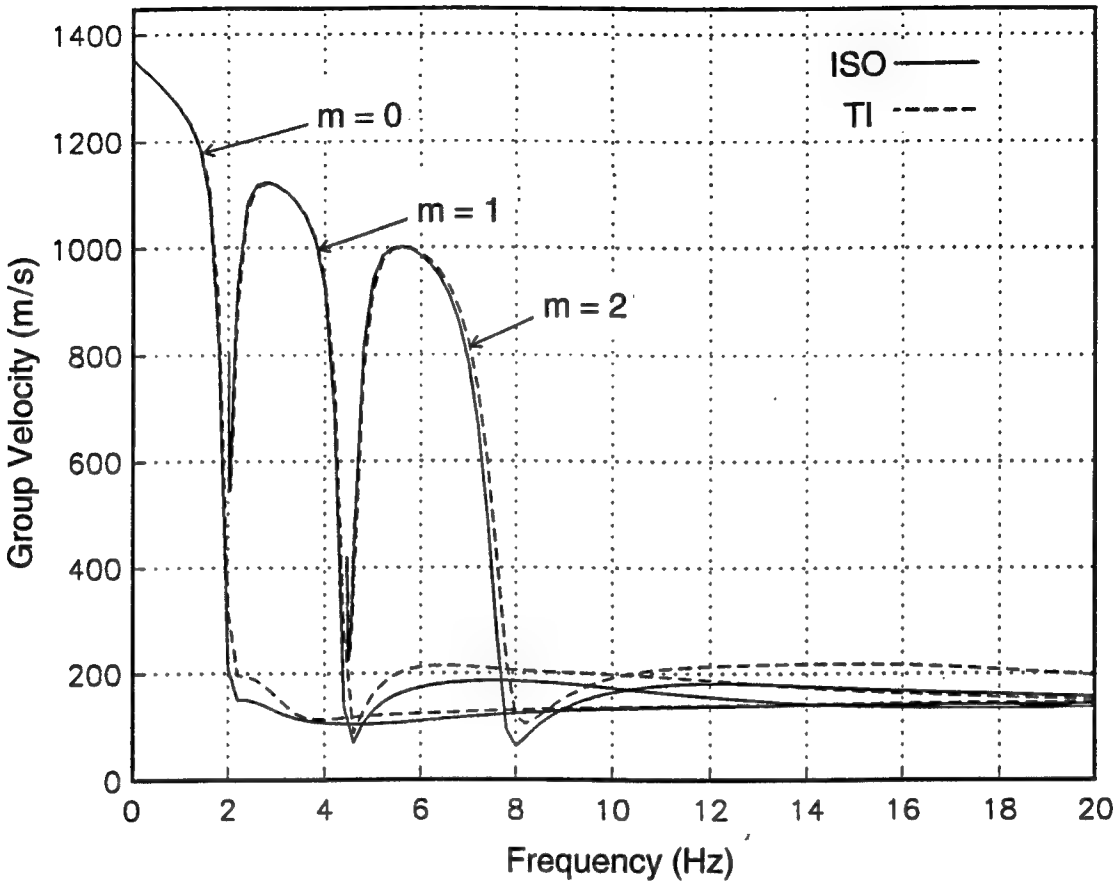
ISO
TI
m = 0
m = 1
m = 2
Group Velocity (m/s)
Frequency (Hz)
0
200
400
600
800
1000
1200
1400
0
2
4
6
8
10
12
14
16
18
20

Fig. 4

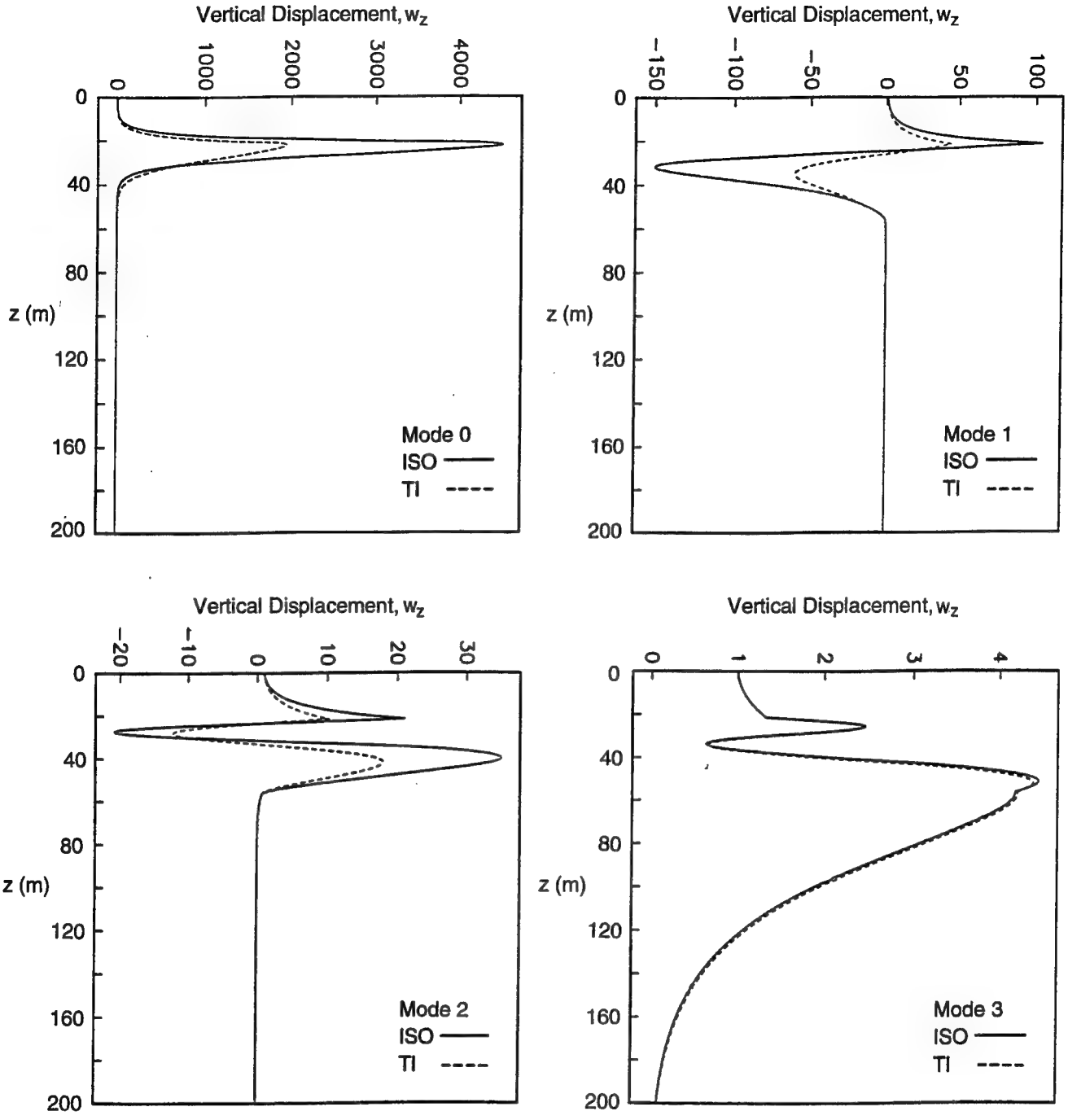
Vertical Displacement, w_z
0
1000
2000
3000
4000
z (m)
0
40
80
120
160
200
Mode 0
ISO
TI
Vertical Displacement, w_z
−150
−100
−50
0
50
100
Mode 1
ISO
TI
Vertical Displacement, w_z
−20
−10
0
10
20
30
Mode 2
ISO
TI
Vertical Displacement, w_z
0
1
2
3
4
Mode 3
ISO
TI

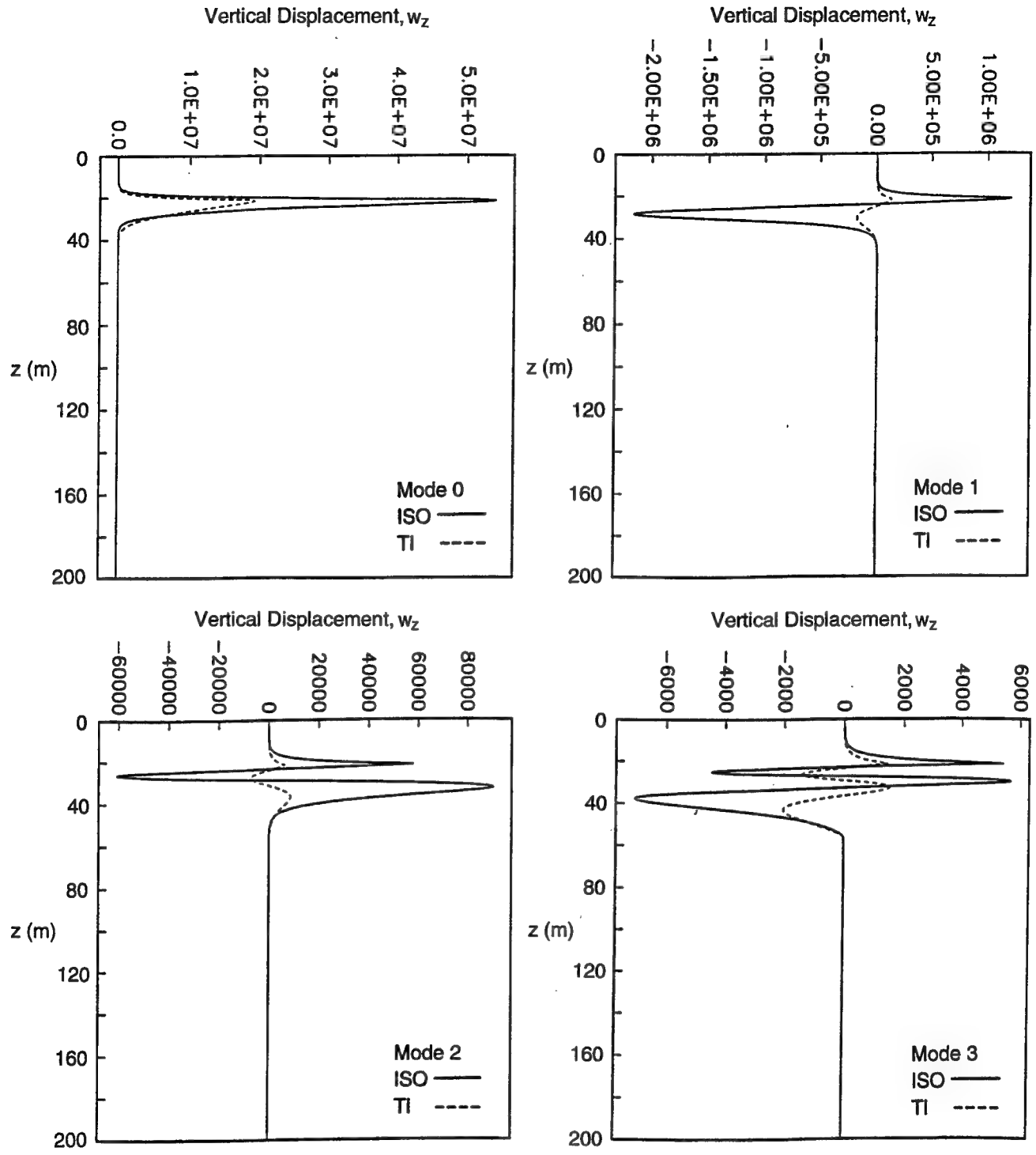
Vertical Displacement, w_z
0.0
1.0E+07
2.0E+07
3.0E+07
4.0E+07
5.0E+07
0
40
80
120
160
200
z (m)
Mode 0
ISO
TI
Vertical Displacement, w_z
−2.00E+06
−1.50E+06
−1.00E+06
−5.00E+05
0.00
5.00E+05
1.00E+06
0
40
80
120
160
200
z (m)
Mode 1
ISO
TI
Vertical Displacement, w_z
−60000
−40000
−20000
0
20000
40000
60000
80000
0
40
80
120
160
200
z (m)
Mode 2
ISO
TI
Vertical Displacement, w_z
−6000
−4000
−2000
0
2000
4000
6000
0
40
80
120
160
200
z (m)
Mode 3
ISO
TI

Fig 6

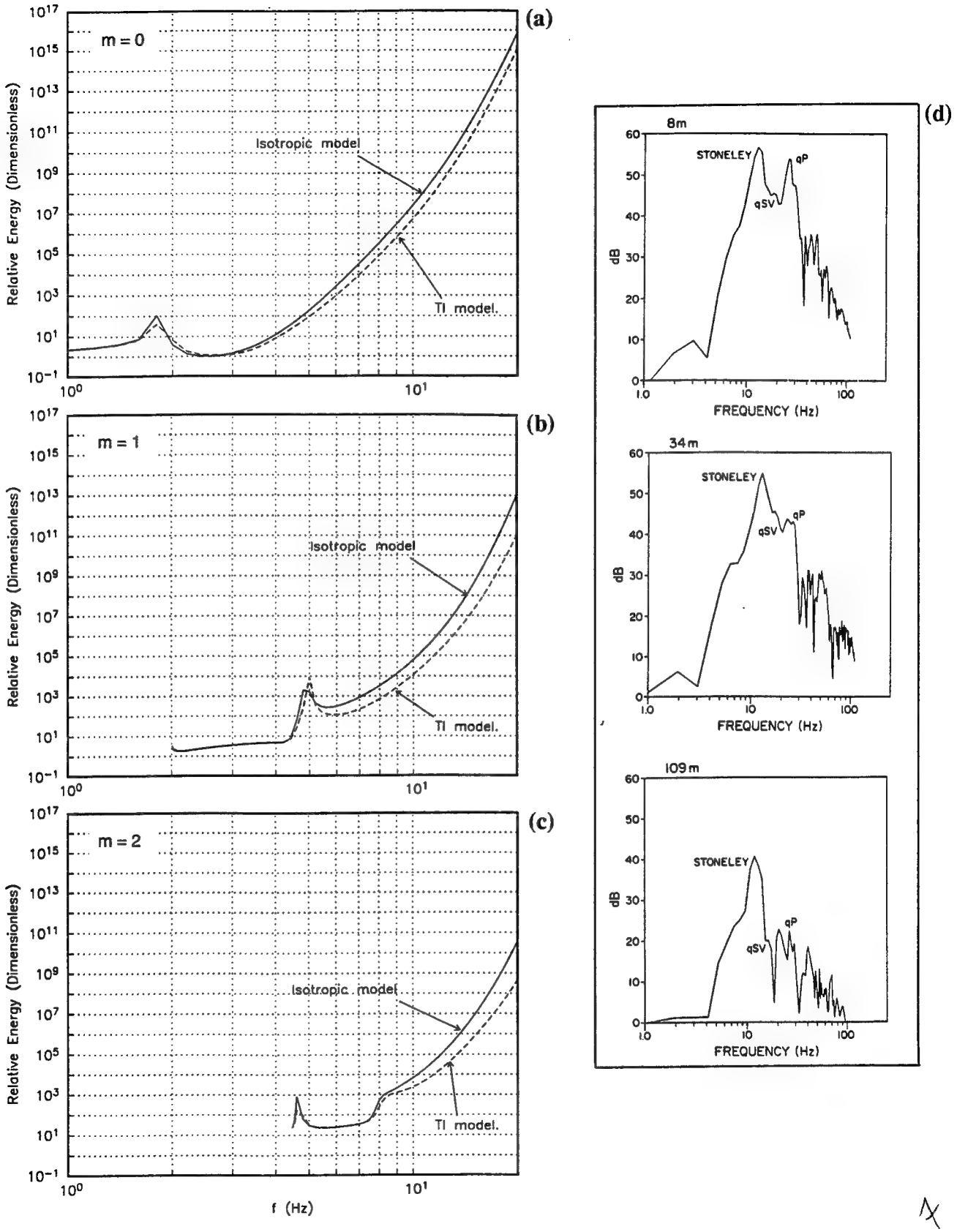
(a)
m = 0
Isotropic model
TI model.
(b)
m = 1
Isotropic model
TI model.
(c)
m = 2
Isotropic model
TI model.
Relative Energy (Dimensionless)
f (Hz)
(d)
8m
34m
109m
STONELEY
qP
qSV
dB
FREQUENCY (Hz)

Fig 7

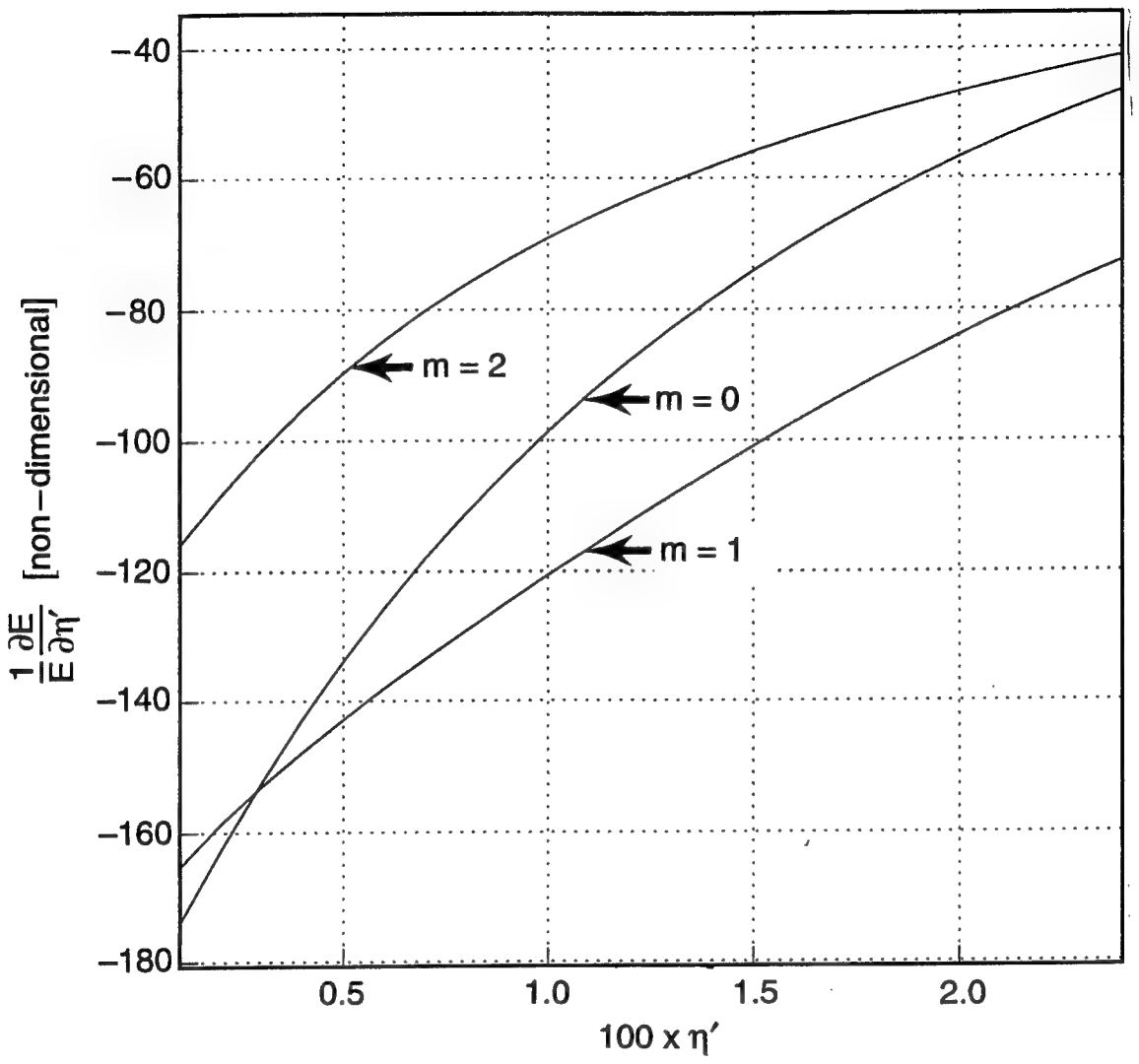
−40
−60
−80
−100
−120
−140
−160
−180
0.5
1.0
1.5
2.0
100 x η′
$\frac{1}{E}\frac{\partial E}{\partial \eta'}$ [non−dimensional]
m = 2
m = 0
m = 1

Fig. 8

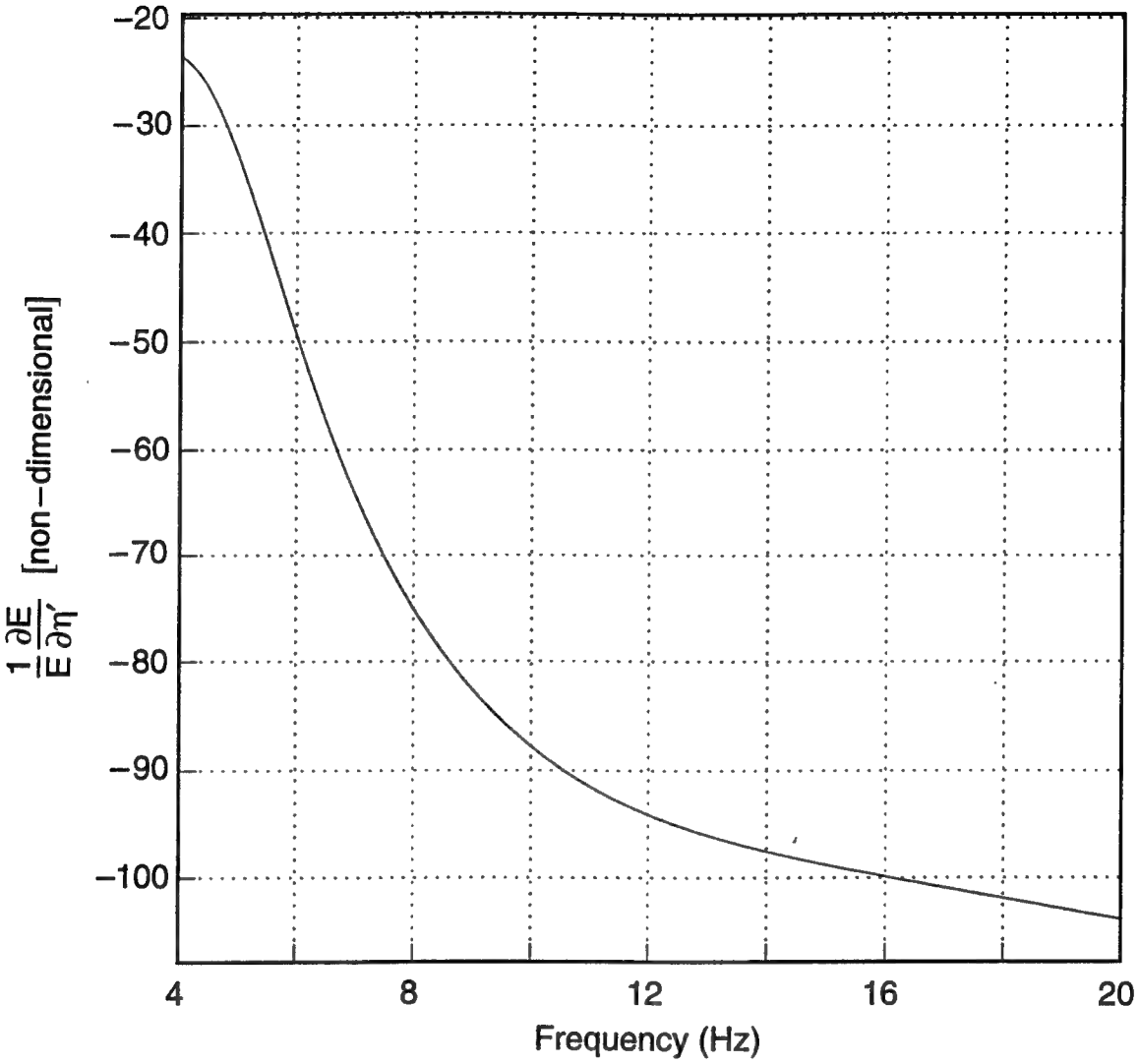
−20
−30
−40
−50
−60
−70
−80
−90
−100
4
8
12
16
20
Frequency (Hz)
$\frac{1}{E}\frac{\partial E}{\partial \eta'}$ [non−dimensional]

a
Fig

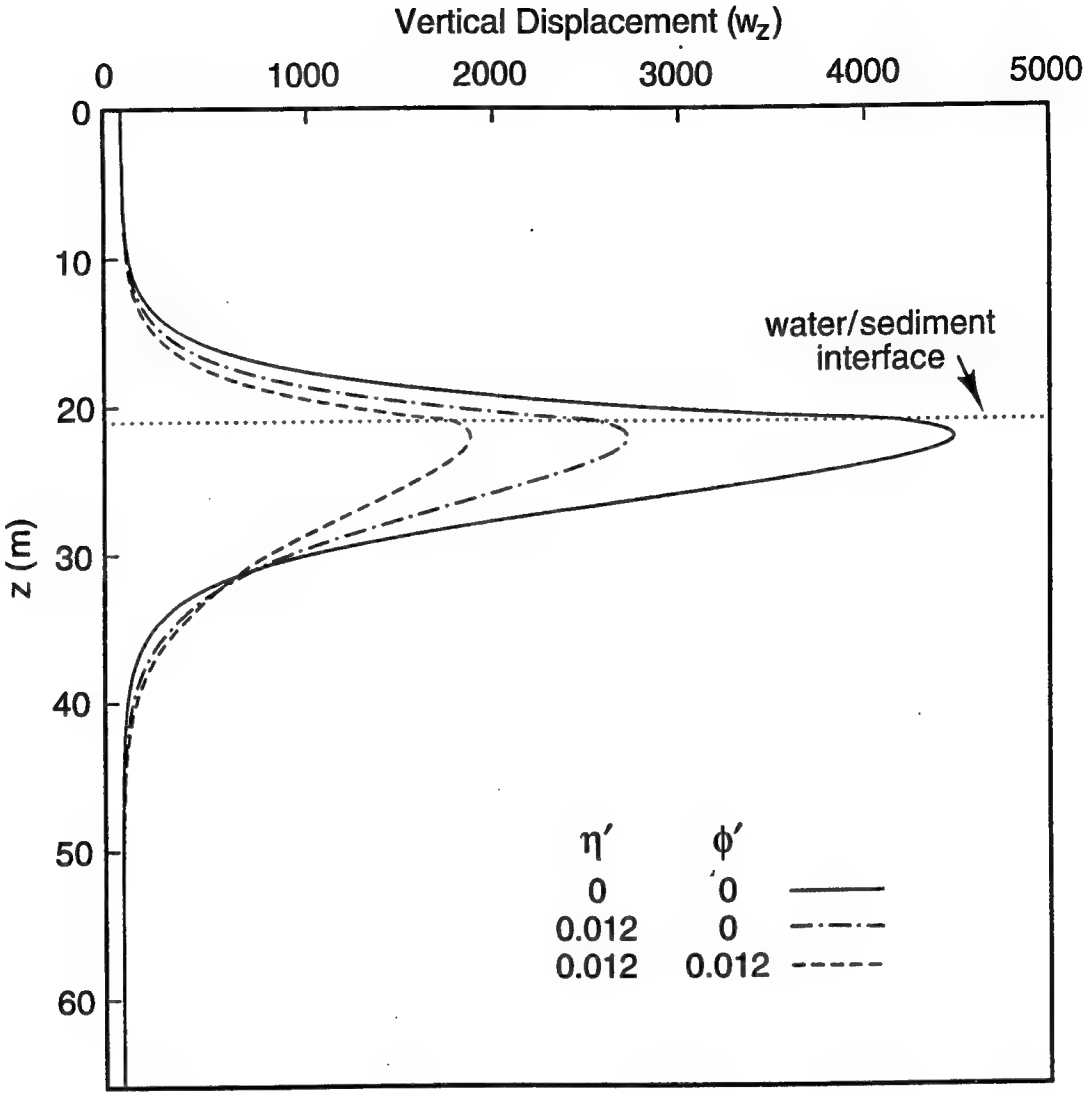
Vertical Displacement (w_z)
0
1000
2000
3000
4000
5000
0
10
20
30
40
50
60
z (m)
water/sediment interface
η′
ϕ′
0
0
0.012
0
0.012
0.012

Fig. 10

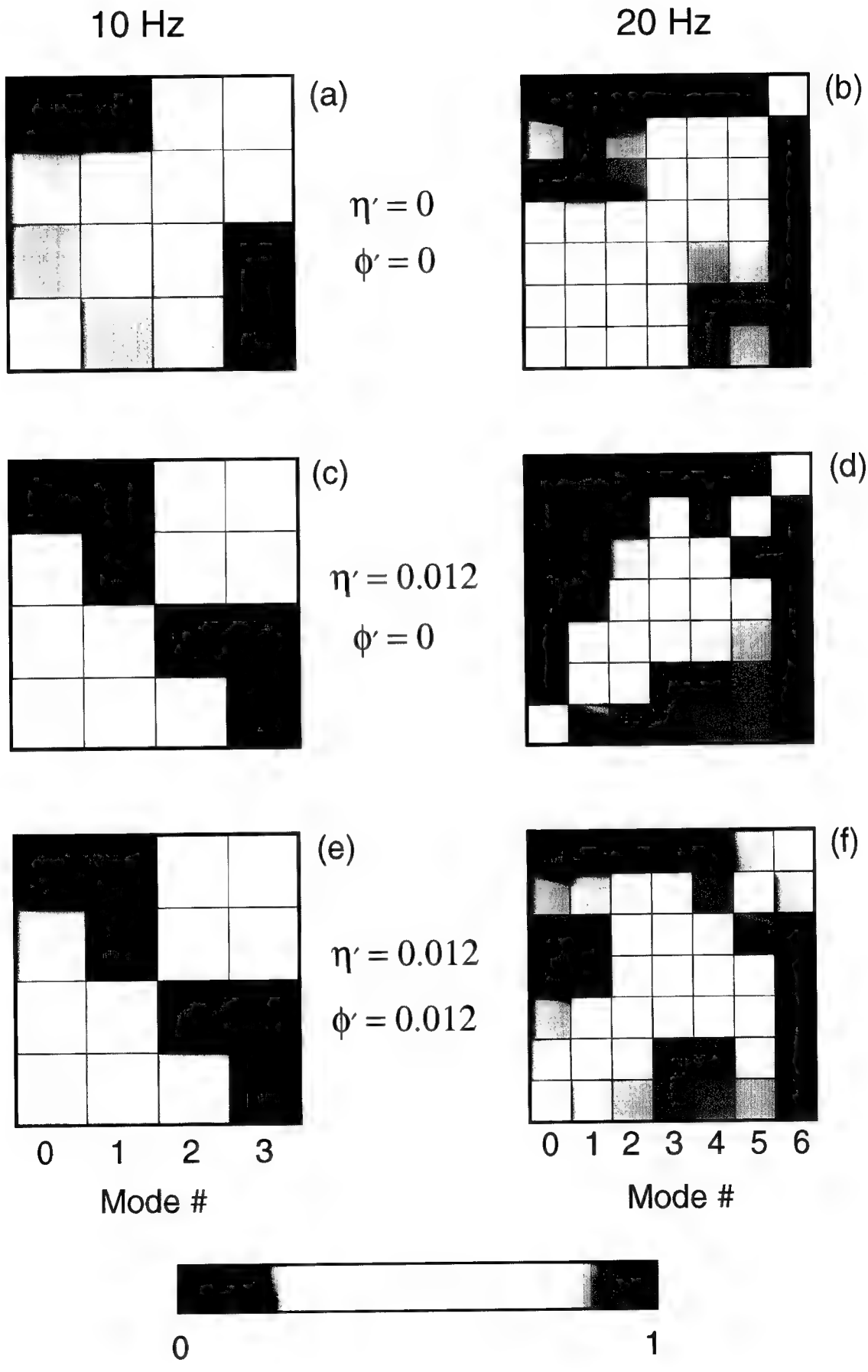
10 Hz
20 Hz
(a)
(b)
$\eta' = 0$
$\phi' = 0$
(c)
(d)
$\eta' = 0.012$
$\phi' = 0$
(e)
(f)
$\eta' = 0.012$
$\phi' = 0.012$
0 1 2 3
Mode #
0 1 2 3 4 5 6
Mode #
0
1

Spectral diffusion of elastic wave energy

Robert I. Odom and James A. Mercer

Applied Physics Laboratory

University of Washington

1013 NE 40th Street

Seattle, WA 98105

USA

Submitted to Geophysical Journal International

SUMMARY

Elastic wave propagation in strongly scattering media is described by an energy diffusion equation derived directly from the coupled mode equations. These equations provide an exact representation of the displacement-stress field in 2-D heterogeneous media. By allowing the mode spacing to approach zero, the continuum limit of the modal representation of the elastic wavefield is derived. The final expressions require neither the location of closely spaced eigenvalues nor construction of eigenfunctions. All assumptions and approximations must be explicitly stated and implemented in the derivation of the energy diffusion equation. Strong forward scattering is assumed to dominate. The energy diffusivity is a range and frequency dependent functional of the displacement-stress field components and the horizontal gradients of the medium properties including anisotropy. The diffusivity functional is derived directly from the continuum limit of the mode coupling matrix; it is essentially the spatial autospectrum of the coupling matrix weighted by a function describing the density of modes in spectral space. The approach presented in this paper is in contrast to energy diffusion equations derived from radiative transfer theory in which the the diffusivity must be specified separately in an *ad hoc* manner. The diffusivity functional is computable from any wavenumber integration type code that generates, or can be modified to generate, the depth dependent Green's function for a fluid-elastic medium. Although our energy diffusion equation is range dependent, the computation of the diffusivity depends on local medium properties and field values for a plane layered medium. An additional difference between the diffusion equation of this paper and previously published treatments of elastic energy diffusion is that this paper describes energy diffusion in spectral space, e.g. slowness, as a function of range rather than diffusion in physical space as a function of time.

Key words: coupled local modes, energy diffusion, forward scattering, random media, surface waves.

1 INTRODUCTION

Deterministic models are quite successful for modeling the large and intermediate scales of the structure of the earth. The scales of the deterministic problems are defined by inhomogeneities that are large compared to the wavelength of the seismic or acoustic waves. Initially coherent signals tend to retain their coherence over long propagation distances. When the scale of the inhomogeneities is small compared to the wavelength and are randomly distributed, propagating signals are scattered, and become progressively more incoherent as the range from the source increases.

A number of different approaches have been used to model the scattered wavefield depending on the spatial density and properties of the inhomogeneities in the medium. For widely spaced scatterers, the Born approximation, which does not conserve energy, has been used (Wu and Aki 1985a, Snieder 1986). (The definition of "widely spaced" depends on the mean free path, correlation length, and frequency.) For more closely spaced scatterers various multiple scattering formulations have been proposed (e.g. Wu 1985). Phase screen methods have recently been extended to to the P-SV problem (Fisk & McCartor 1991; Fisk, Charette & McCartor 1992). Phase screen methods have also been combined with the Born approximation to model propagation in media with large numbers of imbedded scatterers (Wu 1994). When the scatterer density is so high that all the energy is scattered, phase information is lost and the field is completely incoherent. In this case radiative transfer theory has been applied to derive an energy diffusion equation. The application of radiative transfer theory to seismic problems was first suggested by Wesley (1965), followed by applications to lunar seismograms by Dainty *et al.* (1974), Dainty and Toksöz (1977), Nakamura (1977) and Oberst (1985). Wu (1985) applied radiative transfer theory to study the coda of local earthquakes. In this paper a new method of modeling energy diffusion in strongly scattering media is described. Although we also arrive at a diffusion equation for the elastic energy,

there are a number of differences between the theory presented in this paper and radiative transfer theory. The main differences are summarized in the next three paragraphs.

Radiative transfer theory is a phenomenological theory that starts with an assumed seismic energy density defined as an integral over all space. Substitution of the energy density into a continuity equation derived from energy conservation leads to a diffusion equation describing the redistribution of energy in space and time. The derivation of the diffusion equation depends on a number of implicit as well as explicit assumptions. The diffusivity, which should contain details about the physical properties of the scatterers, is specified in an *ad hoc* manner based on plausibility arguments about the size, distribution and scattering strength of the imbedded inhomogeneities and partitioning of energy between . The model that is either explicitly or implicitly assumed is generally of a random distribution of scatterers imbedded in a homogeneous background. An advantage of radiative transfer theory over the theory presented in this paper is that it is inherently a three dimensional theory, and backscattering is automatically accounted for.

We derive an energy diffusion equation directly from the exact coupled mode representation of the solution to the elastic wave equation. This makes the theory of this paper a physically based theory rather than a phenomenological theory. The assumptions and approximations must be explicitly stated in order to extract a diffusion equation from the starting coupled mode representation. One key assumption is that backscattering is neglected. Because the scattered energy is assumed to be forward scattered, our theory is most appropriately applied to scattering from velocity heterogeneities which affect the wavefield phase. Backscattering produced by strong impedance heterogeneities is not modeled by this approach (Wu & Aki 1985a). Whereas previously published treatments of elastic energy diffusion model energy diffusion in space and time, we model energy diffusion in spectral space as a function of propagation range.

As shown below, the diffusivity arises from the continuum limit of the mode coupling

matrix, and it contains all the interaction physics and medium properties so that the background medium and imbedded inhomogeneities are treated on an equal footing. The coupling between the compressional and shear waves is automatically included. The frequency dependence of the diffusion process and correlations of the horizontal gradients of the elastic moduli, density and layer boundaries appear explicitly in the diffusivity. All the required quantities are readily computable.

The coupled mode equations for an elastic medium are reviewed in Section 2. From the coupled mode equations, a coupled energy equation is derived, and then reduced to an energy diffusion equation. The derivation is 2-D and valid for general anisotropic fluid-elastic media.

In Section 3. an approximate solution of the coupled mode equations in the forward scattering limit is described, to be used later in the derivation of the coupled energy equations.

In Section 4. energy conservation in a range dependent medium, and its relation to the anti-Hermiticity of the mode coupling matrix is discussed.

In Section 5. the coupled energy equations are derived from the coupled mode equations. The phase information carried by individual modes is relinquished for a description of the evolution of the average energy of a mode propagating in a range dependent medium.

In Section 6. the energy diffusion equation is derived from the coupled energy equations. The energy diffusivity functional is shown to be essentially the spatial autospectrum of the coupling matrix weighted by the local density of modes in the random medium. The diffusion equation can be transformed to a Schrödinger equation, which may offer some advantages for numerical implementation. However, the form of the potential is somewhat complicated.

In Section 7. an initial condition and physically reasonable choices for two boundary conditions are discussed. The boundary conditions must be satisfied in spectral space, rather than physical space.

In Section 8. solutions to two elementary spectral diffusion problems are presented and

discussed. The solutions are represented as Fourier series of the energy spectrum in p_x – space. The homogenization of the spectrum with increasing propagation distance through the scattering medium is readily apparent upon examining the elementary solutions. The final two sections include a brief discussion of attenuation and our conclusions.

2 THE COUPLED MODE EQUATIONS

Seismic wave modeling in fluid-elastic media with variations in 2 and 3 dimensions is complicated by the non-separability of the spatial independent variables of the equations of motion. However the normal mode representation can still be used with modification. A local separation of the equations of motion is effected by representing the wavefield components as the superposition of a set of range varying basis functions, the "local modes," with range dependent amplitude and phase. The elements of this local basis are the modes of the plane layered structure that corresponds locally to the range dependent structure in terms of material properties and layer thicknesses. The derivation uses the coupled mode theory of Maupin (1988), which is an extension to elastic media of the acoustic coupled mode theory of Odom (1981, 1986). Kennett's (1984) theory uses the modes of a reference structure; this theory will suffer in accuracy if the boundaries of the reference structure diverge from those of the actual structure. Bostock (1992) has extended Kennett's reference structure method to 3-D, and Tromp (1994) has made a partial extension of the local mode method to 3-D.

Maupin's (1988) theory is summarized here, since it forms the basis of the derivation of the energy diffusion equation. The theory is valid for solid-solid as well as fluid-solid and fluid-fluid boundaries. It is also valid for general anisotropic media.

A Cartesian coordinate system is used where the x axis (or x_1 axis) is the direction of the range dependence, and z-axis (or x_3 axis) is the depth axis and taken to be positive downward. The medium is assumed to be 2-D, laterally heterogeneous and composed of n

layers. The layers may have non-planar interfaces $h_n(x)$, where the free surface is designated $h_0(x)$. Material properties, the density $\rho(x,z)$ and stiffnesses $c_{ijkl}(x,z)$, may vary smoothly in both the x and z directions.

For the elastic moduli, the matrix notation of Woodhouse (1974) is employed such that

$$(C_{ij})_{kl} = c_{kilj}. \tag{1}$$

The equations of motion for an elastic medium are

$$\rho \frac{\partial^2 \mathbf{w}}{\partial t^2} = \nabla_i \mathbf{t}_i + \mathbf{f}, \tag{2}$$

where ρ is the density, $\mathbf{f}$ is an external force and the traction vector $\mathbf{t}$ is defined by

$$\mathbf{t}_i = C_{ij} \left(\frac{\partial \mathbf{w}}{\partial x_j} \right). \tag{3}$$

The displacement is Fourier transformed with respect to t, as

$$\mathbf{w}(x,z,\omega) = \int_{-\infty}^{+\infty} \mathbf{w}(x,z,t) \exp(-i\omega t) dt. \tag{4}$$

The same symbol $\mathbf{w}$ is used for both the transformed and untransformed displacement. The equations of motion for a 2-D heterogeneous medium, rewritten to isolate the derivatives with respect to x, the propagation direction, on the left hand side are

$$\frac{\partial \mathbf{u}}{\partial x} = A\mathbf{u} + \sum_n \dot{h}_n \begin{Bmatrix} 0 \\ [\mathbf{t}]_n \delta(z - h_n(x)) \end{Bmatrix} \tag{5}$$

with the interface conditions

$$[\mathbf{t}_3]_n = [\mathbf{w}]_n = 0. \tag{6}$$

The square brackets $[\cdot]_n$ indicate the jump of the enclosed quantity across the n^{th} interface, taken from bottom to top. The free surface condition for an elastic (fluid) medium is that the traction (pressure) vanishes and a radiation condition is assumed as $z \to \infty$. The

4-component vector $\mathbf{u} = (\mathbf{w}, \mathbf{t})^{\mathbf{T}}$ where $\mathbf{w} = (w_x, w_z)$ and $\mathbf{t} = \mathbf{t}_1 = (\tau_{xx},\ \tau_{xz})$, and the differential operator A is

$$A = \begin{pmatrix} -C_{11}^{-1}C_{13}\frac{\partial}{\partial z} & C_{11}^{-1} \\ -\rho\omega^2 - \frac{\partial}{\partial z}\left(Q_{33}\frac{\partial}{\partial z}\right) & -\frac{\partial}{\partial z}C_{31}C_{11}^{-1} \end{pmatrix}, \tag{7}$$

and $Q_{ij} = C_{ij} - C_{i1}C_{11}^{-1}C_{1j}$.

Continuity of the traction normal to a sloping interface in the laterally heterogeneous medium is equivalent to a jump in traction along the vertical axis. Maupin & Kennett (1987) transformed the traction discontinuity in the interface boundary conditions to a localized volume force located along the interface by applying a representation theorem for elastic media (Burridge & Knopoff 1964). The resulting equivalent volume force becomes the source term on the right hand side of eq. (5), and the interface boundary conditions become homogeneous.

Eqs. (5) and (6) are a first order system of inhomogeneous equations with homogeneous boundary conditions that formally describes the evolution of the stress-displacement fields along the propagation direction. The solution to this system is expressed in terms of coupled local modes. These local modes, defined below, are the eigenfunctions of the range independent medium that locally share the same depth dependence as the range dependent medium. Hence locally at some point x_0 in range, the density $\rho(x_0, z)$ and the elastic moduli $C_{ij}(x_0, z)$ are functions of depth only so that

$$\rho(x_0, z) = \rho(z) \quad \text{and} \quad C_{ij}(x_0, z) = C_{ij}(z). \tag{8}$$

The wave propagation problem for a 2-dimensional range dependent medium can be solved exactly in terms of the local eigenfunctions of the range independent medium. These eigenfunctions are the homogeneous solutions to eq. (5) with homogeneous boundary con-

ditions eq. (6). The boundary conditions at the irregular interfaces are satisfied exactly by including the effective source term in eq. (5). No approximations have been made (Maupin 1988).

Local solutions of the equations of motion (eq. (5)) which depend parametrically on x are represented as

$$\mathbf{u}(x_o, z)\exp(-ik^r(x_o)x) \tag{9}$$

satisfying

$$-ik^r(x_o)\mathbf{u}^r(x_o, z) = A\mathbf{u}^r(x_o, z) \tag{10}$$

and the homogeneous boundary conditions $[\mathbf{w}^r]_n = 0$ and $[\mathbf{t}_3^r]_n = 0$ across interfaces. The horizontal wave number in the x-direction is k^r, and taken to be real.

Maupin (1988) introduced the following Hermitian scalar product between two local eigenfunctions of index r and q.

$$(\mathbf{u}^q, \mathbf{u}^r) = i\int_0^\infty (\mathbf{w}^{q*}\mathbf{t}^r - \mathbf{t}^{q*}\mathbf{w}^r)dz \tag{11}$$

where $*$ indicates complex conjugation. The local modes are orthogonal with respect to this scalar product at fixed values of frequency and p. The local modes are normalized such that

$$(\mathbf{u}^q, \mathbf{u}^r) = \delta_{rq}. \tag{12}$$

Thus, they all carry the same energy flux across planes $x =$ constant.

The coupled local mode technique seeks a solution for the equations of motion as a coupled set of local modes whose amplitudes and phases vary with laterally varying structure. The evolution of the range dependent amplitude determines how energy is exchanged between modes as a signal propagates through the medium. The solution of the equations of motion

for the stress-displacement field in the range dependent medium is thus represented as the sum over local modes

$$\mathbf{u} = \begin{Bmatrix} \mathbf{w} \\ \mathbf{t} \end{Bmatrix} = \sum_q c_q(x) \exp\left(-i \int_0^x k^q(\xi) d\xi\right) \begin{Bmatrix} \mathbf{w}^q(x,z) \\ \mathbf{t}^q(x,z) \end{Bmatrix}, \tag{13}$$

where $k(\xi)$ is the local horizontal wavenumber at $x = \xi$. The local modes satisfy the homogeneous boundary conditions, eq. (6), of a plane layered medium, and are therefore readily computed.

The derivation of the evolution equation for the range dependent amplitude coefficients $c_r(x)$ proceeds by substituting the representation eq. (13) into the equations of motion eq. (5). The scalar product of the resulting expression is formed with the displacement-stress vector of the qth mode $\mathbf{u}^q$, yielding:

$$\frac{\partial c_q}{\partial x} = B_{qr} c_r, \tag{14}$$

which describes the evolution of the range dependent amplitude coefficients.

The explicit form for the coupling matrix B_{qr} has been reproduced for reference from Maupin (1988), and is listed in the Appendix (eq. (A1)). The coupling matrix B_{qr} is composed of products of components of the displacement-stress field, their vertical derivatives and lateral gradients of the medium properties. There are no range derivatives of the local eigenfunctions. The explicit expression for the coupling matrix eq. (A1) describes the coupling in a fully anisotropic 2-D medium.

3 APPROXIMATE SOLUTION OF THE COUPLED MODE EQUATIONS

In this section we derive an approximate solution of the coupled mode equations that will be required for the derivation of the coupled energy equation in the next section.

For a complete description of propagation in a general heterogeneous medium, the evolution eq. (14) for the mode amplitudes must be solved for both forward(+) and backward(−) propagating modes.

$$\frac{\partial}{\partial x}\begin{pmatrix}\mathbf{c}^+(x)\\ \\ \mathbf{c}^-(x)\end{pmatrix} = \begin{pmatrix}\mathbf{B}^{++}(x) & \mathbf{B}^{+-}(x)\\ \\ \mathbf{B}^{-+}(x) & \mathbf{B}^{--}(x)\end{pmatrix}\begin{pmatrix}\mathbf{c}^+(x)\\ \\ \mathbf{c}^-(x)\end{pmatrix} \tag{15}$$

where $\mathbf{c}^+$ and $\mathbf{c}^-$ are n-dimensional vectors whose components are the amplitude coefficients of n forward and backward propagating modes. If we specify a geometry defined by a heterogeneous region sandwiched between two homogeneous (plane layered) regions and assume a signal incident from the left onto the heterogeneous region, eq. (15) defines a $2n \times 2n$ boundary value problem for the amplitudes of the forward and backward propagating modes. The boundary values are $\mathbf{c}^+(x_L)$ known at $x = x_L$ on the left side of the heterogeneous region, and $\mathbf{c}^-(x_R) = 0$ on the right side of the heterogeneous region at $x = x_R$. Figure 1. illustrates the medium geometry and various length scales employed in this paper.

We now assume that energy is scattered predominantly in the forward direction so that backscattering can be neglected. The forward scattering assumption also implies that this theory is applicable to scattering from medium heterogeneities that are predominantly velocity heterogeneities rather than impedance heterogeneities. Backscattering is controlled primarily by impedance contrast (Wu & Aki 1985a,b).

Applying the forward scattering assumption eq. (15) can be written

$$\frac{\partial c_q^+}{\partial x} = B_{qr}^{++}(x) c_r^+(x) \tag{16}$$

which can be approximately integrated (Marquering & Snieder 1994)

$$c_q^+(x) = \exp\left(\int_{x_L}^{x} B_{qr}^{++}(\xi)\, d\xi\right) c_r^+(x_L). \tag{17}$$

The validity of this approximate solution to eq. (16) requires that the commutator of B_{qr}^{++} and $\partial B_{qr}^{++}/\partial x$ be small. A derivation of the approximate solution eq. (17), and an excellent discussion of the subtleties involved is given by Marquering & Snieder (1994). We represent the matrix exponential in eq. (17) by its power series expansion (e.g. Golub & Van Loan 1983, p. 396)

$$\exp(A_{qr}) = \sum_{j=0}^{\infty} \frac{A_{qr}^j}{j!}, \tag{18}$$

so that eq. (17) becomes

$$c_q^+(x) = c_q(x_L) + \sum_{r=0}^{N} A_{qr} c_r(x_L) + \frac{1}{2} \sum_{r=0}^{N} A_{qr} \sum_{l=0}^{N} A_{rs} c_s(x_L) + \ldots \tag{19}$$

where

$$A_{qr} = \int_{x_L}^{x} B_{qr}^{++}(\xi)\, d\xi. \tag{20}$$

Marquering & Snieder (1994) have used the same power series representation of the matrix exponential (eq. (19)) to derive a very efficient algorithm for the solution of the coupled mode equations in the forward scattering limit that takes second order coupling interactions into account. In our derivation of the coupled energy equations below, we retain only the first two terms of eq. (19).

4 ENERGY CONSERVATION

As indicated by eq. (12), the local modes are normalized to carry the same energy flux across planes $x =$ constant. We can obtain a statement of energy conservation for a lossless range dependent medium by substituting the local mode representation of the stress displacement field eq. (13) into the scalar product eq. (11) and setting the derivative with respect to x equal to 0. A concise proof of this statement of energy conservation for the general 3-D problem has been given by Tromp (1994). Carrying out the indicated differentiation and employing eq. (14) yields

$$\begin{aligned}
\frac{\partial}{\partial x}(\mathbf{u}^q, \mathbf{u}^r) &= \frac{\partial}{\partial x} \sum_q |c_q(x)|^2 \\
&= \sum_q \left(\frac{\partial c_q(x)}{\partial x} c_q^*(x) + c_q(x) \frac{\partial c_q^*(x)}{\partial x} \right) \\
&= \sum_{q,r} \left(B_{qr} + B_{rq}^* \right) c_r(x) c_q^*(x) \\
&= 0. \qquad (21)
\end{aligned}$$

We have used the fact that

$$\sum_q c_q(x) \left(\sum_r B_{qr}^* c_r^*(x) \right) = \sum_r c_r(x) \left(\sum_q B_{rq}^* c_q^*(x) \right), \qquad (22)$$

since the mode indices $\{q, r\}$ are summed over the same set.

The only way for eq. (21) to be satisfied generally is for the coupling matrix to be anti-Hermitian, i.e.

$$B_{qr} = -B_{rq}^*. \qquad (23)$$

This anti-Hermiticity is a necessary consequence of energy conservation in a lossless medium. It can be seen by inspection that the coupling matrix B_{qr} given by eq. (A1) is anti-Hermitian.

5 THE COUPLED ENERGY EQUATIONS

As the frequency increases, the discrete mode spacing becomes fine enough that the displacement-stress field may be treated as a continuum of trapped modes. Random fluctuations of material parameters and layer thicknesses and boundary slopes can cause energy to be exchanged among modes. Within the limits of a very well defined set of assumptions, it is possible to derive a diffusion equation to describe this energy exchange. If the medium consists of densely packed scatterers imbedded in a matrix, and if the field is characterized by a large number of closely spaced modes, all the propagating energy is scattered energy. This leads us to relinquish information about individual mode phases in exchange for a description of the average energy transport. Marcuse (1974) derived coupled power equations for propagation in an optical waveguide with random rough boundaries. While our derivation of the coupled energy equations roughly parallels that of Marcuse (1974), there are differences. Marcuse (1974) assumed that the coupling matrix B_{qr} was independent of range, which is not necessary. Another difference is that Marcuse's final results for the energy diffusivity depend on the autocorrelation of the boundary function itself. Our results depend on an autocorrelation functional on the horizontal gradients of the boundary functions and material parameters.

Referring to eq. (21), the average energy flux of local mode q across planes $x =$ constant is

$$E_q = \left\langle c_q c_q^* \right\rangle . \tag{24}$$

The angle brackets $\langle \cdot \rangle$ indicate an ensemble average taken over statistically similar realizations of the medium.

Differentiating eq. (24) with respect to x, we get

$$\frac{\partial E_q}{\partial x} = \left\langle \frac{\partial c_q}{\partial x} c_q^* \right\rangle + \left\langle c_q \frac{\partial c_q^*}{\partial x} \right\rangle \tag{25}$$

and substitute eq. (14) to get

$$\frac{\partial E_q}{\partial x} = \sum_r \left\langle B_{qr}(x)\, c_r(x)\, c_q^*(x) \right\rangle + cc, \tag{26}$$

where cc refers to the complex conjugate of the first expression on the right hand side of eq. (26).

The displacement-stress field in a random medium characterized by heterogeneities distributed over a range of scales is statistically nonuniform. We deal with this statistical nonuniformity by dividing the medium into a sequence of approximately statistically uniform segments of length

$$\mathcal{L}(\omega) = x - x'. \tag{27}$$

for a specified frequency band (Wu & Aki 1985b). We also assume that the frequency dependent correlation length scale of the medium heterogeneities $l(\omega)$ is small compared to the statistically uniform region (Fig. 1)

$$l(\omega) \ll \mathcal{L}(\omega). \tag{28}$$

We assume that over the region of approximate statistical uniformity $\mathcal{L}(\omega)$, we can approximate the forward scattered mode amplitudes $c_q(x)$ and $c_r(x)$ with the first two terms from the power series expansion of the matrix exponential eq. (17). So using the first two terms of eq. (17) substitute

$$c_r(x) \approx c_r(x') + \sum_{n=0}^{N} A_{rn}(x) c_n(x') \tag{29}$$

and

$$c_q^*(x) \approx c_q^*(x') + \sum_{r=0}^{N} A_{qr}^*(x) c_r^*(x') \tag{30}$$

for c_r and c_q^* in the first term of eq. (26). Corresponding substitutions are made in the complex conjugate term, yielding

$$\begin{aligned}
\frac{\partial E_q}{\partial x} &= \sum_r \left\langle B_{qr}(x) c_r(x') c_q^*(x') \right\rangle \\
&+ \sum_{r,n} \left\langle B_{qr}(x) A_{rn}(x) c_n(x') c_q^*(x') \right\rangle \\
&+ \sum_r \left\langle B_{qr}(x) A_{qr}^*(x) c_r(x') c_r^*(x') \right\rangle \\
&+ \sum_{r,n} \left\langle B_{qr}(x) A_{rn}(x) A_{qr}^*(x) c_n(x') c_r^*(x') \right\rangle \\
&+ cc.
\end{aligned} \tag{31}$$

Because of the double summation over r and n, the elements of the product terms in eq. (31) commute without requiring the interchange of indices.

By making several assumptions about the statistics of the random heterogeneities, eq. (31) can be reduced in a systematic way to yield the coupled energy equations. We assume that the range dependent displacement-stress field amplitudes $c_i(x)$ are slowly varying over the correlation distance $l(\omega)$ of the medium properties. This permits us to express the ensemble averages of the products in eq. (31) as products of the ensemble averages (Bendat &Piersol 1986, pp. 465-471)

$$\begin{aligned}
\frac{\partial E_q}{\partial x} &= \sum_r \langle B_{qr}(x) \rangle \left\langle c_r(x') c_q^*(x') \right\rangle \\
&+ \sum_{r,n} \langle B_{qr}(x) A_{rn}(x) \rangle \left\langle c_n(x') c_q^*(x') \right\rangle \\
&+ \sum_r \left\langle B_{qr}(x) A_{qr}^*(x) \right\rangle \langle c_r(x') c_r^*(x') \rangle \\
&+ \sum_{r,n} \langle B_{qr}(x) A_{rn}(x) A_{qr}(x)^* \rangle \langle c_n(x') c_r^*(x') \rangle \\
&+ cc.
\end{aligned} \tag{32}$$

The coupling matrix terms B_{qr}, and the horizontally integrated matrices A_{rn} and A^*_{qr} are sums of terms directly proportional to the horizontal gradients of the density $(\partial\rho/\partial x)$, stiffness tensor $(\partial c_{ijkl}/\partial x)$ and layer boundary configurations $(\partial h/\partial x)$. We assume that the distribution of horizontal gradients of these medium properties within the ensemble of statistically similar models are zero mean so that

$$\langle B_{qr} \rangle = \langle A_{rn} \rangle = \langle A_{qr} \rangle = 0. \tag{33}$$

The zero mean assumption allows us to eliminate the first term on the right hand side of eq. (32). We have already assumed that the coupling is weak enough to approximate the matrix exponential eq. (17) by the first two terms of its power series. The third term on the right hand side of eq. (32) will therefore be much smaller than the second and third terms, and we ignore it.

The second term in eq. (32) contains a double summation over r and n. Physically, this term includes the effects of all modes n which couple to all modes r which then couple to mode q. We make the assumption that the main contribution to the double summation comes from modes $n = q$. This is consistent with the previous assumption that the mode amplitudes can be expressed by the first two terms of the series expansion of the matrix exponential.

After dropping the first and fourth terms on the right hand side of eq. (32), eliminating the summations over n in the second and third terms, and using the anti-Hermiticity of B_{qr}, we have

$$\begin{aligned} \frac{\partial E_q}{\partial x} = & - \sum_r \left\langle B_{qr} A^*_{qr} \right\rangle \left\langle c_q(x') c^*_q(x') \right\rangle \\ & + \sum_r \left\langle B_{qr} A^*_{qr} \right\rangle \left\langle c_r(x') c^*_r(x') \right\rangle \\ & + cc. \end{aligned} \tag{34}$$

The remaining terms proportional to $\left\langle B_{qr}(x)A^*_{qr}(x)\right\rangle$ can be rewritten using the definition of A_{qr} (eq. (20)), so that the coupling terms form the autocorrelation of the coupling matrix

$$\begin{aligned}\left\langle B_{qr}(x)A^*_{qr}(x)\right\rangle &= \int_{x'}^{x}\left\langle B_{qr}(x)B^*_{qr}(x'')\right\rangle\, dx'' \\ &= \int_{-\infty}^{0}\mathcal{R}_{qr}(\tau)\, d\tau, \end{aligned} \tag{35}$$

where

$$\mathcal{R}_{qr}(\tau) = \langle B_{qr}(x)B^*_{qr}(x-\tau)\rangle \tag{36}$$

is the autocorrelation of the coupling matrix, and

$$\tau = x - x''. \tag{37}$$

The lower limit of the integral has been extended from x' to $-\infty$ because we assume that $\mathcal{R}_{qr}(\tau)$ contributes only over the distance of a medium correlation length $l(\omega)$, and

$$l(\omega) \ll x - x'. \tag{38}$$

Since B_{qr} is evaluated at x and the integration for A_{qr} is over x'', we are able to take B_{qr} inside the integral, and introduce the correlation variable τ. The complex conjugate term contributes the complex conjugate of the integral term we already have. The final result for the coupled energy equation is then

$$\frac{\partial E_q}{\partial x} = \sum_r b_{qr}(E_r - E_q) \tag{39}$$

where

$$b_{qr} = \int_{-\infty}^{+\infty}\mathcal{R}_{qr}(\tau)\, d\tau, \tag{40}$$

the symmetric energy coupling matrix, is essentially the spatial autospectrum of the square of the coupling matrix B_{qr}. It can be seen from eq. (A1) that the leading order phase dependence of the integrand of eq. (40) will be $exp(i(k^q - k^r)\tau)$ which gives b_{qr} the form of an autospectrum to leading order.

Referring to eq. (A1), it can be seen that B_{qr} is a sum of terms made up of field components, the vertical derivatives of the field components and horizontal derivatives of the field components. If we write B_{qr} to emphasize the horizontal derivatives of the material properties,

$$B_{qr} = \frac{1}{k^q - k^r}\left\{\tilde{B}^{(1)}_{qr}\frac{\partial \rho(x)}{\partial x} + \tilde{B}^{(2)}_{qr}\frac{\partial f(c_{ijkl}(x))}{\partial x} + \tilde{B}^{(3)}_{qr}\frac{\partial h(x)}{\partial x}\right\}\exp\left(i\int_0^x (k^q - k^r)d\xi\right), \quad (41)$$

where $f(c_{ijkl}(x))$ is used to indicate any of the Q_{ij} or matrix products of the C_{ij}, and if we can assume that $\tilde{B}^{(1)}_{qr}$, $\tilde{B}^{(2)}_{qr}$ and $\tilde{B}^{(3)}_{qr}$ are constant over the statistically uniform regions $\mathcal{L}(\omega)$, we find that b_{qr} is proportional to a sum of terms consisting of the spatial autospectra and cross-spectra of $\partial\rho(x)/\partial x$, $\partial f(c_{ijkl}(x))/\partial x$ and $\partial h(x)/\partial x$. If we are able to make this approximation, specification of the random properties of the medium is reduced to the specification of the corresponding autospectra and cross-spectra of the medium properties. In addition the coupling matrix will only have to be computed once for every statistically uniform segment.

6 THE ENERGY DIFFUSION EQUATION

Eq. (39) is an infinite set of coupled first order equations that describes the evolution of mode energy in a random medium with a correlation function that can be computed once the form of the heterogeneities has been specified. Eq. (39) is not particularly useful in the form given because the eigenvalues of the local modes in the random medium must be found,

the eigenfunctions must be calculated and the range dependent energy coupling matrix must be computed before eq. (39) can be solved. By employing several additional assumptions, we can reduce eq. (39) to a diffusion equation for the diffusion of energy in the random medium. Our derivation parallels that of Gloge (1972), who derived a diffusion equation for the propagation of energy in a dielectric optical waveguide with random index of refraction perturbations.

The elements of the coupling matrix eq. (A1) depend on the inverse of the eigenwavenumber spacing. Tromp (1994) has shown that the the relative coupling strength between modal overtones is inversely proportional to the square of the local wavenumber spacing

$$\frac{\delta c_q}{c_q} \propto |k_q - k_r|^{-2} \tag{42}$$

so the strength of the energy coupling is therefore

$$\frac{\delta E_q}{E_q} \propto |k_q - k_r|^{-4}. \tag{43}$$

As the frequency increases, the eigenwavenumber spacing decreases. The $(\Delta k)^{-4}$ dependence of the energy coupling indicates that the coupling interaction between immediately neighboring modes will be much stronger than more distant intermode interactions. If we assume that nearest neighbor coupling between modes comprises the dominant intermode interactions, eq. (39) can be written as the differential-difference equation

$$\frac{\partial E_q}{\partial x} = b_{q+1,q}(E_{q+1} - E_q) + b_{q,q-1}(E_{q-1} - E_q). \tag{44}$$

As the frequency increases, the mode spacing becomes smaller and smaller. In the limit in which the mode spacing goes to zero, the mode spectrum is represented by a continuum, and the differences in eq. (44) can be replaced with differentials

$$E_{q+1} - E_q = \frac{\partial E_q}{\partial q}\Delta q. \tag{45}$$

This allows us to rewrite eq. (44) as

$$\begin{aligned}\frac{\partial E_q}{\partial x} &= b_{q+1,q}(E_{q+1} - E_q) - b_{q,q-1}(E_q - E_{q-1}) \\ &= \Delta q \left(b_{q+1,q} \frac{\partial E_{q+1}}{\partial q} - b_{q,q-1} \frac{\partial E_q}{\partial q} \right). \end{aligned} \tag{46}$$

Finally we collapse the final difference in the same way to get

$$\frac{\partial E_q}{\partial x} = \left\{ \frac{\partial}{\partial q} \left(b_q \frac{\partial E_q}{\partial q} \right) \right\}. \tag{47}$$

We have dropped the second subscript on b_{qr}, and set $\Delta q = 1$.

The mode number q is not particularly useful as the continuous independent variable. However at this point we have quite a bit of flexibility for the choice of continuous independent variable to use as we take the continuum limit. Possible choices include the local horizontal wavenumber k_q, the local horizontal slowness in the propagation direction $p_{x,q}$, the local phase velocity v_q^{ph} or the local ray equivalent angle θ_q. A final choice would be made according to application, mathematical perspective one would like to take and ease of numerical implementation. In any case we need to be able to relate the mode number q to the continuous independent variable of choice. If we let λ represent any appropriate spectral variable we may want to choose, then the local dispersion relation

$$\mathcal{F}(\lambda, q) = 0 \tag{48}$$

provides an implicit relation between the mode index q and λ. Differentiation of eq. (48) provides the needed relation to transform the derivatives with respect to q in eq. (47) to derivatives with respect to λ.

Our final result is then

$$\frac{\partial E}{\partial x} = \varrho^{-1}(q,\lambda,x)\left\{\frac{\partial}{\partial \lambda}\left(\varrho^{-1}(q,\lambda,x) b(\lambda,x)\frac{\partial E(\lambda,x)}{\partial \lambda}\right)\right\}, \tag{49}$$

where

$$\varrho(q,\lambda,x) = \frac{\partial q}{\partial \lambda} \tag{50}$$

is the local mode density function, and

$$b(\lambda,x) = \int_{-\infty}^{+\infty} \mathcal{R}(\tau)\, d\tau, \tag{51}$$

which is the continuum limit of eq. (40) described below.

The form of $b(\lambda,x)$ follows from the continuum limit of eq. (36) and eq. (A1). The coupling matrix B_{qr} (eq. (A1)) is a function of the difference of the eigenwavenumbers $\Delta k = (k_q - k_r)$

$$B_{qr} = \frac{1}{\Delta k(x)}\mathcal{B}_{qr}(x) e^{i\psi(\Delta k,x)}, \tag{52}$$

where $\mathcal{B}_{qr}$ is the part of B_{qr} that does not depend on Δk and $\psi(\Delta k,x)$ is the phase. We can express $\Delta k(x)$ in terms of the mode density function $\varrho(q,\lambda,x)$ as

$$\begin{aligned} \Delta k &= \Delta q \frac{\partial \lambda}{\partial q}\frac{\partial k}{\partial \lambda} \\ &= \Delta q \frac{\partial k}{\partial \lambda}\varrho^{-1}(q,\lambda,x). \end{aligned} \tag{53}$$

Now rewrite the autocorrelation function eq. (36) as

$$\langle B_{qr}(x) B^*_{qr}(x-\tau)\rangle = \frac{1}{(\Delta q)^2}\langle \tilde{\mathcal{B}}(x)\tilde{\mathcal{B}}(x-\tau)\rangle, \tag{54}$$

where

$$\tilde{\mathcal{B}}(x) = \left(\frac{\partial\lambda(x)}{\partial k}\right) \varrho(q,\lambda,x)\mathcal{B}(x)e^{i(\Delta q\tilde{\psi}(x))} \tag{55}$$

and

$$\tilde{\mathcal{B}}^*(x-\tau) = \left(\frac{\partial\lambda(x-\tau)}{\partial k}\right) \varrho(q,\lambda,x-\tau)\mathcal{B}^*(x-\tau)e^{-i(\Delta q\tilde{\psi}(x-\tau))}. \tag{56}$$

The tildes over $\tilde{\psi}(x)$ and $\tilde{\psi}(x-\tau)$ indicate that the Δk term in the phases has also been replaced by the expression given in eq. (53). Allowing the mode spacing to approach zero, and setting $\Delta q = 1$ in eq. (54), we get

$$\begin{aligned} b_{qr} = \int_{-\infty}^{+\infty} \mathcal{R}_{qr}(\tau)\, d\tau \quad &\rightarrow \quad \int_{-\infty}^{+\infty} \langle \tilde{\mathcal{B}}(x)\tilde{\mathcal{B}}^*(x-\tau)\rangle \\ &= \quad \int_{-\infty}^{+\infty} \mathcal{R}(\tau)\, d\tau \\ &= \quad b(\lambda,x). \end{aligned} \tag{57}$$

If it occurs that

$$\varrho(q,\lambda,x) = \varrho(q,\lambda,x-\tau) \approx \text{constant}, \tag{58}$$

for all x and λ, then ϱ^2 can be factored from $b(\lambda,x)$ and canceled by the inverse factors on the right hand side of eq. (49) to eliminate the mode density from the energy diffusion equation. Also note that if we choose $\lambda = k$ then $\partial\lambda/\partial k = 1$, and if we choose $\lambda = p_x$ then $\partial\lambda/\partial k = 1/\omega$. Either of these choices for λ will significantly simplify the computation of $b(\lambda,x)$.

Eq. (49) is a parabolic partial differential equation that describes the range dependent diffusion of energy in λ-space in a perfectly elastic 2-D random medium that is so strongly scattering that all the energy is scattered energy. The diffusivity $b(\lambda,x)$ is a range and frequency dependent continuous functional of the displacement-stress field and the range

gradients of the medium properties. Because we have taken the continuum limit in the derivation of eq. (49), the diffusivity $b(\lambda, x)$ can be computed using any program, e.g. reflectivity or finite difference, that can solve for the displacement-stress field as a function of depth in a plane layered medium. The field quantities in the coupling matrix B_{qr} from which the diffusivity $b(\lambda, x)$ is derived, are the field quantities for a plane layered medium. The range dependence enters through the range gradients of the medium.

In order to solve eq. (49), we must be able to evaluate $\varrho(q, \lambda, x)$. There are several special cases for which $\varrho(q, \lambda, x)$ can be evaluated analytically subject to some additional approximations. From a practical numerical standpoint, we need to know the density of modes in the region of interest in the spectral space of choice (k, p_x, v^{ph}, θ, etc.). This is straightforward for SH waves and acoustic waves which are governed by a second order scalar differential equation that defines a Sturm-Liouville problem. The eigenvalues are predictably and evenly spaced, and it is relatively straightforward to determine the density of eigenvalues in some region of spectral space. Determining the density of eigenvalues for the higher order P-SV problem is more difficult because of their irregular spacing.

However, Woodhouse (1981, 1988) has been able to construct a function from the minors of the propagator matrix that exactly yields the density of modes in a specified region of spectral space for the general P-SV problem. The evaluation of this function requires only two integrations of the system of differential equations for the P-SV problem. The existence and form of this function were conjectured quite some time ago (Woodhouse 1981), and a complete proof was given just recently (Woodhouse 1988). An effective algorithm for computing the mode density function has been given by Gomberg & Masters (1988). We discuss the more general P-SV case first, and then the cases for which it is possible to find an approximate analytical expression for $\varrho(q, \lambda, x)$.

Woodhouse's (1988) function is

$$\nu(\lambda_a, \lambda_b), \tag{59}$$

which is the number of eigenvalues(modes) of an $n \times n$ system of equations between the values $\lambda_a < \lambda_b$. We take as the average mode density

$$\varrho(q, \lambda, x) = \frac{\nu(\lambda_a, \lambda_b)}{\lambda_b - \lambda_a}. \tag{60}$$

Eq. (60) should provide a reasonable approximation to the average mode density at high frequencies where the modes are spaced closely together. It is not necessary to precisely locate eigenvalues, nor is it necessary to construct eigenfunctions in order to compute eq. (60). It is only necessary to count the number of zero crossings of a certain product of minors of the propagator matrix. The mode density $\varrho(q, \lambda, x)$ is also range dependent, and must be pre-computed locally and stored along with the quantities necessary to construct the diffusivity functional $b(\lambda, x)$.

Eq. (60) is quite general, and valid for an arbitrary fluid-elastic medium. We should be able to construct a numerical solution to the energy diffusion equation (49) for any 2-D fluid-elastic random medium of interest that satisfies the assumptions already stated. With some additional assumptions it is possible to obtain a precise analytical expression for the mode density.

We choose the horizontal slowness p_x as our independent spectral variable, and restrict it to lie in the range $\alpha_{min}^{-1} < p_x < \beta_{min}^{-1}$ where α_{min} and β_{min} are the minimum compressional and shear speeds, respectively. In this slowness range the shear waves are propagating and the compressional waves are evanescent. If the surface layers consist of water overlying very low shear speed sediments, we take α_{min} equal to the minimum sound speed in the water, and take β_{min} equal to the shear speed in the sediments at the water-sediment interface. We assume further that the sediment shear speed is less than the compressional speed in the

water. If the medium can be modeled as piecewise smooth, the high frequency asymptotic limit of the dispersion relation is (Kennett 1983, p.297)

$$2\omega\tau_\beta(p_x) \sim (2q + 1/2)\pi + \Psi(\omega, p_x), \tag{61}$$

where

$$\tau_\beta(p_x) = \int_0^{Z_\beta(p_x)} p_z^\beta(z)\, dz, \tag{62}$$

the intercept time, is the integral of the vertical shear wave slowness $p_z^\beta(z)$ from the surface to the shear wave turning depth $Z_\beta(p_x)$, and $\Psi(\omega, p_x)$ is a frequency dependent phase shift from the effect of reflection from all interfaces, including the free surface. If the only interface is a solid free surface then

$$\Psi(\omega, p_x) = -\text{arg}\tilde{\text{R}}^{SS}(p_x). \tag{63}$$

where $\tilde{\text{R}}^{SS}(p_x)$ is the SS free surface reflection coefficient, which is frequency independent.

From eq. (61) we get

$$\frac{\partial q}{\partial p_x} = \frac{1}{\pi}\frac{\partial}{\partial p_x}\left\{\omega\tau_\beta(p_x) - \frac{1}{2}\Psi(\omega, p_x)\right\} \tag{64}$$

The first term inside the braces on the right hand side can be simplified further,

$$\frac{\partial \omega\tau_\beta}{\partial p_x} = \omega\tau_\beta(p_x)U_S(p_x) - \omega X_S(p_x), \tag{65}$$

where

$$U_S = \frac{1}{\omega}\frac{\partial \omega}{\partial p_x} \tag{66}$$

is the local shear wave group velocity, and

$$X_S = -\frac{\partial \tau_\beta}{\partial p_x} \tag{67}$$

is the local shear wave range at slowness p_x. Using

$$\tau_\beta(p_x) = T_S(p_x) - p_x X_S(p_x), \tag{68}$$

where $T_S(p_x)$ is the local shear wave traveltime, and

$$X_S(p_x) = T_S(p_x) U_S(p_x), \tag{69}$$

we have for the mode density from eq. (64)

$$\varrho(q, p_x, x) = \frac{\partial q}{\partial p_x} = -\frac{1}{\pi}\left\{\omega p_x X_S(p_x) U_S(p_x) + \frac{1}{2}\frac{\partial \Psi(\omega, p_x)}{\partial p_x}\right\}. \tag{70}$$

By combining eq. (70) with eq. (49), we have an equation that describes the range dependent diffusion of energy in slowness space for the slowness range indicated above,

$$\frac{\partial E}{\partial x} = \varrho^{-1}(q, p_x, x)\left\{\frac{\partial}{\partial p_x}\left(\varrho^{-1}(q, p_x, x) b(p_x, x)\frac{\partial E(p_x, x)}{\partial p_x}\right)\right\}, \tag{71}$$

where $\varrho(q, p_x, x)$ is given by eq. (70), and from eq. (57)

$$b(p_x, x) = \omega^{-2}\int_{-\infty}^{+\infty} \mathcal{R}(\tau)\, d\tau. \tag{72}$$

The factor of ω^{-2} is from $(\partial p_x/\partial k)^2$ in eq. (57), which we have removed from $\mathcal{R}(\tau)$. All the medium dependent factors are computed locally with any suitable one dimensional code that yields the complete displacement-stress field as a function of depth. The range dependence enters explicitly when the diffusivity functional $b(p_x, x)$ is constructed.

Energy diffusion of SH waves or pure acoustic waves is also governed by equations of the form of eqs. (70) and (71). The only difference is that the free surface contribution to

$\Psi(\omega, p_x)$ will be zero. This is because there is no wave type conversion for SH, or for pure acoustic waves, in 2-D media. If the medium is slowly varying, and the free surface is the only interface, then

$$\Psi(\omega, p_x) = 0. \tag{73}$$

If we expand the derivatives with respect to p_x in eq. (71), we get an equation the form of a convection-diffusion equation with non-constant coefficients

$$\frac{\partial E}{\partial x} = \mathcal{D}^2(p_x, x)\frac{\partial^2 E(p_x, x)}{\partial p_x^2} - \Gamma^2(p_x, x)\frac{\partial E(p_x, x)}{\partial p_x}, \tag{74}$$

where the diffusivity

$$\mathcal{D}^2(p_x, x) = \varrho^{-2}(q, p_x, x)b(p_x, x), \tag{75}$$

and $\Gamma^2(p_x, x)$ characterizes the rate at which energy spreads from a particular region of p_x-space

$$\Gamma^2(p_x, x) = -\varrho^{-1}(q, p_x, x)\frac{\partial}{\partial p_x}\left\{\varrho^{-1}(q, p_x, x)b(p_x, x)\right\}. \tag{76}$$

Finally by introducing the transformation

$$\begin{aligned} E(p_x, x) &= \mathcal{E}(p_x, x)\exp\left\{\frac{1}{2}\int^{p_x}\left(\frac{\Gamma(p'_x, x)}{\mathcal{D}(p'_x, x)}\right)^2 dp'_x\right\} \\ &= \mathcal{E}(p_x, x)\{r(p_x, x)\}^{-1/2}, \end{aligned} \tag{77}$$

the first derivative with respect to p_x can be eliminated from eq. (74), reducing it to a Schrödinger equation

$$\frac{\partial^2 \mathcal{E}}{\partial p_x^2} + \mathcal{V}(p_x, x)\mathcal{E} = \mathcal{D}^{-2}\frac{\partial \mathcal{E}}{\partial x}, \tag{78}$$

with the potential

$$\mathcal{V}(p_x, x) = \frac{1}{2}\frac{\partial}{\partial p_x}\left(\frac{\Gamma}{\mathcal{D}}\right)^2 - \frac{1}{4}\left(\frac{\Gamma}{\mathcal{D}}\right)^4 - \frac{1}{2\mathcal{D}^2}\frac{\partial}{\partial x}\int^{p_x}\left(\frac{\Gamma(p'_x, x)}{\mathcal{D}(p'_x, x)}\right)^2 dp'_x. \tag{79}$$

The Schrödinger equation form may be useful because of the large amount of work that has gone into its numerical solution. A drawback may be the complicated form of the potential $\mathcal{V}(p_x, x)$, and the boundary conditions discussed in the next section.

7 INITIAL AND BOUNDARY CONDITIONS

Eq. (71) is first order in x and second order in p_x. In order to completely define the diffusion problem, we need an initial condition and two boundary conditions. As an initial condition, which does not have to satisfy the boundary conditions, we specify the source spectrum at $x = 0$

$$E(p_x, 0) = \mathcal{S}(p_x). \tag{80}$$

For the particular problem defined above at the end of Section 6, the boundary conditions are to be specified at the endpoints of a finite region of spectral space $\alpha_{min}^{-1} < p_x < \beta_{min}^{-1}$. Within this region of p_x – space the propagating waves are almost pure SV. This spectral region was chosen as an illustrative example for which the mode density function was easy to calculate. First we will specify the appropriate boundary conditions for this specific problem, then comment on how they must be changed for more general problems.

For $p_x > \alpha_{min}^{-1}$ the compressional waves are evanescent and carry no energy. For $p_x \leq \alpha_{min}^{-1}$ energy in the SV waves is radiated away as P waves. We assume that this energy is carried away and completely lost to the system. Because of this energy loss we choose

$$E(\alpha_{min}^{-1}, x) = 0 \tag{81}$$

for the lower boundary condition, which corresponds to infinite loss.

For the upper boundary condition at $p_x = \beta_{min}^{-1}$, we also choose

$$E(\beta_{min}^{-1}, x) = 0. \tag{82}$$

The reason for this choice is that for values of $p_x > \beta_{min}^{-1}$, the propagating SV waves can lose energy to the fundamental Rayleigh wave or low speed Stoneley waves. This choice for the upper boundary condition is somewhat artificial since energy can flow into Rayleigh waves, which are ignored by this choice.

If we give up being able to analytically calculate the mode density function in the interests of covering the complete slowness range $0 \leq p_x < \infty$, we need to reexamine the boundary conditions. For the lower boundary condition at $p_{min} = 0$, we must choose

$$\frac{\partial E}{\partial p_x} = 0, \quad \text{for} \quad p_x = 0. \tag{83}$$

Because we have assumed that there is no backscattering, the energy flux into regions of spectral space for which $p_x < 0$ must be zero. Eq. (83) is the mathematical statement of the zero flux condition.

We must choose a finite upper limit for the upper boundary since there are no propagating waves for $p_x > p_{max}$, where p_{max} is the slowness for the fundamental Rayleigh or Stoneley wave, whichever has the greatest slowness. Therefore, at the upper boundary we also have a zero flux condition

$$\frac{\partial E}{\partial p_x} = 0, \quad \text{for} \quad p_x = p_{max}, \tag{84}$$

indicating that no energy is allowed to flow into the spectral region for which $p_x > p_{max}$.

If the Schrödinger equation form eq. (78) is employed, the zero flux boundary conditions eq. (83) and eq. (84) assume the form

$$\frac{\partial \mathcal{E}}{\partial p_x} + \left(\frac{\Gamma}{\mathcal{D}}\right)^2 \mathcal{E} = 0. \tag{85}$$

Mixed boundary conditions of the form eq. (85) complicate the solution process in general. The zero energy boundary conditions such as eq. (81) and eq. (82) retain their same form, as does the initial condition eq. (80).

8 DISCUSSION OF ELEMENTARY SOLUTIONS TO THE DIFFUSION EQUATION

The energy diffusion problems described by eq. (49) or eq. (71) and the boundary conditions given in the previous section must be solved numerically for any realistic problem of interest. However some qualitative insight can be gained by examining simple solutions for constant diffusivity. We define two example problems that illustrate the points. Because we specify constant diffusivity, the "convection" term in eq. (74) vanishes since the coefficient of that term is the derivative of the diffusivity.

Problem I.

The first example problem is

$$\frac{\partial E}{\partial x} = \mathcal{D}^2 \frac{\partial^2 E}{\partial p_x^2} \qquad x \geq 0 \quad \text{and} \quad p_{min} \leq p \leq p_{max}, \tag{86}$$

with initial condition eq. (80) and boundary conditions

$$E(p_{min}, x) = \frac{\partial E(p_{max}, x)}{\partial p_x} = 0. \tag{87}$$

The constant diffusivity is denoted by $\mathcal{D}^2$, and has units of $[slowness^2/length]$. *Problem I* assumes zero energy flux above a maximum value of $p_x = p_{max}$ and assumes that any energy scattered to compressional waves at $p_x = p_{min}$ is completely lost to the system. This problem defines an eigenvalue problem for the energy $E(p_x, x)$ in the region $p_{min} \leq p \leq p_{max}$ that can be solved by a number of different methods, It is treated in detail by most textbooks on partial differential equations, so we simply state the Fourier series representation of the solution

$$E(p_x, x) = \sum_{n=1}^{\infty} a_n e^{-(\lambda_n \mathcal{D})^2 x} \cdot \{\tan(\lambda_n p_{max}) \sin(\lambda_n p_x) + \cos(\lambda_n p_x)\}, \tag{88}$$

where the eigenvalue λ_n, which is not related in any way to the spectral parameter λ used earlier, is

$$\lambda_n = \frac{\pi(2n-1)}{2(p_{max} - p_{min})}, \tag{89}$$

and n is the summation index. The expansion coefficients are

$$a_n = 2\left\{(p_{max} - p_{min}) - \frac{1}{\lambda_n}\cos(\lambda_n((p_{max} + p_{min}))\right\}^{-1} \int_{p_{min}}^{p_{max}} \mathcal{S}(p_x) \cos(\lambda_n p_x)\, dp_x. \tag{90}$$

There are several things to notice about the form of the solution eq. (88). It is apparent that as the propagation distance in the strongly scattering medium $x \to \infty$ that the energy $E \to 0$. All the energy is eventually scattered away to body waves and lost to the system. Also any structure that may initially exist in the p_x-spectrum is smeared out as the propagation distance increases. The sharpest peaks in the spectrum correspond to the largest eigenvalues of the solution eq. (88), but the spectral components with the largest eigenvalues suffer the largest damping proportional to $\exp(-n^2 x)$ with range. The effect of a strongly scattering medium is to homogenize the spectrum and destroy any coherent signal.

Problem II.

The second example problem is defined by replacing the zero energy boundary condition at $p_x = p_{min}$ by the zero flux boundary condition eq. (83) at $p_x = 0$. Because of the zero flux boundary conditions at both ends of the spectral interval, there is no energy loss to the system. The solution is a sum of a steady state (ss) part and a transient (t) part.

$$E(p_x, x) = E_{ss} + E_t, \tag{91}$$

where the steady state part is the total energy divided by the interval length

$$E_{ss} = \frac{1}{p_{max}} \int_0^{p_{max}} \mathcal{S}(p_x) dp_x. \tag{92}$$

The transient part of the solution is

$$E_t(p_x, x) = \sum_{n=1}^{\infty} a_n e^{-(\lambda_n \mathcal{D})^2 x} \cos(\lambda_n p_x), \tag{93}$$

where

$$\lambda_n = \frac{n\pi}{p_{max}}, \tag{94}$$

and

$$a_n = \frac{2}{p_{max}} \int_0^{p_{max}} \mathcal{S}(p_x) \cos(\lambda_n p_x)\, dp_x. \tag{95}$$

In the limit as $x \to \infty$ the transient part of the solution vanishes and the energy is distributed uniformly throughout the spectral region $0 \leq p_x \leq p_{max}$. As with *Problem I* all coherent structure disappears from the spectrum. This is illustrated in Figure 2. The remaining steady state solution corresponds to the zero eigenvalue. For a realistic medium with non-zero intrinsic attenuation there will of course be no steady state solution. The energy will approach zero as $x \to \infty$.

The only requirement for the validity of the Fourier series representation of the solutions to *Problem I* and *Problem II* is that $\mathcal{S}(p_x)$ be continuous. We have previously assumed in the derivation of the diffusion equation that the spectrum could be represented by a continuum. The disadvantage of the representations eq. (88) and eq. (93) from a computational standpoint is that the series have rather poor convergence properties for small x. For very small x the Green's function representation of the solutions is more efficient. We do not reproduce the Green's functions for the problems here. Kevorkian (1990, Chapter 1) has an excellent discussion of the various solution representations for the diffusion equation including a proof of the equivalence of the Fourier series and the Green's function solutions. A final comment on the Green's function representation is that it is very inefficient for large x because a large number of image sources are required in order to satisfy the zero flux boundary conditions for either *Problem I* or *Problem II.*

9 ATTENUATION

The theory presented above is also valid for arbitrary dissipative media if the scalar product eq. (11) is replaced with the more general scalar product defined by Maupin (1992). The form of the energy diffusivity functional is such that it can be locally calculated with a reflectivity program. Most reflectivity codes incorporate arbitrary attenuation by introducing complex frequency dependent velocities or elastic moduli. The viscoelastic correspondence principle states that the governing equations and boundary conditions for the displacement-stress fields are formally identical in the perfectly elastic and dissipative cases. The only difference is that the velocities or the elastic moduli for the perfectly elastic media are replaced with complex velocities or elastic moduli for the dissipative media. Attenuation then enters the problem in a natural and straightforward way, rather than in the *ad hoc* manner used by Gloge (1972), Marcuse (1974) and all the energy diffusion equations (so far as we are aware)

originating from radiative transfer theory.

One problematic practical issue is the computation of the mode density function $\varrho(q, \lambda, x)$, which would have to be done in complex (q, λ) space. Woodhouse's (1988) mode count function $\nu(\lambda_a, \lambda_b)$ for the Rayleigh wave case was derived for real systems of equations, not complex systems. A possible solution might be to estimate it with its real value.

10 CONCLUSIONS

We have derived a very general energy diffusion equation (49) directly from the local coupled mode representation of the displacement-stress field for a randomly heterogeneous 2-D fluid-elastic medium. Eq. (49) describes the diffusion in spectral space as a function of range in media whose propagation processes are dominated by strong scattering in the forward direction. The derivation proceeds in a systematic way following a well defined sequence of assumptions, and is explicitly frequency dependent. Because of the large number of assumptions required to derive the energy diffusion equation, we summarize them here:

1. Backscattering is neglected. This implies that our results are most applicable to media characterized by velocity heterogeneities or very weak impedance heterogeneities.

2. Mode coupling is weak enough to express the forward scattered amplitudes by the first two terms of the series expansion for the matrix exponential. This approximation takes first order mode coupling into account.

3. The statistically non-uniform random medium can be characterized by a series of regions of frequency dependent length $\mathcal{L}(\omega)$ that are approximately statistically uniform.

4. The frequency dependent correlation length scale $l(\omega)$ of the medium heterogeneities is much smaller than the length scale of the statistically uniform regions ($l(\omega) \ll \mathcal{L}(\omega)$).

5. The range dependent displacement-stress field amplitudes $c_q(x)$ vary slowly over the correlation distance $l(\omega)$ of the medium.

6. The distributions of the horizontal gradients of the medium properties are zero mean.

7. The autocorrelation of the coupling matrix $\mathcal{R}_{qr}(\tau) = \langle B_{qr}(x) B^*_{qr}(x-\tau) \rangle$ makes a significant contribution only over the distance of a medium correlation length $l(\omega)$.

8. The mode spectrum can be represented by a continuum in the high frequency limit.

A further useful approximation is that the part of the coupling matrix B_{qr} that depends directly on the displacement-stress field components is constant throughout the statistically uniform regions. If this is the case, the energy diffusivity functional is seen to be directly proportional to the autospectra and cross-spectra of the horizontal derivatives of the medium properties.

The specific example given for the energy diffusion of Rayleigh waves in the slowness range $\alpha_{min}^{-1} < p_x < \beta_{min}^{-1}$ where α_{min} and β_{min} are the minimum compressional and shear speeds of the medium, is also formally identical to the energy diffusion equation for Love waves or for scalar acoustic waves propagating in a waveguide.

Elementary solutions to the diffusion equation for relevant boundary conditions clearly illustrate the the homogenization of the spectrum as the propagation distance increases. The most singular features of the initial spectrum are the most heavily damped with range.

ACKNOWLEDGEMENTS

This research was supported by the Office of Naval Research Contracts N00014-90-J-1369, N00014-94-1-0036 and the Space and Naval Warfare Office PMW-183.

REFERENCES

Aki, K. & Chouet, B., 1975. Origin of coda waves: Source attenuation and scattering effects, *J. geophys. Res.*, **80**, 3322-3342.

Bendat, J.S. & Piersol, A.G., 1986. *Random Data, 2nd edition*, pp 465-471, Wiley, New York.

Burridge, R. & Knopoff, L., 1964. Body-force equivalents for seismic dislocations, *Bull. seism. Soc. Am.*, **54**, 1875-1888.

Dainty, A.M., Toksöz, M.N., Anderson, K.R., Pines, P.J., Nakamura, Y. & Latham, G., 1974. Seismic scattering and shallow structure of the moon in Oceanus Procellarum, *The Moon*, **9**, 11-29.

Dainty, A.M. & Toksöz, M.N., 1977. Elastic wave propagation in a highly scattering medium - A diffusion approach, *J. Geophys.*, **43**, 375-388.

Fisk, M.D. & McCartor, G.D., 1991. The phase screen method for vector elastic waves, *J. geophys. Res.*, **96**, 5985-6010.

Fisk, M.D., Charette, E.E. & McCartor, G.D., 1992. A comparison of phase screen and finite difference calculations for elastic waves in random media, *J. geophys. Res.*, **97**, 12,409-12,423.

Gloge, D., 1972. Optical power flow in multimode fibers, *Bell Sys. Tech. J.*, **51**, 1767-1783.

Golub, G. & Van Loan, 1983. *Matrix Computations*, p. 396, Johns Hopkins University Press, Baltimore.

Gomberg, J.S. & Masters, T.G., 1988. Waveform modelling using locked-mode synthetic and differential seismograms: application to determination of the structure of Mexico, *Geophys. J.*, **94**, 193-218.

Kennett, B.L.N., 1983. *Seismic Wave Propagation in Stratified Media*, Cambridge University Press, Cambridge, England.

Kennett, B.L.N., 1984. Guided-wave propagation in laterally varying media. I. Theoretical development, *Geophys. J. R. astr. Soc.*, **79**, 235-255.

Kevorkian, J., 1990. *Partial Differential Equations*, Wadsworth & Brooks, Pacific Grove, California.

Marcuse, D., 1974. *Theory of Dielectric Optical Waveguides*, Academic, San Francisco.

Marquering, H. & Snieder, R., 1994. Surface wave mode coupling for efficient forward modeling and inversion of body wave phases, *Geophys. J. Int.*, in press.

Maupin, V., 1988. Surface waves across 2-D structures: a method based on coupled local modes, *Geophys. J.*, **93**, 173-185.

Maupin, V., 1992. Modelling of laterally trapped surface waves with application to Rayleigh waves in the Hawaiian swell, *Geophys. J. Int.*, **110**, 553-570.

Maupin, V. & Kennett, B.L.N., 1987. On the use of truncated modal expansions in laterally varying media, *Geophys. J. R. astr. Soc.*,**91**, 837-851.

Nakamura, Y., 1977. Seismic transmission in an intensively scattering environment, *J. Geophys.*, **43**, 389-399.

Oberst, J., 1987. Unusually high stress drops associated with shallow moonquakes, *J. geophys. Res.*, **92**, 1397-1405.

Odom, R.I., 1980. Experimental and Theoretical Investigations of Ocean-Earth Acoustic Coupling, Ph.D. Dissertation, Geophysics, University of Washington, Seattle, 1980.

Odom, R.I., 1986. A coupled mode examination of irregular waveguides including the continuum spectrum, *Geophys. J.R. astr. Soc.*, **86**, 425-453.

Snieder, R., 1986. 3-D linearized scattering of surface waves and a formalism for surface wave holography, *Geophys. J.R. astr. Soc.*, **84**, 581-605.

Tromp, J., 1994. A coupled local-mode analysis of surface-wave propagation in a laterally heterogeneous waveguide, *Geophys. J. Int.*, **117**, 153-161.

Woodhouse, J.H., 1974. Surface waves in laterally varying structure, *Geophys J. R. astr. Soc.*, **37**, 461-490.

Woodhouse, J.H., 1981. The calculation of the complete normal mode spectrum of the earth using finite difference methods, Seismic Discrimination Semiannual Technical Summary, Lincoln Laboratory, MIT, 31 March 1981.

Woodhouse, J.H., 1988. The calculation of eigenfrequencies and eigenfunctions of the free oscillations of the earth and sun, in *SEISMOLOGICAL ALGORITHMS: Computational Methods and Computer Programs*, pp. 321-370, ed. Doornbos, D., Academic, San Diego, California.

Wu, R-S., 1985. Multiple scattering and energy transfer of seismic waves - separation of scattering effect from intrinsic attenuation - I. Theoretical modelling, *Geophys. J. R. astr. Soc.*, **82**, 57-80.

Wu, R-S., 1994. Wide-angle elastic one-way propagation in heterogeneous media and an elastic wave complex screen method, *J. geophys. Res.*, **99**, 751-766.

Wu, R-S. & Aki, A., 1985a. Scattering characteristics of elastic waves by an elastic heterogeneity, *Geophysics*, **50**, 582-595.

Wu, R-S. & Aki, A., 1985b. Elastic wave scattering by a random medium and the small-scale inhomogeneities in the lithosphere, *J. geophys. Res.*, **90**, 10261-10273.

APPENDIX A: MAUPIN'S COUPLING MATRIX FOR FLUID-ELASTIC MEDIA

In this appendix we include for reference, Maupin's (1988) mode coupling matrix for a general range dependent model comprised of a fluid layer of depth $h_1(x)$ lying over a semi-infinite solid halfspace. The incompressibility of the fluid layer is designated by κ, which is a minor deviation from Maupin's (1988) notation. The designations h_1^- and h_1^+ indicate that those terms are to be evaluated in the fluid just above the fluid-solid interface and in the solid just below the fluid-solid interface, respectively. The dot (e.g. $\dot{\rho}$) indicates differentiation with respect to x. The elements of the C_{ij} and the Q_{ij} for isotropic and transversely isotropic media are given in Maupin (1988) and (1992), respectively.

$$
\begin{aligned}
B_{qr} \;=\; & \frac{1}{k^q - k^r}\left\{ \int_0^{h_1(x)} w_1^{q*}\dot{\rho}\omega^2 w_1^r + t^{q*}\left(\frac{\dot{1}}{\kappa}\right)t^r + \frac{\partial t^{q*}}{\partial z}\frac{\dot{1}}{\rho\omega^2}\frac{\partial t^r}{\partial z}dz \right. \\
& + \int_{h_1(x)}^{\infty} (\mathbf{w}^{q*}\dot{\rho}\omega^2\mathbf{w}^r - \frac{\partial \mathbf{w}^{q*}}{\partial z}\dot{Q}_{33}\frac{\partial \mathbf{w}^r}{\partial z} \\
& - \frac{\partial \mathbf{w}^{q*}}{\partial z}(C_{31}\dot{C}_{11}^{-1})\mathbf{t}^r - \mathbf{t}^{q*}(C_{11}^{-1}\dot{C}_{13})\frac{\partial \mathbf{w}^r}{\partial z} + \mathbf{t}^{q*}\dot{C}_{11}^{-1}\mathbf{t}^r)\, dz \\
& - \dot{h}_1\left(-\frac{\partial t^{q*}}{\partial z}\frac{1}{\rho\omega^2}\frac{\partial t^r}{\partial z} - t^{q*}\left(\frac{1}{\kappa}\right)t^r + w_1^{q*}\rho\omega^2 w_1^r\right)_{h_1^-} \\
& - i\dot{h}_1(k^q - k^r)(w_1^{q*}t_{33}^r + t_{33}^{q*}w_1^r)_{h_1^+} \\
& + \sum_{n=2}\dot{h}_n\left[-\mathbf{w}^{q*}\rho\omega^2\mathbf{w}^r - \frac{\partial \mathbf{w}^{q*}}{\partial z}Q_{33}\frac{\partial \mathbf{w}^r}{\partial z} + \frac{\partial \mathbf{w}^{q*}}{\partial z}(C_{31}C_{11}^{-1})\mathbf{t}^r \right. \\
& \left.\left. - \mathbf{t}^{q*}(C_{11}^{-1}C_{13})\frac{\partial \mathbf{w}^r}{\partial z} + \mathbf{t}^q C_{11}^{-1}\mathbf{t}^r\right]_n \right\} \exp\left(i\int_0^x (k^q - k^r)d\xi\right). \qquad \text{(A1)}
\end{aligned}
$$

Figure Captions

Figure 1. Geometry and notation used for the energy diffusion problem. The randomly heterogeneous region is $x_L \rightarrow x_R$, is divided up into N approximately statistically stationary regions $\mathcal{L}_i(\omega)$, $(i = 1, N)$. Within any approximately stationary region $\mathcal{L}_i(\omega)$, we assume $l_j^{(i)}(\omega) \ll \mathcal{L}_i(\omega)$, where $l_j^{(i)}(\omega)$ is the frequency dependent correlation length.

Figure 2. Schematic representation of the evolution of the energy spectrum with propagation distance. The initial condition at $x = 0$ must be continuous, but may have sharp closely space peaks (a). The sharpest spectral features decay most rapidly with range according to eqs. (88) and (93) (b). In the limit that $x \rightarrow \infty$, the energy is distributed uniformly within the propagating wave spectral band with energy amplitude given by eq. (92) (c).

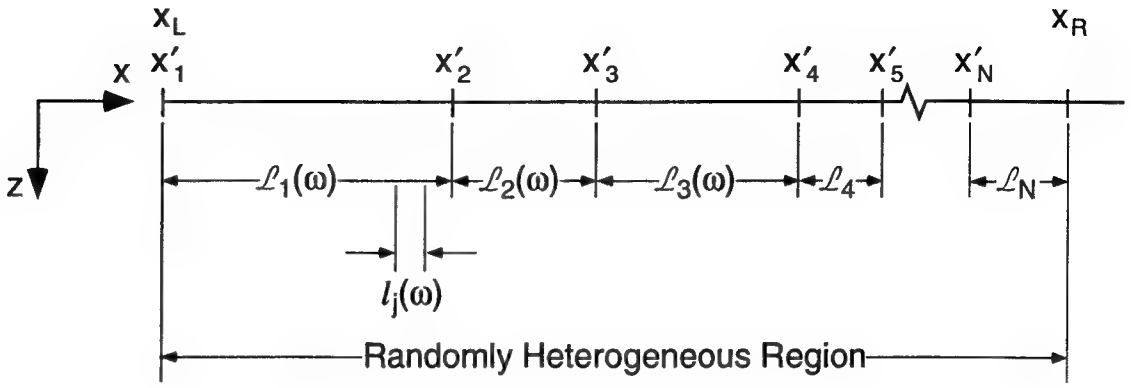
x_L
x_R
x
x'_1
x'_2
x'_3
x'_4
x'_5
x'_N
z
$\mathcal{L}_1(\omega)$
$\mathcal{L}_2(\omega)$
$\mathcal{L}_3(\omega)$
$\mathcal{L}_4$
$\mathcal{L}_N$
$l_j(\omega)$
Randomly Heterogeneous Region

Fig. 1

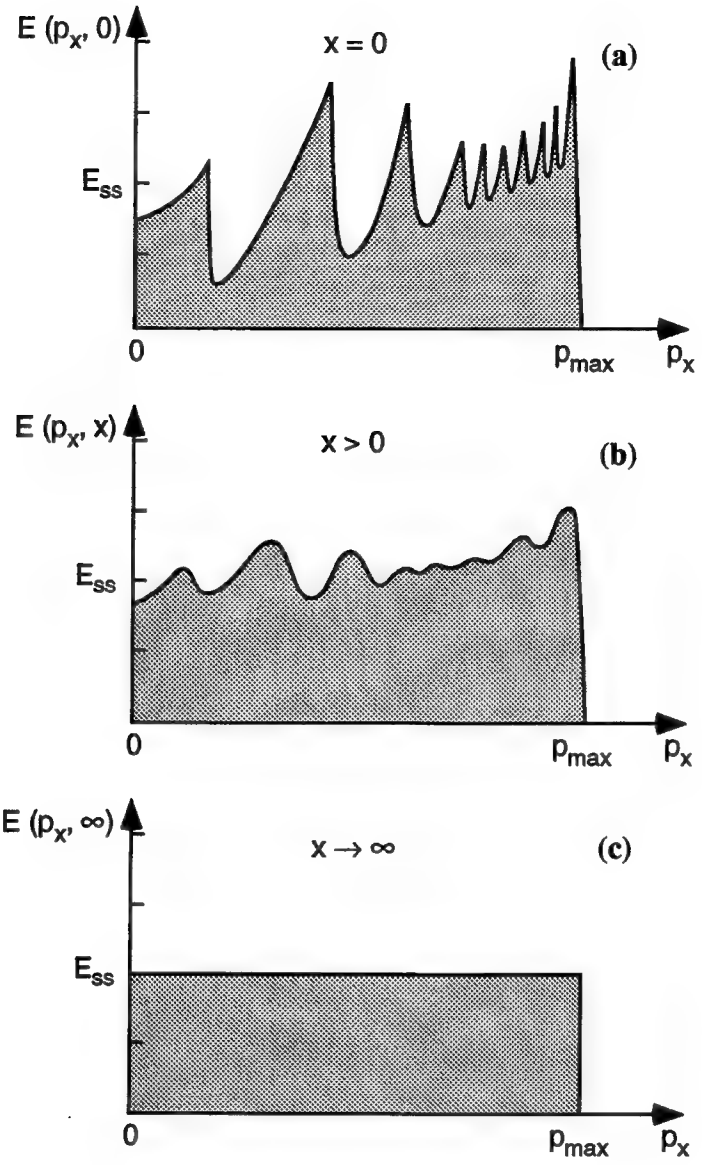

Fig. 2

EXTENDED ABSTRACT

Modal Attenuation and Interaction with a Transversely Isotropic Viscoelastic Bottom in Shallow Water Acoustic Propagation

R.I. Odom and J.A. Mercer
Applied Physics Laboratory
University of Washington, 1013 NE 40th St., Seattle, WA 98105
206-685-3788; odom@apl.washington.edu

Introduction

An acoustic signal propagating in shallow water can be conveniently represented as a linear superposition of orthogonal modes. Our definition of shallow water is frequency dependent since, by "shallow" we mean that the water is a "few" acoustic wavelengths in depth. A "few" is somewhat arbitrary, but may be as many as 100. The main point is that acoustic signal propagation in shallow water exhibits interference and diffraction phenomena that are not well modelled with ray theory.

When modal representations of the acoustic field have been applied to shallow water sound propagation by the ocean acoustics community, it has been fairly common practice to include the effects of attenuation as a first order perturbation to modal eigenvalues (e.g. Ingenito, 1973; Zhou, 1985). First order perturbation theory ignores anelastic coupling between modes and requires that $k/(Q\delta k) \ll 1$ where k is the unperturbed wavenumber, δk is the unperturbed wavenumber spacing and Q is the spatial quality factor. Because at low frequencies a significant fraction of a shallow water acoustic signal propagates in low Q bottom sediments, $k/(Q\delta k)$ can be $O(1)$. This makes the use of perturbation theory invalid, and can introduce serious errors in mode sum acoustic signal synthesis. Ewing et al. (1992) report shear Q values in the range 20 - 50 for continental shelf sediments off the New Jersey.

The severity of the error resulting from the improper treatment of attenuation in mode sum signal synthesis has been graphically illustrated by Day et al. (1989). Day et al. calculated synthetic seismograms for stratified models consisting of a high Q layer over a layered half space. The shear Q of the underlying half space was lower than the Q in the overlying layer, and half space shear speeds were lower than the compressional wave speed in the overlying layer. The signals calculated from modal summation dramatically overestimate the effect of the low shear Q on the complete signal. The mode summation results are compared with the results from a wavenumber integration routine (Apsel, R.J. and J.E. Luco, 1983) that is similar to SAFARI (Schmidt and Tango, 1986), at least in the way in which attenuation is incorporated into the model. Serious errors in the mode sum seismograms are traced by Day et al. to the way in which perturbation theory is applied to treat the anelastic problem. Specifically, the difficulty occurs with the use of the

unperturbed elastic eigenfunctions in the anelastic problem. Because the problem is with the eigenfunctions themselves, it cannot be repaired with higher order perturbation corrections to the eigenvalues. The problem does not appear when using wavenumber integration routines, because the attenuation is incorporated directly through the use of complex, frequency dependent compressional and shear speeds.

If one wishes to retain the physical insight inherent in a modal representation of the acoustic field, and properly incorporate the effects of anelasticity, one approach is to invoke the correspondence principle (e.g. Leitman and Fisher, 1973), and solve for the anelastic modes directly. The correspondence principle states that the equations of motion for a linear viscoelastic material are just the equations for a perfectly elastic material with the elastic moduli replaced with the complex, frequency dependent anelastic moduli. The anelastic moduli must be frequency dependent to preserve causality.

The correspondence principle approach has been used by Yuen and Peltier (1982) and Buland et al. (1985) to model aspects of the free oscillations of the whole earth. To a limited extent, it has also been applied to shallow water propagation problems. Bucker and Morris (1965) employed the correspondence principle to solve for the anelastic eigenwavenumbers and model the propagation loss for a shallow water problem with a fairly simple structure.

We adopt a different approach in that we represent the anelastic modes as a complex superposition of elastic eigenfunctions. The effects due to anelastic mode coupling are explicitly included and there is no restriction on the magnitude of the damping. Our approach is a traveling wave adaptation of Tromp and Dahlen (1990), who derived an elegant solution for the free oscillations of an anelastic spherical earth in terms of the elastic eigenfunctions and eigenfrequencies. Advantages of using the elastic eigenfunctions as a basis for the anelastic eigenfunctions are: 1. The effect of anelasticity on individual modes can be examined in detail; 2. The effect of range dependent attenuation can be studied by making the complex expansion coefficients range dependent. If the environment is not geometrically range dependent, we can employ the same elastic basis; 3. Used in conjunction with a general range dependent coupled mode program, the propagation physics of a strongly range dependent shallow water environment can be studied in detail. We have the ability to isolate the influence of the geometry, and different aspects of the rheology of the medium on a propagating shallow water signal.

We have derived a generalized eigenvalue equation for the complex eigenwavenumbers and complex coefficients used in the superposition of the elastic eigenfunctions to construct the anelastic eigenfunctions. Our generalized eigenvalue equation is strictly linear for the complex anelastic eigenwavenumbers. This is in contrast to the nonlinear eigenvalue equation for the anelastic eigenfrequencies of the free oscillations of the earth (Dahlen, 1981; Tromp and Dahlen, 1990). The reason for this difference is our choice of the frequency ω as the independent variable. Because of the standing wave nature of the earth free oscillation problem, ω is taken as the dependent variable in the dispersion relation. Since the anelastic moduli are frequency dependent, the eigenvalue equation for the anelastic free oscillations is nonlinear.

Our derivation also includes the effects of transverse isotropy, which has a single vertical

axis of symmetry. It is commonly observed that horizontally propagating SH waves have higher speeds than horizontally propagating, vertically polarized (SV) or vertically propagating shear waves. In addition, higher compressional wave speeds for horizontally propagating compressional waves than for vertically propagating compressional waves are observed (Ewing et al., 1992). Berge et al. (1991) report shear wave anisotropy of 12% - 15% in the same shelf region off of New Jersey studied by Ewing et al.

Definitions and notation

The derivation of the generalized eigenvalue equation for the anelastic eigenwavenumbers will be sketched briefly. A more detailed treatment is currently being prepared for publication. We adopt the notational conventions of Takeuchi and Saito (1972), who treat seismic surface waves and free oscillations explicitly for a transversely isotropic earth. As mentioned above, the case of transverse isotropy is probably the most relevant for bottom interacting shallow water propagation. Berge et al.(1991) felt that additional azimuthal anisotropy induced by ripples in the sediment surface or cracks would be very weak. A particular feature of transversly isotropic media is that the P - SV motion still decouples from the SH motion. This is not true for more general anisotropy. We include the SH problem for completeness, but discuss it only briefly. It is the P - SV problem that describes, when the appropriate limits are taken, the propagation of an acoustic signal propagating in shallow water over a plane layered viscoelastic bottom.

Our coordinate system is a right handed coordinate system with the propagation direction along the x axis, y positive into the paper, and z positive upward. As mentioned the P - SV (Rayleigh) motion decouples from the SH (Love) motion. The perfectly elastic displacements u_i and stresses σ_{ij} for P - SV are

$$\begin{aligned} u_x &= -i\, y_3(z;\omega,k)e^{i(\omega t - kx)} \\ u_y &= 0 \\ u_z &= y_1(z;\omega,k)e^{i(\omega t - kx)} \end{aligned} \tag{1}$$

and

$$\sigma_{xx} = \left[\mathrm{F}\frac{dy_1}{dz} - k\mathrm{A}y_3\right] e^{i(\omega t - kx)}$$

$$\sigma_{yy} = \left[\mathrm{F}\frac{dy_1}{dz} - k(\mathrm{A}-2\mathrm{N})y_3\right] e^{i(\omega t - kx)}$$

$$\begin{aligned} \sigma_{zz} &= y_2 e^{i(\omega t - kx)} \\ \sigma_{zx} &= -i\, y_4 e^{i(\omega t - kx)} \\ \sigma_{yz} &= \sigma_{xy} = 0 \end{aligned} \tag{2}$$

The boundary conditions on the y_i for P - SV are

$$\begin{aligned} & y_i\,(i=1,2,3,4) \quad \text{continuous} \\ & y_2 = y_4 = 0 \quad \text{at the free surface} \quad z=0 \\ & y_i\,(i=1,2,3,4) \quad \to 0 \quad \text{as} \quad z \to -\infty \end{aligned} \tag{3}$$

The displacements and stress for SH motion are

$$\begin{aligned} & u_x = u_z = 0 \\ & u_y = y_1(z;\omega,k)e^{i(\omega t - kx)} \end{aligned} \tag{4}$$

and

$$\sigma_{yz} = \left[\mathrm{L}\frac{dy_1}{dz}\right] e^{i(\omega t - kx)}$$

$$\sigma_{xy} = -i\,k\,\mathrm{N}y_1 e^{i(\omega t - kx)} \tag{5}$$

$$\sigma_{xx} = \sigma_{yy} = \sigma_{zz} = \sigma_{zx} = 0$$

In addition, we introduce the definition for y_2

$$y_2(z;\omega,k) = \mathrm{L}\frac{dy_1}{dz} \tag{6}$$

so that

$$\sigma_{yz} = y_2 e^{i(\omega t - kx)} \tag{7}$$

The boundary conditions for the y_i for SH are

$$\begin{aligned} & y_1, y_2 \quad \text{continuous} \\ & y_2 = 0 \quad \text{at the free surface} \quad z=0 \\ & y_1, y_2 \to 0 \quad \text{as} \quad z \to -\infty \end{aligned} \tag{8}$$

In order to minimize the notational overhead, we make no distinction between the y_i's for the P - SV and SH problems. We will concentrate mainly on the P - SV problem. The meaning of the y_i's will be clear from context. The P - SV and SH problems are treated separately since they do not couple in transversly isotropic media.

The above equations of motion for a perfectly elastic medium may be represented in first order form as

$$\partial_z \mathbf{b}_{R,L} = \mathbf{M}_{R,L}\, \mathbf{b}_{R,L} \tag{9}$$

where the subscripts R, L indicate whether we are referring to the P - SV [Eq. (1) - (3)] or the SH [Eq. (4) - (8)] systems of equations. The vectors $\mathbf{b}_{R,L}$ and the matrices $\mathbf{M}_{R,L}$ are defined for P - SV motion as

$$\mathbf{b}_R = (y_1, y_2, y_3, y_4)^T \tag{10}$$

and

$$\mathbf{M}_R = \begin{bmatrix} 0 & C^{-1} & k\,F/C & 0 \\ -\omega^2 \rho & 0 & 0 & k \\ -k & 0 & 0 & L^{-1} \\ 0 & -k\,F/C & \left[k^2\left[A - F^2/C\right] - \omega^2 \rho\right] & 0 \end{bmatrix} \tag{11}$$

and for SH motion as

$$\mathbf{b}_L = (y_1, y_2)^T \tag{12}$$

and

$$\mathbf{M}_L = \begin{bmatrix} 0 & L^{-1} \\ \left(k^2 N - \omega^2 \rho\right) & 0 \end{bmatrix} \tag{13}$$

In the matrices $\mathbf{M}_{R,L}$, ω is the real angular frequency, ρ is the density, k is the horizontal wavenumber for a perfectly elastic medium, and A, C, F, L and N are the five elastic moduli necessary to characterize a transversly isotropic medium. When

$$A = C = \lambda + 2\mu \qquad L = N = \mu \qquad F = \lambda \tag{14}$$

the medium is isotropic.

From this point on, we drop the subscripts R, L on the vector **b** and the matrix **M**. It will be apparent from context which system we mean. The following development will be for the P - SV system. Analogous results for the SH system are summarized at the endof the paper.

There are inherent symmetries in the equations of motion (Kennett et al., 1978 and Thomson et al., 1986) that can be exploited to construct compact expressions useful for very efficiently deriving the elastic wave dispersion relation, orthogonality relationships and other quantities. Define the matrices **R**, **S**, Λ and Ξ as

$$\mathbf{R} = \begin{bmatrix} \Lambda & \mathbf{0} \\ \mathbf{0} & \Lambda \end{bmatrix} \quad \text{and} \quad \mathbf{S} = \begin{bmatrix} \Xi & \mathbf{0} \\ \mathbf{0} & \Xi \end{bmatrix} \tag{15}$$

and

$$\Lambda = \begin{bmatrix} 0 & 1 \\ -1 & 0 \end{bmatrix} \quad \text{and} \quad \Xi = \begin{bmatrix} 0 & 1 \\ 0 & 0 \end{bmatrix} \tag{16}$$

Using the matrices defined above, we can form various compositions of two stress fields. For example for P - SV, we can form

$$\partial_z(\mathbf{b}^T \mathbf{S} \mathbf{b}) = \mathbf{b}^T \left[\mathbf{M}^T \mathbf{S} + \mathbf{S} \mathbf{M} \right] \mathbf{b} \tag{17}$$

whereby we operate from the left and the right with the same stress displacement vector **b**. When both sides are integrated with respect to z from $-\infty$ to 0, we obtain the dispersion relation for Rayleigh waves in a transversly isotropic medium.

$$\omega^2 I_1 = k^2 I_2 + k I_3 + I_4 \tag{18}$$

where

$$I_1 = \int_{-\infty}^{0} \rho(y_1{}^2 + y_3{}^2)\, dz \tag{19}$$

$$I_2 = \int_{-\infty}^{0} (L y_1{}^2 + A y_3{}^2)\, dz \tag{20}$$

$$I_3 = 2 \int_{-\infty}^{0} \left[L y_1 \frac{dy_3}{dz} - F y_3 \frac{dy_1}{dz} \right] dz \tag{21}$$

$$I_4 = \int_{-\infty}^{0} \left[C \frac{dy_1}{dz}^2 + L \frac{dy_3}{dz}^2 \right] dz \tag{22}$$

The left hand side of Eq. (17) is a perfect differential in z, and after integration it vanishes when the boundary conditions are applied.

Derivation of the generalized eigenvalue equation

The complex generalized eigenvalue equation for the complex eigenwavenumbers is derived in a straightforward manner. Invoking the correspondence principle, we represent the equations of motion for an anelastic transversly isotropic medium as

$$\partial_z \mathbf{c} = \tilde{\mathbf{M}} \mathbf{c} \tag{23}$$

where $\mathbf{c}$ and $\tilde{\mathbf{M}}$ represent the stress-displacement vector and wave operator matrix, respectively for anelastic media. For our definition of $\tilde{\mathbf{M}}$, we take

$$\tilde{\mathbf{M}} = \begin{bmatrix} 0 & \tilde{C}^{-1} & \kappa\tilde{F}/\tilde{C} & 0 \\ -\sigma^2\rho & 0 & 0 & \kappa \\ -\kappa & 0 & 0 & \tilde{L}^{-1} \\ 0 & -\kappa\tilde{F}/\tilde{C} & \left[\kappa^2\left[\tilde{A}-\tilde{F}^2/\tilde{C}\right]-\sigma^2\rho\right] & 0 \end{bmatrix} \tag{24}$$

The symbols $\tilde{A}$, $\tilde{C}$, $\tilde{F}$, $\tilde{L}$ and $\tilde{N}$ are the five complex frequency dependent elastic moduli for an anelastic transversly isotropic solid; κ is the eigenwavenumber for the anelastic solid; σ is the frequency, which we take to be real for propagating waves.

We take

$$\mathbf{c} = \mathbf{c}_n \tag{25}$$

where $\mathbf{c}_n$ is an eigenfunction of the anelastic medium and is a solution of Eq. (23). In addition, we represent $\mathbf{c}_n$ as a complex linear superposition of the eigenfunctions of the perfectly elastic problem

$$\mathbf{c}_n = \sum_m Q_{m\,n}\mathbf{b}_m \tag{26}$$

$Q_{m\,n}$ is the matrix of complex coefficients that transforms the elastic eigenfunctions $\mathbf{b}_m$ to the anelastic solutions.

Employing the matrix $\mathbf{R}$ defined above, we form the composition of an anelastic mode $\mathbf{c}_n$ as represented by Eq. (26) and an elastic mode $\mathbf{b}_n$

$$\partial_z(\mathbf{b}_n{}^{\mathrm{T}}\,\mathbf{R}\,\mathbf{c}_n) = \mathbf{b}_n{}^{\mathrm{T}}\left[\mathbf{M}^{\mathrm{T}}\mathbf{R} + \mathbf{R}\tilde{\mathbf{M}}\right]\mathbf{c}_n \tag{27}$$

and integrate over z from $-\infty$ to 0. The elastic and anelastic problems satisfy the same boundary conditions, so the left hand side of Eq. (27) vanishes after the integration.

By assuming that the elastic eigenfunction $\mathbf{b}_n$ and the anelastic eigenfunction $\mathbf{c}_n$ have the same real frequency so that

$$\omega^2 = \sigma^2 \tag{28}$$

we arrive at the following infinite generalized quadratic eigenvalue equation for the anelastic eigenwavenumbers κ_n

$$\mathbf{A}\,\mathbf{q}_n + \kappa_n\,\mathbf{B}\,\mathbf{q}_n + \kappa_n{}^2\mathbf{C}\,\mathbf{q}_n = 0 \tag{29}$$

where

$$\mathbf{A} = -\int_{-\infty}^{0} \Big\{ k_n^{\,2} \left[\mathrm{A} - \mathrm{F}^2/\mathrm{C} \right] y_3^{(n)} y_3^{(m)} + k_n \left[\left[y_1^{(n)} y_4^{(m)} + y_4^{(n)} y_1^{(m)} \right] - \frac{\mathrm{F}}{\mathrm{C}} \left[y_2^{(n)} y_3^{(m)} + y_3^{(n)} y_2^{(m)} \right] \right] - \left[\mathrm{C}^{-1} - \tilde{\mathrm{C}}^{-1} \right] y_2^{(n)} y_2^{(m)} - \left[\mathrm{L}^{-1} - \tilde{\mathrm{L}}^{-1} \right] y_4^{(n)} y_4^{(m)} \Big\} \, dz \tag{30}$$

$$\mathbf{B} = \int_{-\infty}^{0} \left[\left[y_1^{(n)} y_4^{(m)} + y_4^{(n)} y_1^{(m)} \right] - \frac{\tilde{\mathrm{F}}}{\tilde{\mathrm{C}}} \left[y_2^{(n)} y_3^{(m)} + y_3^{(n)} y_2^{(m)} \right] \right] dz \tag{31}$$

$$\mathbf{C} = \int_{-\infty}^{0} \left[\left[\tilde{\mathrm{A}} - \tilde{\mathrm{F}}^2/\tilde{\mathrm{C}} \right] y_3^{(n)} y_3^{(m)} \right] dz \tag{32}$$

The eigenvectors $\mathbf{q}_n$ are the columns of the matrix $\mathbf{Q}$

$$\mathbf{Q} = (\ldots, \mathbf{q}_n, \ldots) \tag{33}$$

By making the assignment

$$\mathbf{I}\,\mathbf{r}_n = \kappa_n \mathbf{I}\,\mathbf{q}_n \tag{34}$$

the quadratic generalized eigenvalue problem Eq. (29) can be converted to a linear generalized eigenvalue problem (Garbow et al., 1977) at the expense of doubling the dimension of the system

$$\begin{bmatrix} \mathbf{A} & \mathbf{B} \\ \mathbf{0} & \mathbf{I} \end{bmatrix} \begin{bmatrix} \mathbf{q}_n \\ \mathbf{r}_n \end{bmatrix} = \kappa_n \begin{bmatrix} \mathbf{0} & -\mathbf{C} \\ \mathbf{I} & \mathbf{0} \end{bmatrix} \begin{bmatrix} \mathbf{q}_n \\ \mathbf{r}_n \end{bmatrix} \tag{35}$$

Equation (35) is the main result of this paper. The solution of this linear generalized matrix eigenvalue problem yields the complex eigenwavenumbers κ_n for the modes of an anelastic transversly isotropic medium and the eigenvectors $\mathbf{q}_n$. The eigenvectors $\mathbf{q}_n$ of Eq. (35) are the columns of the transformation matrix $Q_{n\,m}$ used to construct the anelastic eigenfunctions from the elastic eigenfunctions from Eq. (26). The linearity of Eq. (35) is an important point and should be contrasted with the result derived by Tromp and Dahlen (1990) for the free oscillations of the earth. Their equation (3.5) is

$$\left[\Omega^2 + \mathbf{V}(\sigma_k) \right] \mathbf{q}_k = \sigma_k^{\,2} \mathbf{q}_k \tag{36}$$

The matrix Ω is a diagonal matrix of eigenfrequencies for the perfectly elastic earth; $\mathbf{q}_k$ is the k^{th} column of the transformation matrix $\mathbf{Q}$; σ_k is the complex eigenfrequency of the k^{th} anelastic mode; and $\mathbf{V}(\sigma)$ is an anelastic potential energy matrix that is a functional of products of the elastic eigenfunctions and the complex frequency dependent elastic moduli. The standing wave nature of the earth free oscillation problem leads to the choice of the frequency as the dependent variable. Because of the dependence of the elastic moduli on frequency, the problem, Eq. (36), is nonlinear. The choice of frequency as the independent variable for the traveling wave problem leads to the linear problem we have derived above, Eq.(35).

We have also derived similar results for the SH problem. We form the compostion

$$\partial_z(\mathbf{b}_n{}^{\mathrm{T}}\,\Xi\,\mathbf{c}_n) = \mathbf{b}_n{}^{\mathrm{T}}\left[\mathbf{M}^{\mathrm{T}}\,\Xi + \Xi\,\tilde{\mathbf{M}}\right]\mathbf{c}_n \tag{37}$$

As definitions of $\mathbf{M}$ and $\mathbf{b}$, we take Eqs. (12) and (13) for SH motion. For $\tilde{\mathbf{M}}$ we take Eq. (13) with k replaced by κ, and N and L replaced by $\tilde{\mathrm{N}}$ and $\tilde{\mathrm{L}}$, respectively. Likewise the definition of $\mathbf{c}$ follows from Eq. (12) and (25). Upon integrating Eq. (37) with respect to z from 0 to $-\infty$, carrying out some additional algebra and again setting

$$\omega^2 = \sigma^2 \tag{38}$$

we arrive at

$$\left(k_n{}^2\mathbf{I} - \kappa_n{}^2\mathbf{N} - \mathbf{L}\right)\mathbf{q}_n = \kappa_n{}^2\,\mathbf{q}_n \tag{39}$$

where

$$\mathbf{N} = \left[\int_{-\infty}^{0} \mathrm{N}\,y_1{}^{(n)2}\,dz\right]^{-1} \int_{-\infty}^{0} \delta\mathrm{N}\,y_1{}^{(n)}y_1{}^{(m)}\,dz \tag{40}$$

and

$$\mathbf{L} = \left[\int_{-\infty}^{0} \mathrm{N}\,y_1{}^{(n)2}\,dz\right]^{-1} \int_{-\infty}^{0} \delta\mathrm{L}\frac{dy_1{}^{(n)}}{dz}\frac{dy_1{}^{(m)}}{dz}\,dz \tag{41}$$

The two terms $\delta\mathrm{L}$ and $\delta\mathrm{N}$ are the complex frequency dependent parts of the two shear moduli $\tilde{\mathrm{L}}$ and $\tilde{\mathrm{N}}$. The anelasticity tensor $\tilde{c}_{ijkl}$ for a linear viscoelastic material can be written

$$\tilde{c}_{ijkl} = c_{ijkl} + \delta c\,(\omega)_{ijkl} \tag{42}$$

We were able to separate the perfectly elastic part from the frequency dependent anelastic part for the SH problem. There is no restriction on the magnitude of $\delta\mathrm{L}$ and $\delta\mathrm{N}$. Also note that Eq. (39) is linear in $\kappa_n{}^2$.

A final point is that both Eq. (35) and Eq. (39) are infinite in dimension. Any practical implementation will necessarily employ a truncated mode set. This should not be much of a restriction, as most low frequency shallow water signals can be adquately modelled with a limited number of modes.

Conclusions

The linear complex generalized eigenvalue equations (35) and (39) appear to be genuinely new results. They are useful for modeling and characterizing acoustic signals propagating in a shallow water environment characterized by high attenuation and transverse isotropy. This is an environment where a perturbation treatment of the bottom properties applied to mode summation signal synthesis will lead to erroneous results. The solution of equations (35) and (36) are used to represent the anelastic modes in terms of the elastic modes, permitting a detailed analysis of the physics of strongly bottom interacting acoustic propagation. The effects of transverse isotropy and attenuation, including attenuation induced dispersion, are properly accounted for. Stable well-behaved numerical algorithms exist for solving the complex generalized eigenvalue problem, even in cases where the the matrices involved are near singular. Our next step is the numerical implementation of Eqs. (35) and (39).

Acknowledgments

This research was sponsored by the ARL Program of the Office of Naval Research under contract N00014-90-J-1369 and ONR contract N00014-94-1-0036.

References

Apsel, R.J. and J.E. Luco, 1983. On the Green's function for a layered half-space, part II, *Bull. Seis. Soc. Am.*, **73**, 931-951.

Berge, P.A., S. Mallick, G.J. Fryer, N. Barstow, J.A. Carter, G.H. Sutton and J.I. Ewing, 1991. *In situ* measurement of transverse isotropy in shallow-water marine sediments, *Geophys. J. Int.*, **104**, 241-254.

Bucker, H.P. and H.E. Morris, 1965. Normal-mode intensity calculations for a constant-depth shallow-water channel, *J. Acoust. Soc. Am*, **38**, 1010-1017.

Buland, R., D. Yuen, K. Konstanty, and R. Widmer, 1985. Source phase shift: a new phemenon in wave propagation due to anelasticity, *Geophys. Res. Lett.*, **12**, 569-572.

Dahlen, F.A., 1981. The free oscillations of an anelastic aspherical earth, *Geophys. J. Roy. Astr. Soc.*, **66**, 1-22.

Day, S.M., K.L. McLaughlin, B. Shkoller and J.L. Stevens, 1989. Potential errors in locked mode synthetics for anelastic earth models, *Geophys. Res. Lett.*, **16**, 203-206.

Ewing, J.I., J.A. Carter, G.H. Sutton and N. Barstow, 1992. Shallow water sediment properties derived from high-frequency shear and interface waves, *J. Geophys. Res.*, **97**, 4739-4762.

Garbow, B., J. Boyle, J. Dongarra and C. Moler, 1977. *Matrix Eigensystem Routines - EISPACK Guide Extension*, Lecture Notes in Computer Science, pp49-50, Springer-Verlag, New York.

Kennett, B.L.N., N.J. Kerry and J.H. Woodhouse, 1978. Symmetries in the reflection and transmission of elastic waves, *Geophys. J. Roy. Astr. Soc.*, **52**, 215-229.

Ingenito, F., 1973. Measurements of mode attenuation coefficients in shallow water, *J. Acoust. Soc. Am*, **53**, 858-863.

Leitman, M.J. and G.M.C. Fisher, 1973. The linear theory of viscoelasticity, *Handbuch der Physik*, Vol. VIa/3 (ed. C. Truesdell), pp1-123, Springer-Verlag, New York.

Schmidt, H. and G. Tango, 1986. Efficient global matrix approach to the computation of synthetic seismograms, *Geophys. J. Roy. Astr. Soc.*, **84**, 331-359.

Takeuchi, H. and M. Saito, 1972. Seismic surface waves, *Methods in Computational Physics*, Vol. 11 (ed. B.A. Bolt), pp217-295. Academic Press, New York.

Thomson, C., T. Clarke, and J. Garmany, (1986). Observations on seismic wave equation and reflection coefficient symmetries in stratified media, *Geophys. J. Roy. Astr. Soc.*, **86**, 675-686.

Tromp, J. and F.A. Dahlen, 1990. Free oscillations of a spherical anelastic earth, *Geophys. J. Int.*, **103**, 707-723.

Yuen, D. and W.R. Peltier, 1982. Normal modes of the viscoelastic earth, *Geophys. J. Roy. Astr. Soc.*, **69**, 495-526.

Zhou, J., 1985. Normal mode measurements and remote sensing of sea-bottom sound velocity and attenuation in shallow water, *J. Acoust. Soc. Am*, **78**, 1003-1009.